

AD-A100 722

COMPUTER SCIENCES CORP FALLS CHURCH VA  
EFFECTS OF PHASE NOISE AND THERMAL NOISE UPON COHERENT PSK DEMO—ETC(U)  
AUG 74 H I PAUL, P A KULLSTAM

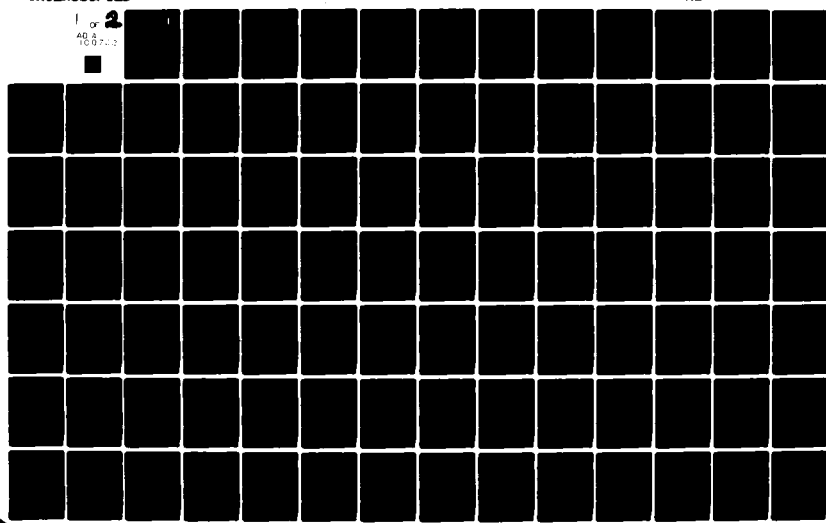
F/6 9/4

DCA100-73-C-0008

NL

UNCLASSIFIED

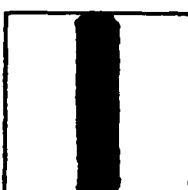
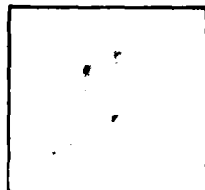
1 or 2  
AD A  
100722



PHOTOGRAPH THIS SHEET

ADA100722

DTIC ACCESSION NUMBER



LEVEL

Computer Sciences Corp.  
Falls Church, VA

INVENTORY

EFFECTS OF PHASE NOISE AND THERMAL NOISE UPON  
COHERENT PSK DEMODULATION AND THEIR IMPACT ON PHASE  
NOISE SPECIFICATIONS FOR TERMINALS OF THE PHASE II  
DSCS. *Final Rept.* Aug. 74

Contract DCA100-73-C-0008

DISTRIBUTION STATEMENT A

Approved for public release  
Distribution Uncontrolled

DISTRIBUTION STATEMENT

ACCESSION FOR

NTIS GRA&I

DTIC TAB

UNANNOUNCED

JUSTIFICATION



BY Per Ltr. on File

DISTRIBUTION /

AVAILABILITY CODES

DIST

AVAIL AND/OR SPECIAL

A

DISTRIBUTION STAMP



DATE ACCESSIONED

DATE RECEIVED IN DTIC

PHOTOGRAPH THIS SHEET AND RETURN TO DTIC-DDA-2

ADA100722

CSC DATA SHEET

FINAL REPORT

EFFECTS OF PHASE NOISE AND THERMAL NOISE UPON COHERENT  
PSK DEMODULATION AND THEIR IMPACT ON PHASE NOISE  
SPECIFICATIONS FOR TERMINALS OF THE PHASE II DSCS

Prepared for  
THE DEFENSE COMMUNICATIONS AGENCY

by  
COMPUTER SCIENCES CORPORATION  
6565 Arlington Boulevard  
Falls Church, Virginia 22046

under  
Contract No. DCA 100-73-C-0008  
Task Order No. 0208, Part 3

August 1974

Prepared by: H. I. Paul P. A. Kullstam  
H. I. Paul, P. A. Kullstam

Reviewed by: D. J. Maxwell  
D. J. Maxwell, Director  
Systems Technology Operation

Approved by: W. Schmidt  
W. Schmidt  
Program Director

DISTRIBUTION STATEMENT  
Approved for public release  
Distribution Unlimited

REPORT DOCUMENTATION PAGE		READ INSTRUCTIONS BEFORE COMPLETING FORM
1. REPORT NUMBER	2. GOVT ACCESSION NO.	3. RECIPIENT'S CATALOG NUMBER
4. TITLE (and Subtitle) EFFECTS OF PHASE NOISE AND THERMAL NOISE UPON COHERENT PSK DEMODULATION AND THEIR IMPACT ON PHASE NOISE SPECIFICATIONS FOR TERMINALS OF THE PHASE II DSCS.		5. TYPE OF REPORT & PERIOD COVERED FINAL
7. AUTHOR(s) H. S. PAUL, P. A. Kulltan		6. PERFORMING ORG. REPORT NUMBER u
8. CONTRACT OR GRANT NUMBER(s) DCA100-73-C-0008		
9. PERFORMING ORGANIZATION NAME AND ADDRESS Computer Services Corporation Fall Church, Virginia		10. PROGRAM ELEMENT, PROJECT, TASK AREA & WORK UNIT NUMBERS Task 0208 Part 3
11. CONTROLLING OFFICE NAME AND ADDRESS		12. REPORT DATE August 1974
14. MONITORING AGENCY NAME & ADDRESS (if different from Controlling Office)		13. NUMBER OF PAGES 1X 014
16. DISTRIBUTION STATEMENT (of this Report)		15. SECURITY CLASS. (of this report) UNCLASSIFIED
17. DISTRIBUTION STATEMENT (of the abstract entered in Block 20, if different from Report)		15a. DECLASSIFICATION/DOWNGRADING SCHEDULE
18. SUPPLEMENTARY NOTES		
19. KEY WORDS (Continue on reverse side if necessary and identify by block number)		
20. ABSTRACT (Continue on reverse side if necessary and identify by block number)		

SECURITY CLASSIFICATION OF THIS PAGE(When Data Entered)

SECURITY CLASSIFICATION OF THIS PAGE(When Data Entered)

EFFECTS OF PHASE NOISE AND THERMAL  
NOISE UPON COHERENT PSK DEMODULATION  
AND THEIR IMPACT ON PHASE NOISE  
SPECIFICATIONS FOR TERMINALS OF THE  
PHASE II DSCS

August 1974

## TABLE OF CONTENTS

<u>Summary</u> .....	S-1
<u>Section 1 - Introduction</u> .....	1-1
<u>Section 2 - System Definitions, Phase Noise Terminology and the Impact of any Color Phase Noise on Partially Coherent PSK System</u> .....	2-1
2. 1    System Definitions .....	2-1
2. 2    Phase Noise Terminology .....	2-1
2. 3    General Impact of any Color Phase Noise on Partially Coherent PSK Systems .....	2-4
<u>Section 3 - Effects of Additive Gaussian Noise and Phase Noise Upon Coherent PSK Demodulation</u> .....	3-1
3. 1    Analytical Studies and Tradeoff Analysis .....	3-1
3. 2    Analytical Difficulties and Their Resolution .....	3-17
<u>Section 4 - Optimum Performance of BPSK and QPSK Signaling With Viterbi (Rate 1/2, K = 7) Decoding in the Presence of Oscillator Phase Noise Expected for Terminals of the DSCS</u> .....	4-1
4. 1    Optimum Performance Results With Terminals Obeying the "HT-MT" Modified Phase Noise Specification .....	4-1
4. 2    Optimum Performance With Realistic Terminal Phase Noise .....	4-5
4. 2. 1    Phase Noise Synthesized Using Comtech Lab. Inc. L-Band Oscillator, Fluke Frequency Synthesizer and Selected Atomic and Crystal Standards .....	4-8
4. 2. 2    BPSK and QPSK System Performance Optimization With Synthesized Phase Noise Data .....	4-12
<u>Section 5 - Demodulation Performance of Current Modulation Systems Operating in the Presence of Phase Noise in the Phase II DSCS</u> .....	5-1
5. 1    Radiation Inc. BPSK (MD-921G) .....	5-1
5. 2    Magnavox Research Lab. Inc. (MRL) USC-28 BPSK Spread Spectrum System .....	5-7
5. 2. 1    General .....	5-7
5. 2. 2    Phase Noise Effects in the USC-28 .....	5-7
5. 2. 3    Performance of the USC-28 Operating with Terminals of the Phase II DSCS .....	5-10

TABLE OF CONTENTS (Continued)

5.3	Raytheon Inc. TDMA (EDM) . . . . .	5-11
5.3.1	General . . . . .	5-11
5.3.2	Impact of Phase Noise Upon TDMA System Performance . . . . .	5-13
<u>Section 6 - Phase Noise Specifications for Terminals of the DSCS . . . . .</u>		6-1
6.1	Analytical Study . . . . .	6-1
6.2	Applications . . . . .	6-6
6.2.1	General . . . . .	6-6
6.2.2	BPSK System Specifications . . . . .	6-6
6.2.3	QPSK System Specifications . . . . .	6-7
6.2.4	Phase Noise Specifications for MRL's USC-28 BPSK Spread Spectrum . . . . .	6-8
6.2.5	Phase Noise Specifications for Raytheon Inc.'s Burst Coherent TDMA . . . . .	6-9
6.2.6	Summary . . . . .	6-10
6.3	Phase Noise Specifications for the AN/MSC-46 "Upgrade" . . . . .	6-10
<u>Annex</u>	. . . . .	N-1
<u>Appendix A - Partially Coherent M-ary PSK Demodulation Loss Functions . . . . .</u>		A-1
<u>Appendix B - Verification of Worst Case Phase Noise Assumption . . . . .</u>		B-1
<u>Appendix C - Evaluation of Integrals Associated with Phase Noise Influence on Coherent PSK Demodulation . . . . .</u>		C-1
C.1	Even K-Values . . . . .	C-1
C.2	Odd K-Values . . . . .	C-3
<u>Appendix D - Tabulated Results . . . . .</u>		D-1
<u>References . . . . .</u>		R-1

## LIST OF ILLUSTRATIONS

### Figure

S-1	Phase Noise Specification Bands . . . . .	S-12
2-1	M-ary PSK System . . . . .	2-2
2-2	Phase Noise Density; Definitions Adopted in This Report . . . . .	2-3
3-1	Spectral Densities at Various Points of a (Partially) Coherent PSK Receiver . . . . .	3-5
3-2	Frequency Characteristics of a Second-Order Phase-Locked Loop with Damping Factor = 0.707 . . . . .	3-7
4-1	HT-MT Incidental FM Specification Converted to Single Sideband Phase Noise Density $\{f(f)\}$ at Carrier Frequency . . . . .	4-2
4-2	Demodulation Loss (dB) and Total Phase Variance Versus Information Bit Rate (BPSK + HT-MT Mod Phase Noise, 2 Terminals) . . . . .	4-4
4-3	Demodulation Loss (dB) and Total Phase Variance Versus Information Bit Rate (BPSK - HT-MT Mod Phase Noise, 2 Terminals and 1 Equivalent Satellite) . . . . .	4-5
4-4	Demodulation Loss (dB) and Total Phase Variance Versus Information Bit Rate (QPSK - HT-MT Mod Phase Noise, 2 Terminals) . . . . .	4-6
4-5	Demodulation Loss (dB) and Total Phase Variance Versus Information Bit Rate (QPSK + HT-MT Mod Phase Noise, 2 Terminals and 1 Equivalent Satellite) . . . . .	4-7
4-6	L-Band Reference Signal Generator . . . . .	4-9
4-7	Synthesized Single Sideband Phase Noise Densities $\{f(f)\}$ for "Cesium II" and "Crystal II" at 7800 MHz . . . . .	4-10
4-8	Demodulation Loss (dB) and Total Phase Variance Versus Information Bit Rate (BPSK and "Cesium II" Phase Noise, 2 Terminals and 1 Equivalent Satellite) . . . . .	4-13
4-9	Demodulation Loss (dB) and Total Phase Variance Versus Information Bit Rate (QPSK and "Cesium II" Phase Noise, 2 Terminals and 1 Equivalent Satellite) . . . . .	4-14
4-10	Demodulation Loss (dB) and Total Phase Variance Versus Information Bit Rate (BPSK and "Crystal II" Phase Noise, 2 Terminals and 1 Equivalent Satellite) . . . . .	4-15
4-11	Demodulation Loss (dB) and Total Phase Variance Versus Information Bit Rate (QPSK and "Crystal II" Phase Noise, 2 Terminals and 1 Equivalent Satellite) . . . . .	4-16
5-1	Radiation Inc. MD-921G BPSK Demodulation Loss and Total Phase Variance Versus Information Bit Rate (HT-MT Mod Phase Noise) . . . . .	5-2

## LIST OF ILLUSTRATIONS (Continued)

### Figure

5-2	Radiation Inc. MD-921G BPSK Demodulation Loss and Total Phase Variance Versus Information Bit Rate ("Crystal II" Phase Noise) .....	5-3
5-3	Radiation Inc. MD-921G BPSK Demodulation Loss and Total Phase Variance Versus Information Bit Rate ("Cesium II" Phase Noise) .....	5-4
5-4	Radiation Inc. MD-921G BPSK Demodulation Loss and Total Phase Variance Versus Information Bit Rate, $\tau = 1.0$ ("Cesium II" Phase Noise) .....	5-6
5-5	Worst Case LOW and R T Configuration .....	5-8
5-6	TDMA Frame and Demodulator Details .....	5-12
5-7	Raytheon Inc. BPSK TDMA Demodulation Loss and Total Phase Variance Versus Information Bit Rate (HT-MT Mod Phase Noise) .....	5-17
5-8	Raytheon Inc. QPSK TDMA Demodulation Loss and Total Phase Variance Versus Information Bit Rate (HT-MT Mod Phase Noise) .....	5-18
5-9	Raytheon Inc. BPSK TDMA Demodulation Loss and Total Phase Variance Versus Information Bit Rate ("Cesium II" Phase Noise) .....	5-19
5-10	Raytheon Inc. QPSK TDMA Demodulation Loss and Total Phase Variance Versus Information Bit Rate ("Cesium II" Phase Noise) .....	5-20
5-11	Raytheon Inc. BPSK TDMA Demodulation Loss and Total Phase Variance Versus Information Bit Rate ("Crystal II" Phase Noise) .....	5-21
5-12	Raytheon Inc. QPSK TDMA Demodulation Loss and Total Phase Variance Versus Information Bit Rate ("Crystal II" Phase Noise) .....	5-22
A-1	Comparison of Degradation Incurred for Auxiliary Carrier, Suppressed Carrier BPSK and QPSK Systems With and Without Viterbi Decoding .....	A-8

## LIST OF TABLES

### Table

S-1	Allowable Information Rates for Suppressed Carrier BPSK and QPSK Signaling With Several Possible Phase Noise Sources in the DSCS and With Soft Decision (3-bit), Rate 1/2, Constraint Length 7 Viterbi Decoding at $BER = 10^{-5}$ . . . . .	S-5
S-2	Allowable Information Rates for Radiation BPSK (Power Loop) Modem With Several Possible Phase Noise Sources in the DSCS and With Soft Decision (3-bit), Rate 1/2 Constraint Length 7 Viterbi Decoding at $BER = 10^{-5}$ . . . . .	S-6
S-3(a)	Allowable Information Rates for Raytheon TDMA With PLL Noise Bandwidth of 100 Hz. Operation With Possible Phase II DSCS Noise Contributors and With Soft Decision (3-bit), Rate 1/2, Constraint Length 7, Viterbi Decoding at $BER = 10^{-5}$ . . . . .	S-7
S-3(b)	Allowable Information Rates for Raytheon TDMA With Optimum PLL Noise Bandwidth. Operation With Possible Phase II DSCS Phase Noise Contributors and With Soft Decision (3-bit), Rate 1/2, Constraint Length 7, Viterbi Decoding at $BER = 10^{-5}$ . . . . .	S-8
S-4	Phase Noise Specification Bands Assuming Worst Case, $f^{-3}$ , Phase Noise Characteristics . . . . .	S-10
S-5	Equivalent Power Loss and Corresponding Phase Noise Variances Based on Conservative $f^{-3}$ Phase Noise Characteristic Design and Gaussian Loss Approximation . . . . .	S-11
S-6	Proposed Specification on Spectral Purity for the Follow-On AN MSC-60 (HT) . . . . .	S-13
S-7	Proposed Specification on Spectral Purity for the AN MSC-46 "Upgrade" Terminal . . . . .	S-14
3-1	Optimum Distribution of Carrier Reference Phase Error Variance . . . . .	3-16
6-1	Algorithm for Generating Frequency Specification Bands $\{f_0, R_s\}$ $\{R_s = \text{PSK symbol rate}\}$ . . . . .	6-5
A-1	Performance Comparison of Decision-Feedback and Power Loop Implementations for M-ary PSK Demodulation . . . . .	A-2
D-1	BPSK Decision Feedback With HT-MT Mod Phase Noise (2 Terminals) . . . . .	D-1
D-2	QPSK Decision Feedback With HT-MT Phase Noise (2 Terminals) . . . . .	D-2
D-3	BPSK Power Loop With HT-MT Mod Phase Noise (2 Terminals) . . . . .	D-3

LIST OF TABLES (Continued)

Table

D-4	QPSK Power Loop With HT-MT Mod Phase Noise (2 Terminals) . . . . .	D-4
D-5	BPSK Decision Feedback With HT-MT Mod Phase Noise (3 Terminals) . . . . .	D-5
D-6	QPSK Decision Feedback With HT-MT Mod Phase Noise (3 Terminals) . . . . .	D-6
D-7	BPSK Power Loop With HT-MT Mod Phase Noise (3 Terminals) . . . . .	D-7
D-8	QPSK Power Loop With HT-MT Mod Phase Noise (3 Terminals) . . . . .	D-8
D-9	Demodulation Performance - BPSK, Power Loop, "Cesium II" Phase Noise (2 Terminals) . . . . .	D-9
D-10	Demodulation Performance - QPSK, Power Loop, "Cesium II" Phase Noise (2 Terminals) . . . . .	D-10
D-11	Demodulation Performance - QPSK, Decision Feedback, "Cesium II" Phase Noise (2 Terminals) . . . . .	D-11
D-12	Demodulation Performance - BPSK, Power Loop, "Cesium II" Phase Noise (2 Terminals and 1 Equivalent Satellite) . . . . .	D-12
D-13	Demodulation Performance - QPSK, Power Loop, "Cesium II" Phase Noise (2 Terminals and 1 Equivalent Satellite) . . . . .	D-13
D-14	Demodulation Performance - QPSK, Decision Feedback, "Cesium II" Phase Noise (2 Terminals and 1 Equivalent Satellite) . . . . .	D-14
D-15	Demodulation Performance - BPSK, Power Loop, "Crystal II" Phase Noise (2 Terminals and 1 Equivalent Satellite) . . . . .	D-15
D-16	Demodulation Performance - QPSK, Power Loop, "Crystal II" Phase Noise (2 Terminals and 1 Equivalent Satellite) . . . . .	D-16
D-17	Demodulation Performance - QPSK, Decision Feedback, "Crystal II" Phase Noise (2 Terminals and 1 Equivalent Satellite) . . . . .	D-17
D-18	Demodulation Performance - Radiation Inc. BPSK With Modified HT-MT Phase Noise (2 Terminals) . . . . .	D-18
D-19	Demodulation Performance - Radiation Inc. BPSK With Modified HT-MT Phase Noise (2 Terminals + 1 Equivalent Satellite) . . . . .	D-19

## LIST OF TABLES (Continued)

### Table

D-20	Demodulation Performance - Radiation Inc. BPSK With "Crystal II" Phase Noise (2 Terminals) . . . . .	D-20
D-21	Demodulation Performance - Radiation Inc. BPSK With "Cesium II" Phase Noise (2 Terminals) . . . . .	D-21
D-22	Demodulation Performance - Radiation Inc. BPSK With "Crystal II" Phase Noise (2 Terminals and 1 Equivalent Satellite) . . . . .	D-22
D-23	Demodulation Performance - Radiation Inc. BPSK With "Cesium II" Phase Noise (2 Terminals and 1 Equivalent Satellite) . . . . .	D-23
D-24	Demodulation Performance - Radiation Inc. BPSK With "Cesium II" Phase Noise (2 Terminals and 1 Equivalent Satellite) . . . . .	D-24
D-25	Demodulation Performance - Raytheon Inc. BPSK TDMA With HT-MT Mod Phase Noise (2 Terminals) . . . . .	D-25
D-26	Demodulation Performance - Raytheon Inc. QPSK TDMA With HT-MT Mod Phase Noise (2 Terminals) . . . . .	D-26
D-27	Demodulation Performance - Raytheon Inc. BPSK TDMA With "Cesium II" Phase Noise (2 Terminals) . . . . .	D-27
D-28	Demodulation Performance - Raytheon Inc. BPSK TDMA With "Cesium II" Phase Noise (2 Terminals and 1 Equivalent Satellite) . . . . .	D-28
D-29	Demodulation Performance - Raytheon Inc. QPSK TDMA With "Cesium II" Phase Noise (2 Terminals) . . . . .	D-29
D-30	Demodulation Performance - Raytheon Inc. QPSK TDMA With "Cesium II" Phase Noise (2 Terminals and 1 Equivalent Satellite) . . . . .	D-30
D-31	Demodulation Performance - Raytheon Inc. BPSK TDMA With "Crystal II" Phase Noise (2 Terminals) . . . . .	D-31
D-32	Demodulation Performance - Raytheon Inc. BPSK TDMA With "Crystal II" Phase Noise (2 Terminals and 1 Equivalent Satellite) . . . . .	D-32
D-33	Demodulation Performance - Raytheon Inc. QPSK TDMA With "Crystal II" Phase Noise (2 Terminals) . . . . .	D-33
D-34	Demodulation Performance - Raytheon Inc. QPSK TDMA With "Crystal II" Phase Noise (2 Terminals and 1 Equivalent Satellite) . . . . .	D-34
D-35	Demodulation Performance - Raytheon Inc. BPSK TDMA With HT-MT Modulation Phase Noise (2 Terminals) . . . . .	D-35

LIST OF TABLES (Continued)

Table

D-36	Demodulation Performance - Raytheon Inc. BPSK TDMA With HT-MT Modulation Phase Noise (2 Terminals and 1 Equivalent Satellite) . . . . .	D-36
D-37	Demodulation Performance - Raytheon Inc. QPSK TDMA With HT-MT Modulation Phase Noise (2 Terminals) . . . . .	D-37
D-38	Demodulation Performance - Raytheon Inc. QPSK TDMA With HT-MT Modulation Phase Noise (2 Terminals and 1 Equivalent Satellite) . . . . .	D-38
D-39	Demodulation Performance - Raytheon Inc. BPSK TDMA With "Cesium II" Phase Noise (2 Terminals) . . . . .	D-39
D-40	Demodulation Performance - Raytheon Inc. BPSK TDMA With "Cesium II" Phase Noise (2 Terminals and 1 Equivalent Satellite) . . . . .	D-40
D-41	Demodulation Performance - Raytheon Inc. QPSK TDMA With "Cesium II" Phase Noise (2 Terminals) . . . . .	D-41
D-42	Demodulation Performance - Raytheon Inc. QPSK TDMA With "Cesium II" Phase Noise (2 Terminals and 1 Equivalent Satellite) . . . . .	D-42
D-43	Demodulation Performance - Raytheon Inc. BPSK TDMA With "Crystal II" Phase Noise (2 Terminals) . . . . .	D-43
D-44	Demodulation Performance - Raytheon Inc. BPSK TDMA With "Crystal II" Phase Noise (2 Terminals and 1 Equivalent Satellite) . . . . .	D-44
D-45	Demodulation Performance - Raytheon Inc. QPSK TDMA With "Crystal II" Phase Noise (2 Terminals) . . . . .	D-45
D-46	Demodulation Performance - Raytheon Inc. QPSK TDMA With "Crystal II" Phase Noise (2 Terminals and 1 Equivalent Satellite) . . . . .	D-46

## SUMMARY

Future communication systems such as the Phase II DSCS will use coherent phase-shift keyed (PSK) modulation with forward error control (FEC) coding and will be transmitted at X-band frequencies. Since coherent PSK systems using FEC are especially sensitive to signal spectral purity and since spectral purity is directly proportional to the transmission frequency, very careful system designs must be used in X-band transmission systems. These systems will require various frequency generation equipment such as atomic standards for long-term frequency accuracy, and various combinations of crystal oscillators, frequency synthesizers and frequency multipliers which are necessary to provide flexible transmit and receive frequency assignments.

The ultimate objective of this effort is to provide guidance on spectral purity requirements for the Phase II DSCS terminals and associated frequency generation equipment.

In this report we have limited ourselves to the following immediate objectives:

- Evaluate expected phase noise performance of various combinations of existing modulation and terminal subsystems operating in the Phase II DSCS.
- Use this insight to generate methods for specification of allowable phase noise as a function of desired system performance.

To reach these objectives it has been necessary to evaluate effects of phase noise upon (partially) coherent PSK demodulation performance and thereby gain insight into the dynamics of system performance. It is known that demodulation of coherent PSK signals requires knowledge of the phase of the original (unmodulated) carrier waveform. Estimates of carrier phase may be derived from the received signal by the well known techniques of phase-locked loop (PLL) theory. Here it is shown that optimum demodulation performance (i. e.,

minimum bit error rate (BER)) in the presence of phase noise and thermal noise is obtained by optimizing the bandwidth of the carrier tracking PLL. Using this technique, optimum demodulation performance for BPSK and QPSK systems is derived for terminals conforming to phase noise specifications designated "modified HT-MT" which is a modified version of an early DSCS HT-MT earth terminal incidental FM specification (SCA-2080A; see also Figure 4-1 which appears at the end of this summary). Results obtained also include the effects of rate 1/2, constraint length 7, convolutional encoding with 3 bit, soft decision Viterbi decoding.\* Two other phase noise curves have also been synthesized, designated cesium II\*\* and crystal II\*\* (Figure 4-5), which are now considered to be realistic estimates of phase noise expected for terminal of the Phase II DSCS. Using these three types of terminal phase noise sources and convolutional encoding; an allowable interval of signaling rates are determined for BPSK and QPSK modulation systems when demodulation losses due to imperfect carrier tracking are limited to 0.2 dB. Results are summarized in Table S-1 (found at end of summary).

#### Subsystem Performance Evaluations

1. Using the "modified HT-MT" phase noise specification, Table S-1 shows that inadequate phase noise performance leads to both minimum and maximum signal rates even with the use of optimized phase estimators when using convolutional encoding and Viterbi decoding. However, with the most recent estimates of phase noise spectral densities (cesium II and crystal II) expected for the Phase II DSCS terminals, the upper bound on signaling rate is far greater than the data rates of interest.

---

\*See note 1.

\*\*A roman numeral II has been used here to help differentiate current data from that which appeared in a prior memorandum.

System performance has also been determined for three modems being designed for the Phase II DSCS using frequency converters conforming to the modified version of the incidental FM noise specification SCA-2080A (Figure 4-1), and the synthesized phase noise data of Section 4 (Figure 4-7).

2. Expected performance of the Radiation, Inc. BPSK modem (MI-921G) is summarized in Table S-2.
3. Results for the Raytheon, Inc. TDMA are summarized in Tables S-3(a) and (b) when the modem is operated with a 100 Hz one-sided PLL noise bandwidth and an optimized bandwidth, respectively. Dramatic improvements in system performance are noted here for a small increase in system complexity caused by the use of a variable bandwidth PLL.
4. Results for the Magnavox Research Laboratory, Inc. AN/USC-28 spread-spectrum modem are presented in detail in. <sup>[1]</sup> In the cited reference it is shown that the most critical performance requirements on carrier phase estimation performance occurred at the lowest information rates, where the phase noise of an improved AN ASC-18 terminal would be similar to that of the synthesized phase noise (cesium II of Figure 4-7) expected for the HT-MT (AN/MSC-60) and the upgraded MSC-46 terminals. Therefore, at low data rates, demodulation performance for the USC-28 operating with the above DSCS terminals will be similar to that given in <sup>[1]</sup> when this modem is operated with the improved AN, ASC-18 terminal. At high frequency offsets from the carrier frequency, the synthesized phase noise curve (cesium II of Figure 4-7) will be better than that of the improved AN ASC-18; therefore at high data rates performance of the USC-28 with the HT-MT or upgraded MSC-46 will be better than that shown in. <sup>[1]</sup>

### Phase Noise Specification

A method of generating specification on oscillator phase noise has been devised based on phase noise power in a band specification. Analysis reveals that the shape of the oscillator phase noise spectral density is of secondary importance to the area under the phase noise spectral density curve in the region between the tracking filter 3-dB bandwidth (i.e., for a PLL this quantity is  $f_n$ ) and the 3-dB bandwidth of the demodulator filter (for a matched filter this occurs at 1/2 the PSK symbol rate).

The design specifications on phase noise power in frequency bands as a function of demodulation losses for systems with rate 1/2, constraint length 7, convolutional encoding and 3 bit soft decision Viterbi decoding are summarized in Tables S-4, S-5 and Figure S-1.

Based on this method results are presented in Tables S-6 and S-7 which are the desired Phase II DSCS terminal phase noise specifications for the AN MSC-60(HT) "Follow-on" and the AN/MSC-46 "Upgrade," respectively.

Finally, it should be pointed out that recent computer simulations on the performance of rate 1/2, constraint length 7, convolutional encoding with 3 bit soft decision Viterbi decoding performed at CSC indicates that the theoretical loss versus phase error variance functional derived in [2] and used in this report, may not be as severe as indicated. However, all of the phase noise specifications derived here are not unreasonable since they can be satisfied with state of the art techniques.

Table S-1. Allowable\* Information Rates for Suppressed Carrier BPSK and QPSK Signaling With Several Possible Phase Noise Sources in the DSCS and With Soft Decision (3-bit), Rate 1/2, Constraint Length 7 Viterbi Decoding at BER  $\leq 10^{-5}$

		Phase Noise Type **			
Information Rate bps	Mod. HT-MT Phase Noise Specifications	Synthesized Data			
		"Cesium"	"Crystal"		
Minimum	450	< 75	< 75		
	$> 39 \times 10^6$	$> 39 \times 10^6$	$> 39 \times 10^6$		
Maximum	300	< 75	< 75		
	$> 39 \times 10^6$	$> 39 \times 10^6$	$> 39 \times 10^6$		
Minimum	300	< 75	< 75		
	$> 39 \times 10^6$	$> 39 \times 10^6$	$> 39 \times 10^6$		
Maximum	116 $\times 10^3$	$61.4 \times 10^3$	$< 4.8 \times 10^3$		
	$20.6 \times 10^6$	$> 39 \times 10^6$	$> 39 \times 10^6$		
Minimum	93.5 $\times 10^3$	$30.7 \times 10^3$	$< 4.8 \times 10^3$		
	$20.6 \times 10^6$	$> 39 \times 10^6$	$> 39 \times 10^6$		
QPSK					
Minimum	93.5 $\times 10^3$	$30.7 \times 10^3$	$< 4.8 \times 10^3$		
	$20.6 \times 10^6$	$> 39 \times 10^6$	$> 39 \times 10^6$		
BPSK					
Minimum	300	< 75	< 75		
	$> 39 \times 10^6$	$> 39 \times 10^6$	$> 39 \times 10^6$		
Maximum	116 $\times 10^3$	$61.4 \times 10^3$	$< 4.8 \times 10^3$		
	$20.6 \times 10^6$	$> 39 \times 10^6$	$> 39 \times 10^6$		

\*Acceptable loss  $\leq .2$  dB with bandwidth optimized carrier tracking PLI.

\*\* Phase Noise contribution from 2 terminals and 1 equivalent satellite

Table S-2. Allowable\* Information Rates for Radiation BPSK (Power Loop) Modem With Several Possible Phase Noise Sources in the DSCS and With Soft Decision (3-bit), Rate 1/2 Constraint Length 7 Viterbi Decoding at BER  $10^{-5}$

Information Rate bps	Phase Noise Type**
Minimum	$2.8 \times 10^3$
Maximum	$> 39 \times 10^6$

\*Acceptable Loss  $\leq 0.2$  dB

\*\*Phase Noise Contribution from 2 Terminals and 1 Equivalent Satellite

Table S-3(a). Allowable\* Information Rates for Raytheon TDMA With PLL Noise Bandwidth of 100 Hz, Operation With Possible Phase II DSCS Noise Contributors and With Soft Decision (3-bit), Rate 1/2, Constraint Length 7, Viterbi Decoding at  $BER = 10^{-5}$

		Phase Noise Type ***		
		Mod. HT-MT Specification	"Cesium II"	Synthesized "Crystal II"
Information Rate Mbps				
BPSK	Minimum	1.2	1.2	1.2
	Maximum	> 38	> 39	> 39
QPSK	Minimum	**	~ 78	39
	Maximum	**	~ 78	> 78

\*Acceptable Demodulation loss < 0.2 dB

\*\*Losses always > 0.2 dB

\*\*\*Terminal phase contribution from 2 terminals and 1 equivalent satellite.

Table S-3(b). Allowable\* Information Rates for Raytheon TDMA With Optimum PLI, Noise Bandwidth, Operation With Possible Phase II DSCS Phase Noise Contributors and With Soft Decision (3-bit), Rate 1/2, Constraint Length 7, Viterbi Decoding at BER  $10^{-5}$

		Phase Noise Type**		
		Mod. HT-MT Specification	"Cesium II"	"Crystal II"
Information Rate Mbps				
BPSK	Minimum	0.307	< 0.15	< 0.07
	Maximum	> 39	> 39	> 78
QPSK	Minimum	2.4	-78	1.2
	Maximum	> 39	-78	> 78

\*Acceptable Demodulation Loss < 0.2 dB

\*\*Terminal phase contributions from 2 terminals and 1 equivalent satellite.

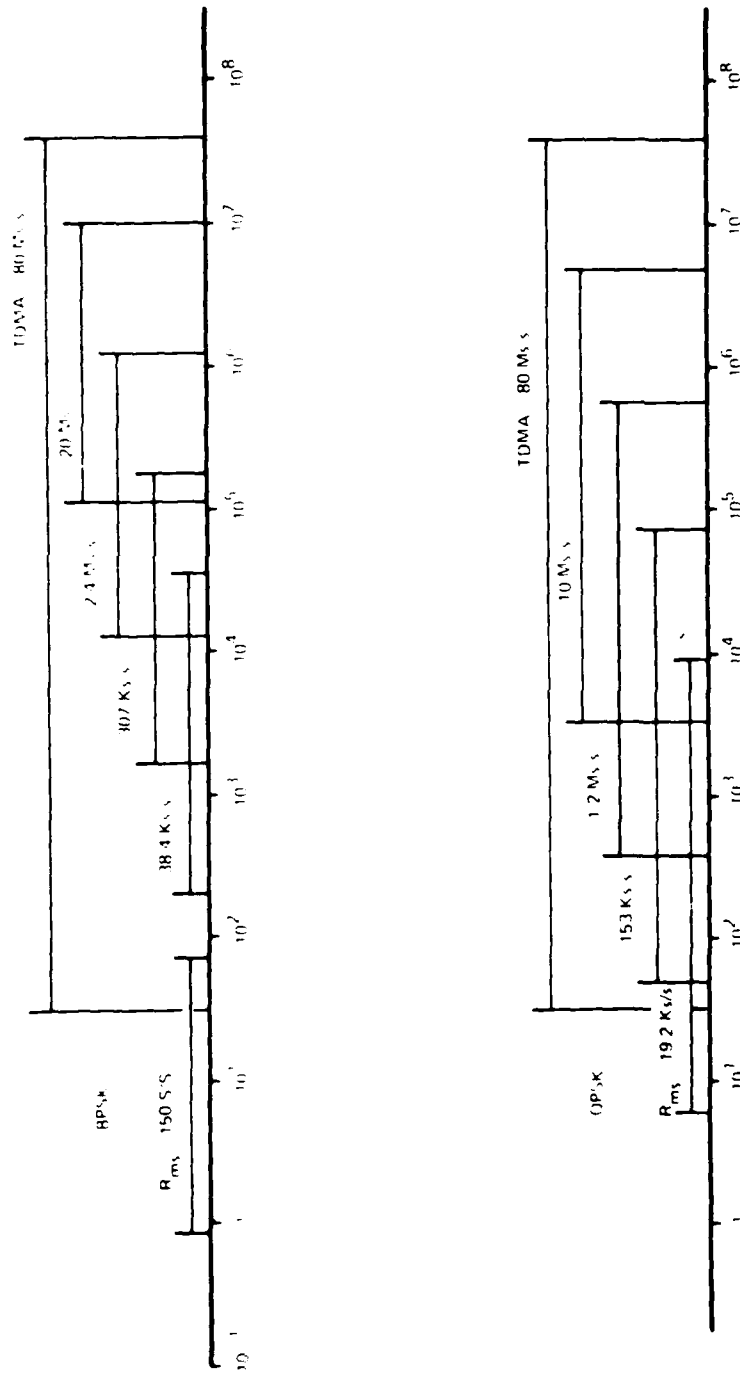
Table S-1. Phase Noise Specification Bands Assuming Worst Case,  $f^{-3}$ , Phase Noise Characteristics

Type of PSK Modulation	Data Bit Rate (R <sub>bit</sub> )	PSK Symbol Rate (R <sub>ms</sub> )	Phase Noise Specification Bands	
			D/F Loop Implementation	Power Loop (MF) Implementation
BPSK M = 2	75 b/s	150 s/s	0.82 Hz - 7.5 Hz	0.68 Hz - 7.5 Hz
	19.2 kb/s	38.4 ks/s	0.2 kHz - 19.2 kHz	0.17 kHz - 19.2 kHz
	15.3 kb/s	30.7 ks/s	1.7 kHz - 153 kHz	1.4 kHz - 153 kHz
	1.2 Mb/s	2.4 Ms/s	13 kHz - 1.2 MHz	11 kHz - 1.2 MHz
	10 Mb/s	20 Ms/s	0.11 MHz - 10 MHz	91 kHz - 10 MHz
QPSK M = 4	19.2 kb/s	19.2 ks/s	6.7 Hz - 9.6 kHz	3.34 Hz - 9.6 kHz
	15.3 kb/s	15.3 ks/s	5.3 Hz - 76 kHz	26 Hz - 76 kHz
	1.2 Mb/s	1.2 Ms/s	0.41 kHz - 0.6 MHz	0.21 kHz - 0.6 MHz
	10 Mb/s	10 Ms/s	3.5 kHz - 5 MHz	1.7 kHz - 5 MHz

Specification Band for TDMA Operation: 23 Hz to 40 MHz

Table S-5. Equivalent Power Loss and Corresponding Phase Noise Variances  
Based on Conservative  $f=3$  Phase Noise Characteristic Design and Gaussian Loss Approximation

Type of Modulation ( $M$ )	Equivalent Power Loss ( $L_{tot}$ dB)	Total Amount of Phase Variance ( $\sigma_{tot}^2$ dB)	Loop Variance ( $\sigma_{th}^2$ dB)	Phase Error Variance due to Phase Noise	
				1 of 2 Terminals (dB)	1 of 3 Terminals (dB)
BPSK $M = 2$	0.1	-18.0	-19.8	-25.8	-27.5
	0.2	-15.0	-16.8	-22.8	-24.5
	0.3	-13.3	-15.1	-21.1	-22.8
	0.4	-12.7	-14.5	-20.5	-22.2
QPSK $M = 4$	0.1	-31.0	-32.8	-38.8	-40.5
	0.2	-28.0	-29.8	-35.8	-37.5
	0.3	-26.0	-27.8	-33.8	-35.5
	0.4	-25.0	-26.8	-32.8	-34.5
	0.5	-24.0	-25.8	-31.8	-33.5



S-11

Figure S-1. Phase Noise Specification Bands ( $\sigma_{\text{th}}^2$  = -17 dB for BPSK and  $\sigma_{\text{th}}^2$  = -30 dB for QPSK; DF Loop implementation)

Table S-6. Proposed Specification on Spectral Purity  
for the Follow-on AN/MSC-60 (HT)

1.0 Spectral Purity

The total spurious content added to any transmitted or received carrier, including phase noise and discrete spurious signals, shall not exceed conditions specified in the following paragraphs.

1.1 Spectral Purity for BPSK-QPSK

- a. Total spurious content from both sides of the carrier at least 25 dB below the carrier level when measured in a band 0.6 Hz to 75 Hz from the carrier frequency.
- b. Total spurious content from both sides of the carrier at least 37.5 dB below the carrier level when measured in the following frequency bands:
  - (b-1) 5 Hz to 16 kHz from the carrier frequency
  - (b-2) 20 Hz to 76 kHz from the carrier frequency
  - (b-3) 200 Hz to 0.6 MHz from the carrier frequency
  - (b-4) 1.7 kHz to 5 MHz from the carrier frequency
  - (b-5) 7 kHz to 20 MHz from the carrier frequency

1.2 Spectral Purity for FDM FM

Total spurious content from both sides of the carrier measured in any 3 kHz bandwidth shall be below the carrier level as follows:

- a. 57 dB minimum from 12 kHz to 20 kHz
- b. 62 dB minimum from 20 kHz to 30 kHz
- c. 65 dB minimum from 30 kHz to 300 kHz

1.3 Spectral Purity for Burst Coherent TDMA

Total spurious content from both sides of the carrier shall be at least 37.5 dB below the carrier level when measured in a band 23 Hz - 40 MHz from the carrier frequency.

Table S-7. Proposed Specification\* on Spectral Purity  
for the AN/MSC-46 "Upgrade" Terminal

1.0 Spectral Purity

The total spurious content added to any transmitted or received carrier, including phase noise and discrete spurious signals, shall not exceed conditions specified in the following paragraphs.

1.0 Spectral Purity for BPSK-QPSK

- a. Total spurious content from both sides of the carrier at least 37 dB below the carrier level when measured in the following frequency bands:
  - (a-1) 0.6 Hz to 75 Hz from the carrier frequency
  - (a-2) 1.8 Hz to 200 Hz from the carrier frequency
- b. Total spurious content from both sides of the carrier at least 37.5 dB below the carrier level when measured in the following frequency bands:
  - (b-1) 5 Hz to 16 kHz from the carrier frequency
  - (b-2) 20 Hz to 76 kHz from the carrier frequency
  - (b-3) 200 Hz to 0.6 MHz from the carrier frequency
  - (b-4) 1.7 kHz to 5 MHz from the carrier frequency
  - (b-5) 7 kHz to 20 MHz from the carrier frequency

1.2 Spectral Purity for FDM FM

Total spurious content from both sides of the carrier measured in any 3 kHz bandwidth shall be below the carrier level as follows:

Table S-7. Proposed Specification\* on Spectral Purity  
for the AN/MSC-46 "Upgrade" Terminal (Cont'd)

- a. 57 dB minimum from 12 kHz to 20 kHz
- b. 62 dB minimum from 20 kHz to 30 kHz
- c. 65 dB minimum from 30 kHz to 300 kHz

1.3 Spectral Purity for Burst Coherent TDMA

Total spurious content from both sides of the carrier shall be at least 37.5 dB below the carrier level when measured in a band 23 Hz - 40 MHz from the carrier frequency.

\*Specifications do not include effects of reference standard. Also assumes that terminal phase noise is dominated by reference at frequencies below 200 Hz.

## SECTION 1 - INTRODUCTION

The need for specifications on phase noise arise because all information conveyed in a coherent PSK signal resides in phase changes added to an unmodulated phase reference (carrier phase reference). The phase reference is, alas, always imperfect even at the transmitter since it always contains noise perturbations<sup>[3,4]</sup> characterized as phase noise for high frequency perturbations and long-term drifts for low frequency perturbations. Because the receiver has no a priori knowledge of these phase perturbations in time, the receiver has to distinguish between the PSK modulation and the phase noise. Our problem at the receiver then becomes one of estimating carrier phase perturbations in the presence of PSK modulation and additive white Gaussian noise (AWGN).<sup>[5,6]</sup>

A perfect reference is, by definition, physically unrealizable. Non-realizability occurs because the parameters which characterize the reference are not truly constant with time but have random noise perturbations superimposed. Optimum performance in PSK systems demands that we estimate phase noise fluctuations of the reference phase so that their effects can be minimized. Since all information is contained in the PSK signal phase, amplitude noise effects are only of significance when passed through devices which cause amplitude noise to be converted to phase noise.

Estimation accuracy may be characterized in the mean square error (MSE) sense by the total phase estimation error variance  $\sigma_{\text{tot}}^2$ . The total error variance is the sum of two terms: (1) a phase error variance due to the effects of thermal noise  $\sigma_{\text{th}}^2$ , and (2) a phase error variance  $\sigma_{\text{pn}}^2$  due to the inability of the carrier phase estimator to completely estimate the entire phase noise process on the received signal.

It is known that the phase error variance due to thermal noise is directly proportional to the noise bandwidth of the reference phase estimator.<sup>[5]</sup> Here we show that the error variance due to phase noise is inversely proportional to various functions of the phase estimator noise bandwidth. (These inverse functions are directly related to the phase noise spectrum present on the reference signal.) Thus, a set of opposing constraints is given for minimizing phase error variance resulting in an optimum phase estimator noise bandwidth (optimum in the sense that it provides the minimum mean square error (MMSE)).

In this report considerable effort is directed towards derivation of this optimum bandwidth, and thus the MMSE for systems using second order PLLs of the power variety (squaring, quadrupling, etc.) or decision-directed feedback type, or pure second order PLLs when an auxiliary unmodulated carrier sinusoid is utilized. Since the order of an optimal linear phase estimator is a function of the order of the oscillator phase noise spectral density, higher order PLLs (i. e., 3rd or 4th) may be desirable in certain instances, however, the analysis could easily be extended with some additional algebraic complexity.

In the preceding we have focused attention on the fidelity of the carrier phase estimator as expressed by its total phase error variance  $\sigma_{\text{tot}}^2$  and we have only hinted that this parameter is directly related to a demodulation performance in a coherent PSK system. In the literature several analyses are available,<sup>[2, 7, 8]</sup> which show demodulation loss from ideal performance in a coherent PSK system when using a noisy phase reference. These analyses account only for thermal noise corruption of the carrier phase estimator. Here the loss functionals derived in these references are extended to include the additional degradations caused by incomplete estimation of the phase noise process on the received signal.

Furthermore, future communication systems (e. g., Phase II DSCS) will be increasingly sensitive to errors in carrier phase estimation due to the use of forward error control coding (FEC). Because of the increased sensitivity

of PSK systems with FEC, it is of utmost importance to: (1) Obtain estimates of all phase noise added to any coherent PSK transmission system, (2) Calculate the exact performance (expressed in the sense of mean square error (MSE) by the phase estimation error variance  $\sigma^2$ ) of various carrier phase estimation techniques in the presence of thermal noise (AWGN) and phase noise, (3) Apply the phase estimation error variance to various decoding loss functions [2, 7, 8] and thereby obtain demodulation loss curves, and finally (4) Derive specifications on adequate phase noise performance for transmission and receive facilities (of the Phase II DSCS).

The use of FEC in suppressed carrier systems allows signaling at extremely low energy per bit to noise density ratios, thus carrier phase estimates must have additional signal processing gain to provide immunity against a relatively large amount of AWGN. This leads to requirements for extremely small bandwidths for carrier phase estimation and therefore places additional restrictions on the allowable level of phase noise.

The problem of estimating coherent PSK system performance in the presence of thermal noise and phase noise may be formulated more precisely by the following mathematical representation. A typical receiver signal in a suppressed carrier coherent PSK modulation system is:

$$r(t) = V(t) + n(t)$$

where

$$V(t) = \left| V_0 + \epsilon(t) \right| \sin \left[ 2\pi\gamma_0 t + \frac{2\pi k}{m} + \delta\phi(t) + \psi \right]$$

and

$n(t)$  = an additive white gaussian noise (AWGN)

$V_0$  = the nominal amplitude

$\gamma_0$  = the nominal frequency

$m$  = the maximum number of phase positions (e.g.,  $m = 4$  QPSK)  
 $k$  =  $0, 1, \dots, m-1$  determines the modulation angle in the interval  $[t, t+T]$   
 $\psi$  = an arbitrary but fixed phase offset  
 $\epsilon(t)$  = an amplitude noise fluctuation  
 $\delta\phi(t)$  = the phase noise fluctuation including all amplitude fluctuations  
 which have been passed through AM to PM conversion devices.

Assuming that  $\frac{\epsilon(t)}{V_0} \ll 1$ , amplitude fluctuations can be ignored. Since the constant angle  $\psi$  is either known or can be estimated, its effects may be ignored. If the estimate of the phase noise term  $\hat{\delta\phi}(t)$  can be made accurately {i.e.,  $|\hat{\delta\phi}(t) - \delta\phi(t)| \ll \delta\phi(t)$ }, then the effects of phase noise can be minimized. Of course carrier phase estimates  $\hat{\delta\phi}(t)$  will be less than perfect since they must be made in the presence of AWGN and, in the case of suppressed carrier system, simultaneously in the presence of phase modulation. Errors in carrier phase estimates which are induced by AWGN can be minimized by using an estimator with long averaging time (small bandwidth). However, if the phase fluctuations  $\delta\phi(t)$  contain high frequency spectral components with high energy content, a phase estimator with short averaging time (large bandwidth) is required leading to a conflicting set of constraints and an optimum averaging time (bandwidth) for optimum performance.

## SECTION 2 - SYSTEM DEFINITIONS, PHASE NOISE TERMINOLOGY AND THE IMPACT OF ANY COLOR PHASE NOISE ON PARTIALLY COHERENT PSK SYSTEM

### 2.1 SYSTEM DEFINITIONS

In a complex satellite communication system such as the DSCS which uses convolutional (rate 1/2) and differential encoding together with M-ary ( $M = 2, 4$ ) PSK modulation, a common source of confusion is the terminology used by different people to describe the same phenomenon. One designer's bits become another designer's symbols especially for people concerned with coding and modulation. Because the arguments for naming these items are extremely convincing, depending upon the designer's area of expertise, the approach used here will be to define symbols via a system diagram and let the reader change the names to suit his requirements.

Figure 2-1 depicts the general system diagram. Since the main item of interest here is the modulation-demodulation system, the term modulation bits at rate  $R_{mb}$  is used to describe the input transition rate to the M-ary modulator which then produces modulation symbols at rate  $R_{ms}$ . Henceforth, unless otherwise stated, all references to symbols or symbol rate refer to modulation symbols and all references to bits refer to modulation bits as described above.

### 2.2 PHASE NOISE TERMINOLOGY

Another source of confusion may arise from the specification of oscillator phase noise spectral density. In this memorandum the definition which has been used is a 1-sided spectrum at low pass (at baseband) as defined by the symbol  $S_{\delta\phi}(f)$  and in Figure 2-2(a). Other possible representations of phase noise spectral density are given by Figures 2-2(b, c, d). Many hardware developers choose to display phase noise spectral density by plotting only the upper sideband of Figure 2-2(d). The ordinate is then referred to as single-side band noise to carrier ratio and sometimes denoted as  $L(f)$ . No problems arise as long as it is clear which spectral density representation is being used. [3], [4]

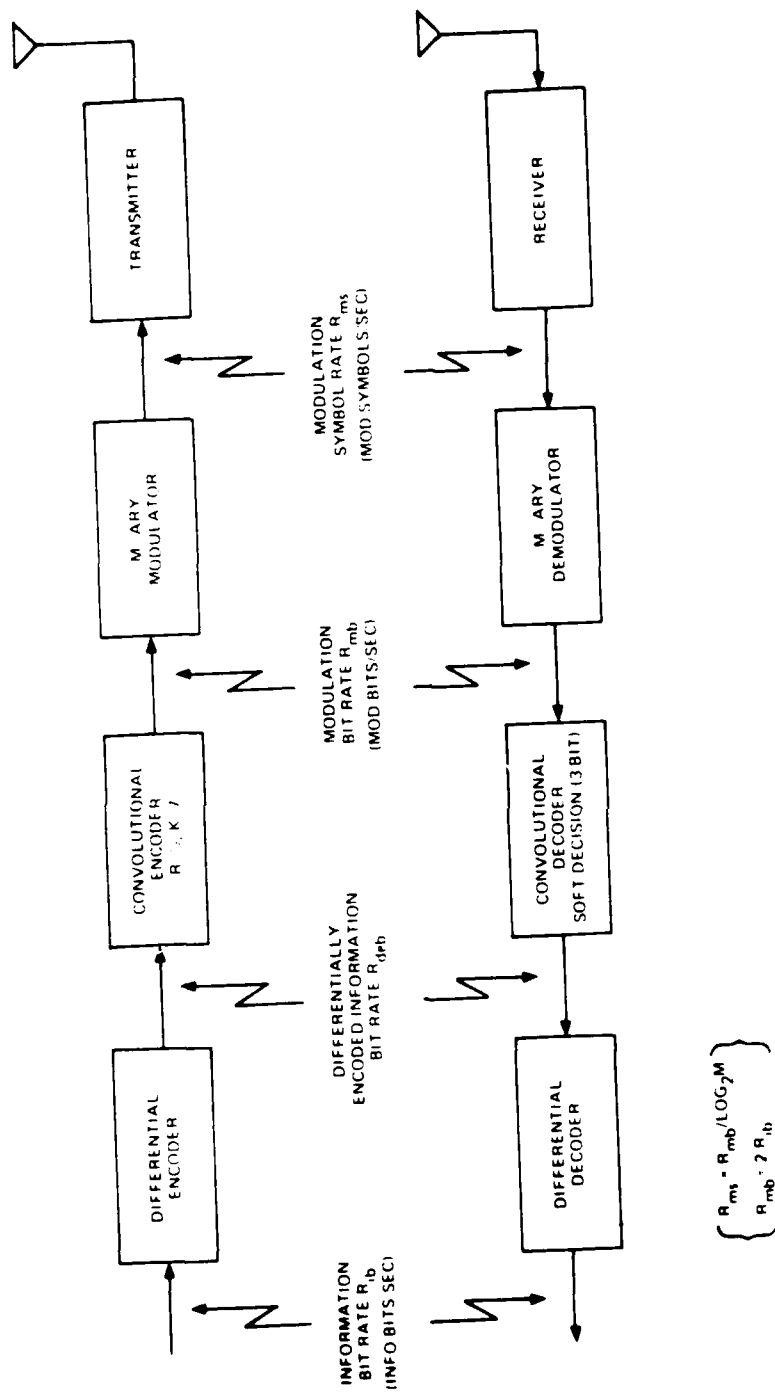


Figure 2-1. M-ary PSK System

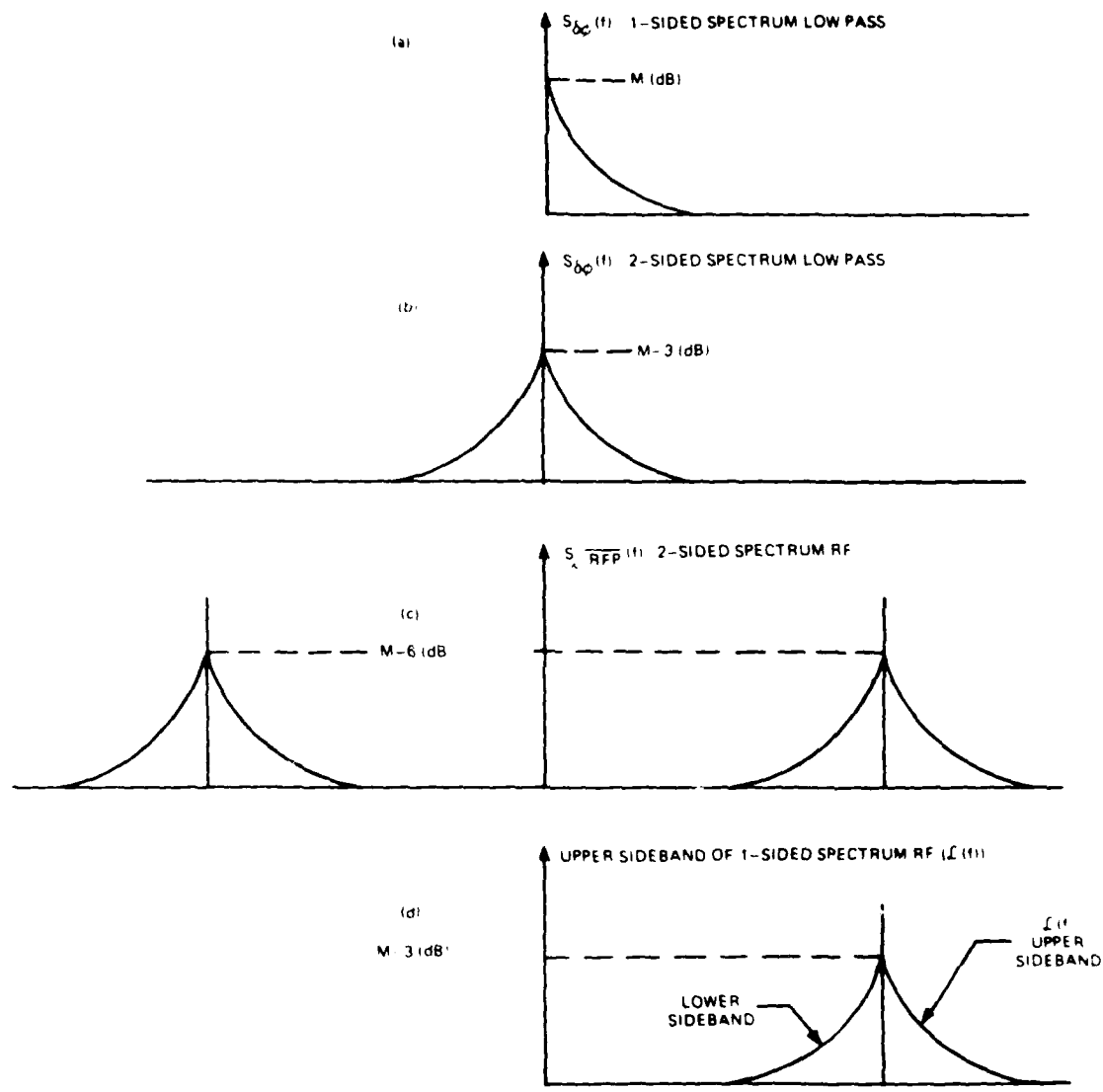


Figure 2-2. Phase Noise Density; Definitions Adopted in This Report

### 2.3 GENERAL IMPACT OF ANY COLOR PHASE NOISE ON PARTIALLY COHERENT PSK SYSTEMS

The introduction of this report has indicated that a demodulation performance tradeoff exists between a design which efficiently tracks out phase noise perturbations present on the transmitted PSK signal and a design that excludes as much thermal noise as possible. A common misunderstanding in the design and description of coherent PSK communications is that the effects of a white oscillator phase noise process on the transmitted signal may somehow be treated as an equivalent additive thermal noise at the receiver front end. The distinction between these two phenomena may be seen from the following arguments. Phase noise results from multiplicative processes which cause a pure rotation of the phase reference relative to the PSK decision region structure. Since a rotation affects decisions on any transmitted PSK symbol in precisely the same manner, i.e., independent of the symbol phase, it is possible by estimating the angle of rotation of the phase reference to compensate for phase noise effects. The phase component caused by the additive, thermal, noise affects the signal in a different manner. That is, a particular thermal noise waveform will cause a phase rotation the magnitude and direction of which is dependent upon the received PSK symbol phase. Therefore, phase rotation of the reference caused by thermal noise cannot be removed in a way that is independent of the receiver symbol sequence as in the case for carrier phase noise.

Since the ultimate aim is to coherently detect the transmitted PSK modulation angle (data symbols) with as few errors as possible, it is desirable to maximize tracking of the carrier phase noise process (including the flat (white)\* portion of the spectrum) simultaneously excluding as much additive thermal noise as possible.

---

\*Of course if the entire oscillator phase noise spectrum is flat (white) and high level, the discussion of coherent system is absurd.

It is shown in Section 3 and in [6] that the demodulation process usually involves a matched filter or integrate-and-dump filter which suppresses the effects of errors in the carrier phase reference at frequencies beyond one-half of the PSK symbol rate. Thus, the most desirable carrier phase tracking system should track as much of the phase noise process (including the flat portion of the phase noise spectral density) as possible, within a bandwidth equal to one-half of the symbol rate, simultaneously excluding as much additive thermal noise as possible.

It is tacitly assumed that when designing a coherent PSK system the design is ultimately limited by thermal noise effects on the phase reference rather than by phase noise. That is, by increasing the carrier tracking system bandwidth, in an attempt to track all the desired carrier phase information, additional additive thermal noise enters the system degrading the coherence of the carrier phase reference and ultimately increasing the total demodulation loss. Thus, a trade-off in carrier tracking bandwidth may be established which minimizes the total demodulation loss due to the untracked portion of carrier phase noise and that due to thermal noise corruption of the carrier phase reference. The preceding results are derived analytically in Section 3.

### SECTION 3 - EFFECTS OF ADDITIVE GAUSSIAN NOISE AND PHASE NOISE UPON COHERENT PSK DEMODULATION

#### 3.1 ANALYTICAL STUDIES AND TRADEOFF ANALYSES

Multiplicative noise on the received signal and its residual effects upon (partially) Coherent PSK signal demodulation are investigated in this section. The multiplicative noise or phase noise originates from frequency converters (mixers) in which the signal is multiplied with another signal containing either phase noise or additive noise which causes phase noise as the signals are multiplied. Another source is AM/PM conversion that is produced by *certain system components*, e.g., TWTs. The phase noise process generally includes both random and deterministic components (spurious signals).

The statistical information about phase noise is generally limited to the second order statistics, i.e., the phase noise process is specified by its power spectral density. By using  $\delta$ -function formalism one can also include the spurious components in the density spectrum. Based on physical characteristics of signal oscillators [3] the power spectral density  $S_{\delta\phi}(f)$  of the phase noise process  $\phi(t)$  is of the form

$$S_{\delta\phi}(f) = h_0 + \frac{h_1}{f} + \frac{h_2}{f^2} + \frac{h_3}{f^3}; \text{ continuous spectrum}$$

$$+ \sum_{k=1}^N \frac{\beta_k^2}{2} \delta(f - f_k); \text{ discrete spectrum}$$

Here  $S_{\delta\phi}(f)$  is defined as the one-sided ( $f > 0$ ) spectrum that would be obtained if the oscillator output signal was coherently demodulated (translated to baseband) by a perfect reference signal. The first four terms containing values of  $\{h_k\}$  specify the continuous spectrum, while the  $\{\beta_k^2/2\}$  are the powers of spurious signals relative to the total signal power at the offset frequencies  $f_k$ .

However, in many cases the output signal from an oscillator is filtered to reduce the phase noise power thereby modifying the spectral representation.

We are not directly interested in the phase noise sources but rather the resulting phase noise (multiplicative noise) present in the received signal influencing the PSK symbol demodulation. In general, the phase noise process of the received signal will have a power spectral density with spectral components given in Equation (3-1). Therefore, the spectral density  $S_{\delta\phi}(f)$  of the phase noise process  $\phi(t)$  at the receiver input lends itself to the determination of the influence or degradation of the PSK demodulation performance since from it the phase error variance at the point of the symbol decision can be obtained. With this variance at hand we can determine the equivalent power loss caused by the phase noise in accordance with [2], [6]-[8].

First, assume that PSK demodulation is performed with a carrier reference which is not corrupted by thermal noise but does not contain information about the phase noise process on the received PSK signal. In this case the phase noise variance  $\sigma_{pn}^2$  due to phase noise at the symbol decision point is given by

$$\sigma_{pn}^2 = \int_0^{\infty} S_{\delta\phi}(f) |M(f)|^2 df \quad (3-2)$$

where  $M(f)$  is the frequency transfer function of the PSK demodulator (usually a matched filter). Equation (3-2) is an approximation that is valid when the amplitude of the phase noise process  $\phi(t)$  is small. A few simple relationships show how Equation (3-2) is derived. For an arbitrary phase angle  $\theta$  we have

$$\begin{aligned} e^{i[\theta + \phi(t)]} &= e^{i\theta} \cdot e^{i\phi(t)} \\ &\approx e^{i\theta} [1 + i\phi(t)] \end{aligned} \quad (3-3)$$

provided  $\phi(t) \ll 1$ . With the impulse responses  $m(t)$  of the filter  $M(f)$  being normalized so that  $\int m(t) dt = 1$ , i.e.,  $M(0) = 1$ , the output of the detection filter

$$\begin{aligned}
 & \int m(t - \tau) e^{i[\theta + \phi(\tau)]} d\tau \\
 & \cong e^{i\theta} [1 + i \int m(t - \tau) \phi(\tau) d\tau] \\
 & \cong \exp\{i[\theta + \int m(t - \tau) \phi(\tau) d\tau]\}
 \end{aligned} \tag{3-4}$$

since  $\phi(t) \ll 1$  also implies that  $\int m(t - \tau) \phi(\tau) d\tau \ll 1$ . This shows that the demodulation filter acts as a linear filter on the phase process  $\phi(t)$ , provided the amplitude of  $\phi(t)$  is small.

A common receiver implementation uses an integrate and dump circuit as a detection filter. The integration operation

$$\frac{1}{T_s} \int_0^{T_s} (\cdot) dt \tag{3-5}$$

over the modulation symbol period  $T_s$  corresponds to the filter characteristic

$$M(f) = \frac{\sin \pi f T_s}{\pi f T_s} \cdot e^{i\pi f T_s} \tag{3-6}$$

With this detection filter Equation (3-2) takes the form

$$\sigma_{pn}^2 = \int_0^{\infty} S_{\delta\phi}(f) \left( \frac{\sin \pi f T_s}{\pi f T_s} \right)^2 df \tag{3-7}$$

An attempt to evaluate this integral with  $S_{\delta\phi}(f)$  according to Equation 3-2-1 will yield an unbounded variance  $\sigma_{pn}^2$  unless  $h_1 = h_2 = h_3 = 0$ . Since at least one of these parameters will not vanish in a real system application, a system using a carrier reference which does not contain information about the phase noise process on the received PSK signal is impossible. It is obvious, however, that noise would have no effect if the carrier reference signal tracked the phase noise perfectly to remove its influence.

A phase-locked loop implementation of the carrier reference signal will track slow changes in the received carrier phase and will therefore at least

partially track the phase noise process. Increased tracking ability is obtained by increasing the phase-locked loop bandwidth. However, this will make the phase estimate more noisy due to less filtering of the additive channel noise. Therefore, a trade-off between phase noise tracking and filtering of additive channel noise is required to determine the optimum phase-locked loop bandwidth that will yield minimum performance degradation in the PSK demodulation process. To perform this trade-off analysis we have to consider the particular frequency characteristic of the phase-locked loop as well as its resulting noise bandwidth,  $B_o$ .

Now given the closed-loop phase-locked loop transfer function  $H(f)$ , the spectral densities at various points of the phase-locked loop and demodulator circuits can be determined (see Figure 3-1). The spectrum associated with the input phase noise process at various points is obtained by multiplying  $S_{\delta\phi}(t)$  by the absolute square of the frequency transfer function to the specific point of interest. In particular, the phase noise spectrum at the input to the symbol demodulator filter is given by

$$S_{\delta\phi}(f) |1 - H(f)|^2 \quad (3-8)$$

The additive Gaussian noise will also cause phase noise via the phase-locked loop. Its spectrum at the demodulator filter input is<sup>[3]</sup>

$$\frac{N_o}{E_s R_s} |H(f)|^2 \quad (f > 0) \quad (3-9)$$

where  $E_s R_s$  equals the received carrier power. Thus at the mixer output before the demodulation filter we have the total phase noise density

$$S_{\delta\phi}(f) |1 - H(f)|^2 + \frac{N_o}{E_s R_s} |H(f)|^2 \quad (3-10)$$

This implies that the total phase noise variance at the output of the demodulator

partially track the phase noise process. Increased tracking ability is obtained by increasing the phase-locked loop bandwidth. However, this will make the phase estimate more noisy due to less filtering of the additive channel noise. Therefore, a trade-off between phase noise tracking and filtering of additive channel noise is required to determine the optimum phase-locked loop bandwidth that will yield minimum performance degradation in the PSK demodulation process. To perform this trade-off analysis we have to consider the particular frequency characteristic of the phase-locked loop as well as its resulting noise bandwidth,  $B_\phi$ .

Now given the closed-loop phase-locked loop transfer function  $H(f)$ , the spectral densities at various points of the phase-locked loop and demodulator circuits can be determined (see Figure 3-1). The spectrum associated with the input phase noise process at various points is obtained by multiplying  $S_{\delta\phi}(t)$  by the absolute square of the frequency transfer function to the specific point of interest. In particular, the phase noise spectrum at the input to the symbol demodulator filter is given by

$$S_{\delta\phi}(f) |1 - H(f)|^2 \quad (3-8)$$

The additive Gaussian noise will also cause phase noise via the phase-locked loop. Its spectrum at the demodulator filter input is<sup>[3]</sup>

$$\frac{N_o}{E_s R_s} |H(f)|^2 \quad (f > 0) \quad (3-9)$$

where  $E_s R_s$  equals the received carrier power. Thus at the mixer output before the demodulation filter we have the total phase noise density

$$S_{\delta\phi}(f) |1 - H(f)|^2 + \frac{N_o}{E_s R_s} |H(f)|^2 \quad (3-10)$$

This implies that the total phase noise variance at the output of the demodulator

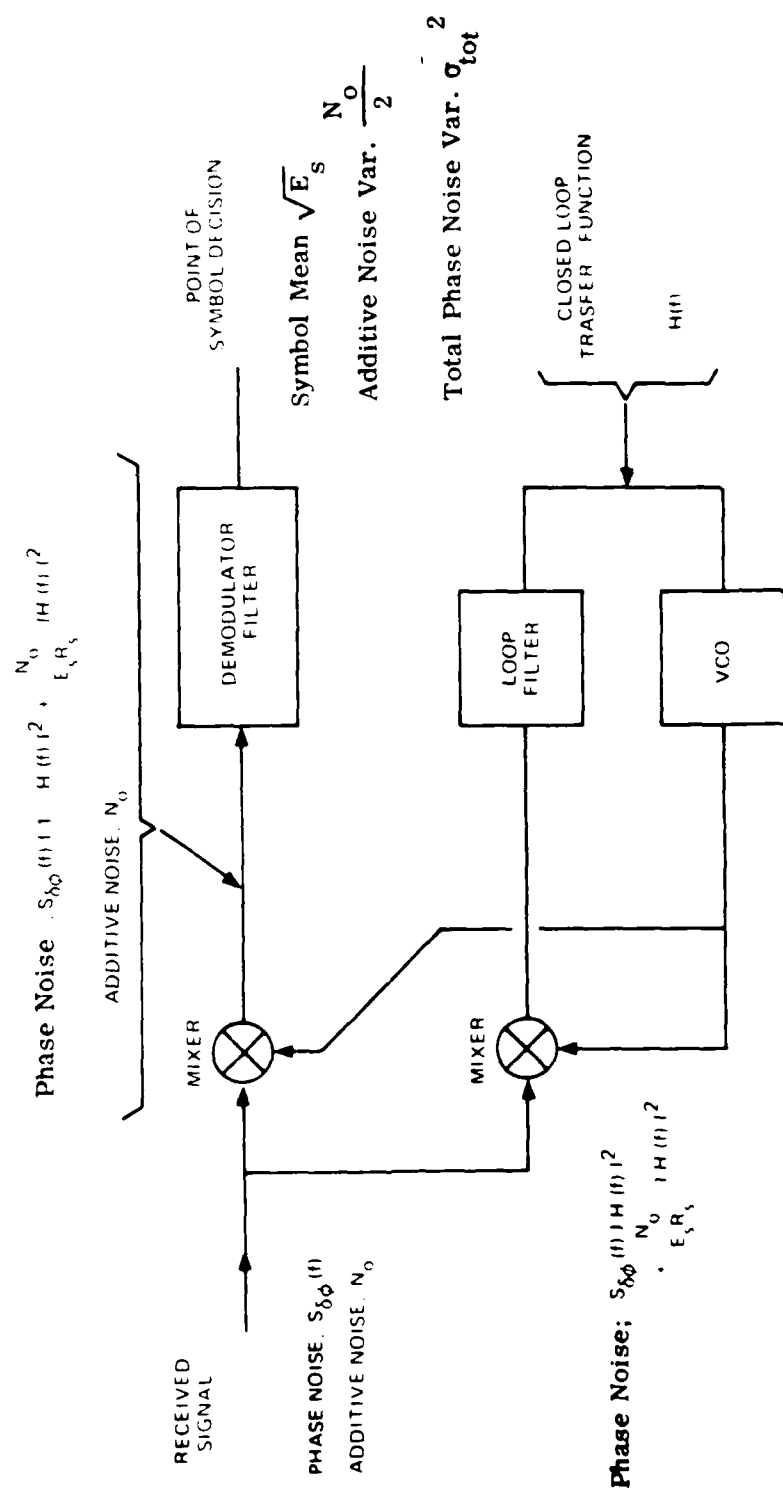


Figure 3-1. Spectral Densities at Various Points of a (Partially) Coherent PSK Receiver

filter, an integrate and dump filter, is given by

$$\sigma_{\text{tot}}^2 = \sigma_{\text{pn}}^2 + \sigma_{\text{th}}^2 \quad (3-10a)$$

where

$$\sigma_{\text{pn}}^2 = \int_0^{\infty} S_{\delta\phi}(f) |1 - H(f)|^2 \left( \frac{\sin \pi f T_s}{\pi f T_s} \right)^2 df \quad (3-10b)$$

and

$$\sigma_{\text{th}}^2 = \int_0^{\infty} \frac{N_o}{E_s R_s} |H(f)|^2 \left( \frac{\sin \pi f T_s}{\pi f T_s} \right)^2 df \quad (3-10c)$$

Figure 3-2 shows the general characteristics of  $|H(f)|^2$  and  $|1 - H(f)|^2$  and indicates that the effect of  $S_{\delta\phi}(f)$  is reduced for low frequencies since  $|1 - H(f)|^2$  approaches zero for decreasing frequencies. In other words, the phase-locked loop partially tracks the low frequency components of the phase noise process. The more the low frequency region is suppressed by  $|1 - H(f)|^2$ , the less the phase noise variance  $\sigma_{\text{pn}}^2$  resulting from the phase noise process  $\phi(t)$ . On the other hand, this increase will make the variance  $\sigma_{\text{th}}^2$  larger since the area under  $|H(f)|^2$  will be larger. Therefore, to minimize the total variance  $\sigma_{\text{tot}}^2$ , the closed-loop filter characteristic  $H(f)$  should be judiciously chosen.

In general,  $S_{\delta\phi}(f)$  will contain the  $f^{-3}$  component [i.e.,  $h_3 > 0$  in Equation (3-1)] that suggests that  $|1 - H(f)|^2$  should approach at least as fast as  $f^3$ . This requires a second- or higher-order phase-locked loop implementation. Considering that we know only that the phase noise spectrum  $S_{\delta\phi}(f)$  is dominated by a spectrum of the form in Equation (3-1), a good system solution is given by a filter that makes  $|1 - H(f)|^2$  maximally flat at  $f = 0$ ; "Butterworth filter."

A second-order maximally flat PLL filter defines

$$|1 - H(f)|^2 = \frac{f^4}{f_n^4 + f^4} \quad (3-11)$$

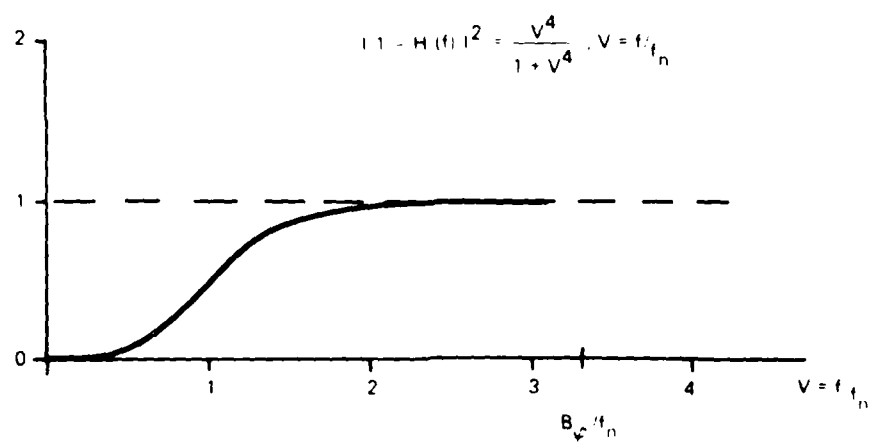
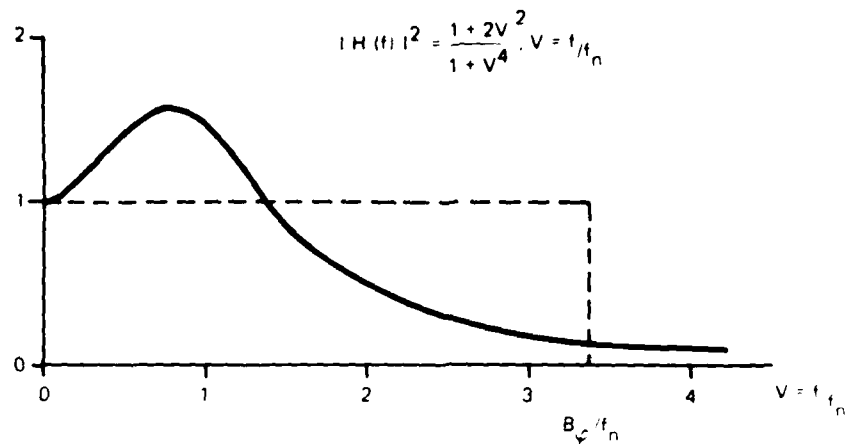


Figure 3-2. Frequency Characteristics of a Second-Order Phase-Locked Loop with Damping Factor = 0.707

which is consistent with the characteristic

$$H(f) = \frac{\frac{f^2}{n} + i\sqrt{2} \frac{f}{n} f}{\frac{f^2}{n} + i\sqrt{2} \frac{f}{n} f - f^2} \quad (3-12)$$

making

$$|H(f)|^2 = \frac{\frac{f^2}{n}(\frac{f^2}{n} + 2f^2)}{f_n^4 + f^4} \quad (3-13)$$

Here  $f_n$  is called the corner frequency of the loop and Equation (3-12) represents a second-order loop. Higher-order PLLs may also be considered, i.e.,  $|1 - H(f)|^2 = f^{2k}/(f_n^{2k} + f^{2k})$ . Such loops are **sometimes** plagued by stability problems and since a second-order loop can handle  $f^{-3}$  phase noise it represents a good system choice. Equations (3-11) and (3-12) are plotted in Figure (3-2).

The loop bandwidth  $B_\varphi$  is directly proportional to the corner frequency  $f_n$ . It is defined as the equivalent noise bandwidth of  $H(f)$ , that is,

$$B_\varphi = \int_0^\infty |H(f)|^2 df$$

$$f_n \int_0^\infty \frac{1 + 2v^2}{1 + v^4} dv \quad (v = \frac{f}{f_n})$$

$$f_n \cdot \frac{3\pi\sqrt{2}}{4} \quad f_n \cdot 3.33 \quad (3-14)$$

Since  $f_n$  is directly proportional to the loop bandwidth  $B_\varphi$ , the transfer function  $H(f)$  is indirectly specified by  $B_\varphi$  so the task of minimizing the total phase noise variance  $\sigma_{\text{tot}}^2$  reduces to one of finding the optimum loop bandwidth  $B_\varphi$ .

Up to this point, no consideration has been given to the fact that the phase-locked loop must be implemented to operate on a modulated signal (except for

auxiliary carrier systems). For power loops, Equation (3-10b) is unaffected but Equation (3-10c) should be multiplied by  $\eta_{\varphi}^p$ , the degradation factor associated with power loops.<sup>[6]</sup> Similarly, in the decision feedback implementation case, Equation (3-10c) is modified by the multiplier  $\eta_{\varphi}^d$  for decision-feedback loop.<sup>[8,9]</sup>

In any case, optimization of loop bandwidth requires minimization of the total phase noise variance at the decision point. Total phase noise variance at the decision point may be written as:

$$\sigma_{\text{tot}}^2 = \sum_{j=0}^3 h_j A_j + \frac{N_0 \eta_{\varphi}}{E_s R_s} \left[ f_n^4 A_4 - 2f_n^2 A_2 \right] \quad (3-15)$$

where:

$$A_j = \int_0^{\infty} \frac{f^{4-j}}{f^4 + f_n^4} \left( \frac{\sin \pi f T_s}{\pi f T_s} \right)^2 df \quad (3-16)$$

and  $j = 0, 1, 2, 3, 4$

Evaluation of integrals  $A_j$  is simplified by letting  $\alpha = \pi f_n T_s$  and  $v = f f_n$  giving:

$$I_{4-j} = f_n^{j-1} A_j = \int_0^{\infty} \frac{v^{4-j}}{1+v^4} \left( \frac{\sin \alpha v}{\alpha v} \right)^2 dv \quad (3-17)$$

Integrals  $I_k$  ( $k = 4-j$ ) have been evaluated in Appendix A taking into account that the greatest interest is for small  $\alpha$ -values. Results are tabulated below.

$$A_0 f_n^{-1} = I_4 = \frac{\pi}{2} \left[ \frac{1}{\alpha} - \frac{1}{\sqrt{2}} \cdot \frac{1}{3\sqrt{2}} \alpha^2 + \dots \right]$$

$$A_1 = I_3 = \frac{1}{\alpha} \cdot 0.24 + 1.04 \alpha^2 + \dots$$

$$f_n A_2 = I_2 = \frac{\pi\sqrt{2}}{4} \left[ 1 - \frac{2\sqrt{2}}{3} \alpha^2 + \dots \right]$$

\*See also Appendix A.

$$f_n^2 A_3 \approx 1_1 = 0.83 + \frac{2}{3} \alpha^2 \ln \alpha + \dots$$

$$f_n^3 A_4 \approx 1_0 = \frac{\pi \sqrt{2}}{4} \left[ 1 - \frac{1}{3} \alpha^2 + \dots \right] \quad (3-18)$$

For small  $\alpha$  values substitution of Equations (3-18) into (3-15) gives the total phase noise variance at the symbol decision point

$$\begin{aligned} \sigma_{\text{tot}}^2 &= h_0 \frac{\pi f_n}{2\alpha} + h_1 (0.24 + t \ln \frac{1}{\alpha}) + h_2 \frac{\pi \sqrt{2}}{4 f_n} + h_3 \frac{0.83}{f_n^2} \\ &+ \frac{N_o \eta_{\phi}}{E_s R_s} + f_n \frac{3\pi \sqrt{2}}{4} \end{aligned} \quad (3-19)$$

Since  $B_{\phi} = f_n \frac{3\pi \sqrt{2}}{4}$  and  $\alpha = \pi f_n T_s = \pi f_n R_s^{-1} = \frac{4}{3\sqrt{2}} \frac{B_{\phi}}{R_s}$ , we may rewrite Equation (3-19) as

$$\begin{aligned} \sigma_{\text{tot}}^2 &= h_0 \frac{R_s}{2} + h_1 \left[ 0.3 + t \ln \frac{R_s}{B_{\phi}} \right] \\ &+ h_2 \frac{3.70}{B_{\phi}} + h_3 \frac{9.22}{B_{\phi}^2} + \frac{N_o B_{\phi}}{E_s R_s} \eta_{\phi} \end{aligned} \quad (3-20)$$

The optimum bandwidth  $B_{\phi}$  that minimizes the total variance  $\sigma_{\text{tot}}^2$  can be found from this expression. Setting the derivative of  $\sigma_{\text{tot}}^2$  with respect to  $B_{\phi}$  equal to zero the optimum value of

$$B_{\phi} = B_0 + \frac{1}{3} h_1 \frac{E_s R_s}{N_o \eta_{\phi}} \quad (3-21)$$

$B_{\phi}$  represents the optimum bandwidth, where

$$B_0 = \sqrt[3]{\frac{1}{2} (G + \sqrt{G^2 - 4 H^3})} \quad (3-22a)$$

if real and

$$B_0 = 2\sqrt{H} \cos \left[ \frac{1}{3} \arccos \left( \frac{G}{2\sqrt{H^3}} \right) \right] \quad (3-22b)$$

otherwise <sup>[10]</sup>. Here

$$H = \frac{1}{3} \left( \tilde{h}_2 + \frac{1}{3} \tilde{h}_1^2 \right) \quad (3-23)$$

and

$$G = -2 \left[ \tilde{h}_3 + \frac{1}{6} \tilde{h}_2 \tilde{h}_1 + \frac{1}{27} \tilde{h}_1^3 \right] \quad (3-24)$$

with

$$\tilde{h}_1 = h_1 \frac{E_s R_s}{N_0 \eta_0} \quad (3-25)$$

$$\tilde{h}_2 = h_2 3.7 \frac{E_s R_s}{N_0 \eta_0} \quad (3-26)$$

$$\tilde{h}_3 = h_3 9.22 \frac{E_s R_s}{N_0 \eta_0} \quad (3-27)$$

Generally, the optimum bandwidth solution is approximated by

$$B_0 = \sqrt[3]{2\tilde{h}_3 + \frac{1}{2}\tilde{h}_2} \quad (3-28)$$

for the very low symbol rates  $R_s$ . By increasing symbol rates the optimum solution of Equation (3-21) is closely approximated by

$$B_0 = \frac{1}{2} \tilde{h}_1 + \sqrt{\tilde{h}_2 + \tilde{h}_1^2/4} \quad (3-29)$$

that finally will approach

$$B_0 = \tilde{h}_1 \quad (3-30)$$

This general trend implies that systems operating at high digital rates will not be plagued by  $f^{-3}$  phase noise because it is effectively tracked out by the phase-locked loop. Having determined the optimum loop bandwidth, one can calculate the resulting total phase noise variance according to Equation (3-20).

Before applying this optimization technique to available phase noise data, it is of great value to present the method by which the optimum choice of the loop bandwidth distributes the total phase noise variance between that due to phase noise on the received signal and the thermally induced loop phase noise. For this purpose we consider a simplified model of the total phase noise variance given by

$$\sigma^2 = \frac{H}{(s-1)x^{s-1}} + Lx \quad (s > 1) \quad \{ R_s \gg x \} \quad (3-31)$$

where

$$h_s = \frac{H}{s-1}$$

and

$$\sigma^2 = h_1 \left[ .3 + h_1 \frac{R_s}{x} \right] + Lx \quad (s > 1) \quad (3-32)$$

and where  $x$  is proportional to the noise bandwidth of the loop (see Equation (3-20)). In other words, we are optimizing the bandwidth of a phase-locked loop in the presence of  $f^{-s}$  noise (the  $\frac{H}{(s-1)x^{s-1}}$  term or the  $h_1 \ln \frac{R_s}{x}$  term) and additive noise (the  $Lx$  term). The value  $x_s$  of  $x$  that minimizes  $\sigma^2$  is the solution of

$$\frac{\partial \sigma^2}{\partial x} = -\frac{H}{x^s} + L = 0 \quad (s > 1) \quad (3-33)$$

or

$$\frac{\delta \sigma^2}{\delta x} = -\frac{h_1}{x} + L \geq 0 \quad (s > 1) \quad (3-34)$$

yielding

$$x_s \leq \sqrt{h/L} \quad (s > 1) \quad (3-35)$$

and

$$x_1 \leq h_1/L \quad (s \leq 1) \quad (3-36)$$

For  $(s > 1)$  the optimum solution distributes the total phase variance (at the symbol decision point) between the untracked portion of carrier phase noise and that due to thermal noise in the proportion  $(1/s)$  to  $(s-1/s)$  giving the minimum total variance

$$\sigma_s^2 \leq \left(\frac{s}{s-1}\right) L x_s \leq \frac{s}{s-1} \sqrt{hL} \quad (s > 1) \quad (3-37)$$

For  $(s \leq 1)$  the optimum solution is slightly more complicated due to the very slow roll off in power for a  $1/f$  type phase noise density. The minimum total phase noise variance is obtained using Equation (3-32),

$$\sigma_1^2 = h_1 \left\{ .3 + \ln \frac{R_s}{x_1} \right\} + L x_1 \quad \left\{ \frac{R_s}{x_1} \gg 1 \right\} \quad (3-38)$$

and using Equation (3-36) gives

$$\sigma_1^2 = h_1 \left\{ \left[ .3 + \ln \frac{R_s}{x_1} \right] + 1 \right\} - h_1 / \left( .3 + \ln \frac{R_s}{x_1} \right) \quad \left\{ \frac{R_s}{x_1} \gg 1 \right\} \quad (3-39)$$

For any typical coherent PSK system it is reasonable to assume that the ratio of modulation symbol rate to PLL bandwidth  $(R_s/x_1)$  will be at least  $\geq 5$  and is typically  $\geq 10$ .<sup>\*</sup> Assuming  $R_s/x_1 \geq 5$  or equivalently,  $(R_s/x_1) \geq 1.6$

<sup>\*</sup> If the optimum bandwidth  $x_1 \approx R_s$  there is no reason to design a "coherent" PSK system since there would be no advantages accrued over performance obtainable from a differentially coherent PSK system which would be much simpler to implement.

and using Equation (3-39) the optimum solution distributes the total phase noise variance between the untracked portion of carrier phase noise and that due to thermal noise in the proportion  $\gamma$  to  $(1-\gamma)$  respectively where  $(.65 \leq \gamma \leq 1)$ .

In the preceding analysis, the optimum tradeoff between colored phase noise  $h_i/f_i$ ,  $i = 1, 2, 3$  and thermal noise has been determined. As discussed in Section 2 of this report, the tradeoff between allowable white oscillator phase noise and additive thermal noise is perhaps the most misunderstood process. It is hoped that the following simple discussion will clarify any conceptual difficulty.

Equation (3-20) shows when the oscillator phase noise process is dominated by white phase noise (i.e.,  $h_0 \gg h_i$ ,  $i = 1, 2, 3$ ) the total phase error variance becomes:

$$\sigma_{\text{tot}}^2 = h_0 \frac{R_s}{2} + \frac{N_o B_\phi}{E_s R_s} \eta_\phi \quad (3-40)$$

However, the first term on the left is an approximation of the filtered white phase noise process which only holds when the PLL corner frequency  $f_n$  is much less than the symbol rate  $R_s$ . When this condition does not hold Equation (3-40) should be given as:

$$\sigma_{\text{tot}}^2 = h_0 \left( \frac{R_s}{2} - f_n \right) + \frac{N_o B_\phi}{E_s R_s} \eta_\phi \quad (3-41)$$

where it is assumed that

$$R_s/2 > f_n$$

and that  $(R_s/2 - f_n)$  is the 3-dB bandwidth of the composite phase noise filter consisting of the PLL filter and integrate-and-dump filter.

A very interesting result is obtained by a simple rearrangement. Noting that  $B_\phi \approx 3.33 f_n$  (second order PLL,  $\zeta = .707$ )

$$\sigma_{\text{tot}}^2 = h_0 \frac{R_s}{2} + B_\phi \left( \frac{N_0}{E_s R_s} \eta_\phi - \frac{h_0}{3.33} \right) \quad (3-42)$$

From Equation (3-42) it is seen that by a judicious choice of parameters it is possible to cause the bracketed quantity to be positive, negative, or zero thus indicating that by increasing the PLL bandwidth  $B_\phi$  with a fixed symbol rate  $R_s$ , it is possible to cause the carrier reference total phase error variance to increase, decrease, or remain the same, respectively. Of course this only holds when  $f_n < R_s/2$  which is a usual requirement for coherent PSK demodulation.

If a set of parameters given are such that the bracket quantity is negative, and the optimum PLL bandwidth thus approaches the symbol rate (noise averaged over only one symbol duration) it is obvious that coherent PSK demodulation holds no advantage over differentially detected PSK since all of the noise of the previous bit interval will appear on the phase reference. Should this situation occur it would be wise to switch to a differentially detected PSK modem and remove the differential decoders normally used to resolve the phase ambiguity problem in coherent PSK systems.

The preceding results are summarized in Table 3-1 which gives the relative phase noise distribution for various  $s$ -values that occur. The results of this optimization also indicate, for example, in the case of dominating  $f^{-3}$  phase noise, the loop bandwidth should be set so large that only one-third of the total phase noise originates from the carrier phase noise. In addition, even though only one phase noise characteristic was considered here ( $f^{-8}$  phase noise), it is clear that from a bandwidth optimization point of view the important consideration is the characteristic of the phase noise about the corner frequency  $f_n$  of the loop (see Equation (3-19)). From a purely analytical point of view, it can be argued that the only things that matter to achieve the MMSF is the differential gain or loss of the total phase noise variance obtained by varying the loop bandwidth.

Table 3-1. Optimum Distribution of Carrier Reference Phase Error Variance

Phase Noise Characteristic	Portion of Phase Noise Variance Due to Carrier Phase Noise		Portion of Phase Noise Variance Due to Thermal Noise	Assumptions
	1	0		
$f^0$	0 dB	0	- $\infty$ dB	$h_0 \sim 3, 33 \frac{N_0}{E_s R_s} \eta_0$
	- $\infty$ dB	1	0 dB	$h_0 \sim 3, 33 \frac{N_0}{E_s R_s} \eta_0$
$f^{-1}$	0.65 to 1.0	-2.1 to 0 dB	0.35 to 0	-1.6 dB to - $\infty$ dB
$f^{-2}$	1.2	-3 dB	1/2	-3 dB
$f^{-3}$	1.3	-5 dB	2/3	-2 dB
$f^{-4}$	1.1	-6 dB	3/4	-1.3 dB

### 3.2 ANALYTICAL DIFFICULTIES AND THEIR RESOLUTION

The analytical optimization procedures described in the preceding section assume well behaved spectral density shapes with monotonically non-increasing density versus frequency and, also assume integer values for the exponent which describes the slope of the phase noise curve. It becomes apparent, however, from measured performance data that various filtering techniques used in real equipment do not always provide such well behaved phase noise spectra. Two techniques are available to supplant the preceding analysis when necessary. One technique which is currently available [11] is a graphical solution to the equations of the preceding section (computer integration) and the second technique is a state variable solution to the phase noise problem. [12] The state variable solution also provides the capability for studying the effects of time gated operation, required for TDMA systems. However, computer graphical procedures are perhaps the most straightforward and can be accurate for TDMA systems over a specified range of parameters as discussed in Paragraph 5.3 of this report.

In any event, the solutions derived in the preceding section provide great insight into most of the systematic variations experienced. In the following sections, any one of the preceding analytical tools is used depending upon which is judged best for the particular application.

SECTION 4 - OPTIMUM PERFORMANCE OF BPSK AND QPSK  
SIGNALING WITH VITERBI (RATE 1/2, K=7) DECODING IN THE  
PRESENCE OF OSCILLATOR PHASE NOISE EXPECTED  
FOR TERMINALS OF THE DSCS

4.1 OPTIMUM PERFORMANCE RESULTS WITH TERMINALS OBTAINING THE  
"HT-MT" MODIFIED PHASE NOISE SPECIFICATION

Since the advent of practical coherent PSK modulation techniques for the DSCS has been relatively recent, the "original" phase noise specifications for the HT-MT earth terminals of the DSCS were derived from an incidental FM model as stated below in a paragraph from SCA-2080A.

Incidental FM. Transmitted carrier and receive carriers after frequency translation shall be spectrally pure so that:

$\Delta f \times f_m$  is not greater than 2 Hz squared for values of  $f_m$  between 1,000 Hz and 20 Hz. For values of  $f_m$  above 20 Hz,  $\Delta f$  shall not exceed 0.1 Hz to the value of  $f_m$  where the single-sided phase noise density to signal ratio equals -105 dB. The -105 dB single-sided phase noise density to signal ratio shall not be exceeded from 10 kHz to 62.5 MHz on either side of carrier  $\Delta f$  - peak deviation of the carrier  $f_m$  - deviation rate.

Using this model the HT-MT single sideband phase noise  $L(f)$  was derived<sup>13</sup> and is shown in Figure 4-1. It is known, however, that the  $f^{-4}$  phase noise indicated in close to the carrier is unrealistic given currently available oscillators and that this type of spectral shape is due to the assumed validity of the incidental FM model. Frequency synthesizers are known to provide an  $f^{-1}$  density close to the carrier and are ultimately limited by the effects of either crystal or atomic standards which exhibit  $f^{-3}$  phase noise characteristics extremely close to the carrier. Thus, the HT-MT specification has been modified for the purposes of this memorandum as shown by the broken line curve of Figure 4-1 labelled HT-MT-modulation.

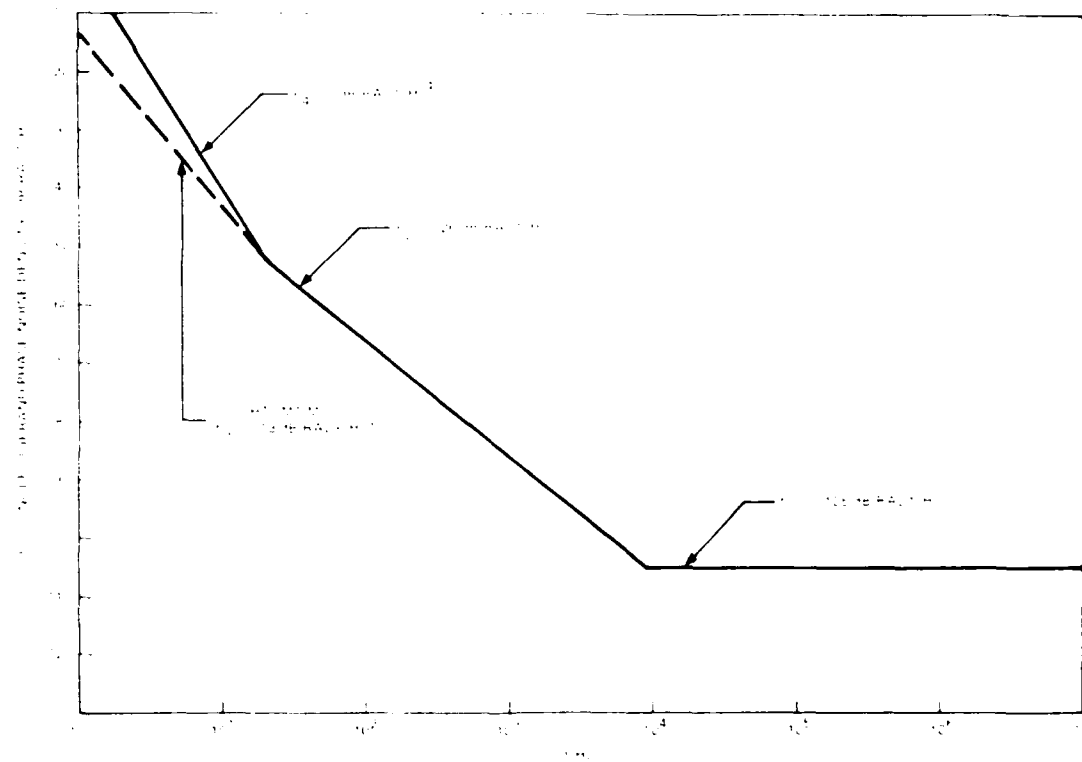


Figure 4-1. HT-MF Incidental FM Specification Converted to Single Sideband Phase Noise Density ' $f(t)$ ' at Carrier Frequency

Based on this modified specification, the total phase noise variance given by Equation (3-20) has been determined using the optimum bandwidth solution of Equation (3-21). The variance has been calculated using both decision-feedback and power loop implementations for two and three times the terminal phase noise according to the specification, since two terminals and one satellite are always involved. This calculation is used because reliable phase noise data about the satellite is not available. (Some very sketchy and incomplete information pertaining to the satellite phase noise is available, but by neglecting the satellite influence and equating the satellite as one terminal, the influence of the satellite can be assessed.) Figures 4-2 through 4-5 illustrate results for two and three terminals, power PLLs, decision-feedback loops, and also for both BPSK ( $M = 2$ ) and QPSK ( $M = 4$ ) operations. Demodulation losses have been plotted as a function information bit rate  $R_{ib}$  for  $\sim$ -level soft decision (3-bit), rate 1/2, constraint length 7, Viterbi decoding followed by differential decoding with a resultant BER  $10^{-5}$ .

A loss cutoff of 0.2 dB has been drawn in the figures to indicate allowable regions of operation for the various configurations. The upward trend in the loss curves with high data rates are caused by the white phase noise floor shown in Figure 4-1.

Figures 4-2 through 4-5 show that when carrier recovery is provided by decision feedback loops a reduction in demodulation losses is obtained as compared with results for power loop implementations. However, significant improvement is only obtained with QPSK with negligible improvement noted with BPSK.

Table S-1 contains a summary of permissible (0.2 dB maximum loss) rates for two terminals and one equivalent satellite all conforming to the HT-MT modulation phase noise specifications (Figure 4-1).

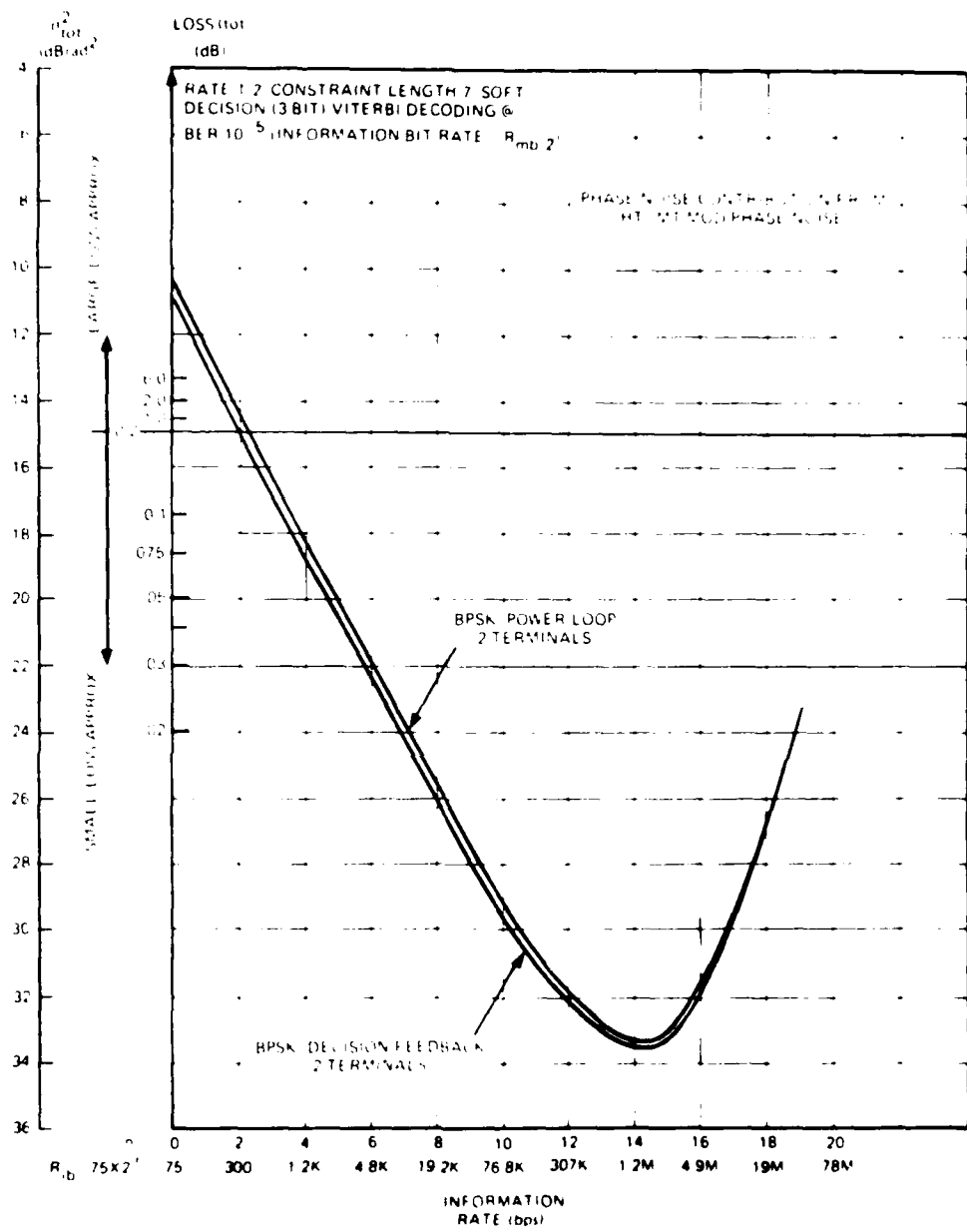


Figure 4-2. Demodulation Loss (dB),  $L_{tot}$ , and Total Phase Variance,  $\sigma_{tot}^2$ , versus Information Bit Rate,  $R_{ib}$  (bps), at Optimum BW

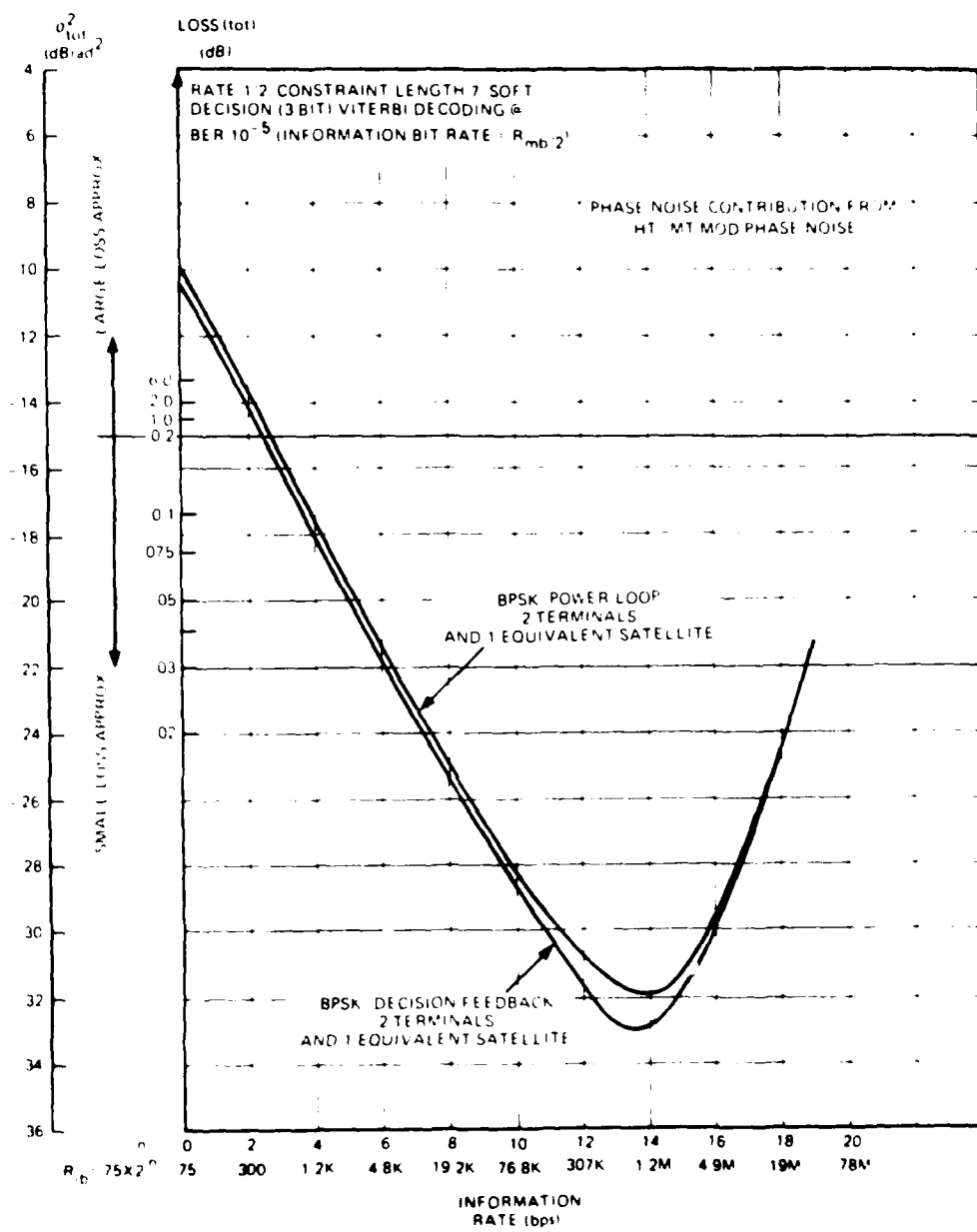


Figure 4-3. Demodulation Loss (dB),  $L_{tot}$ , and Total Phase Variance,  $\sigma_{tot}^2$ , versus Information Bit Rate,  $R_{ib}$  (bps), at Optimum BW

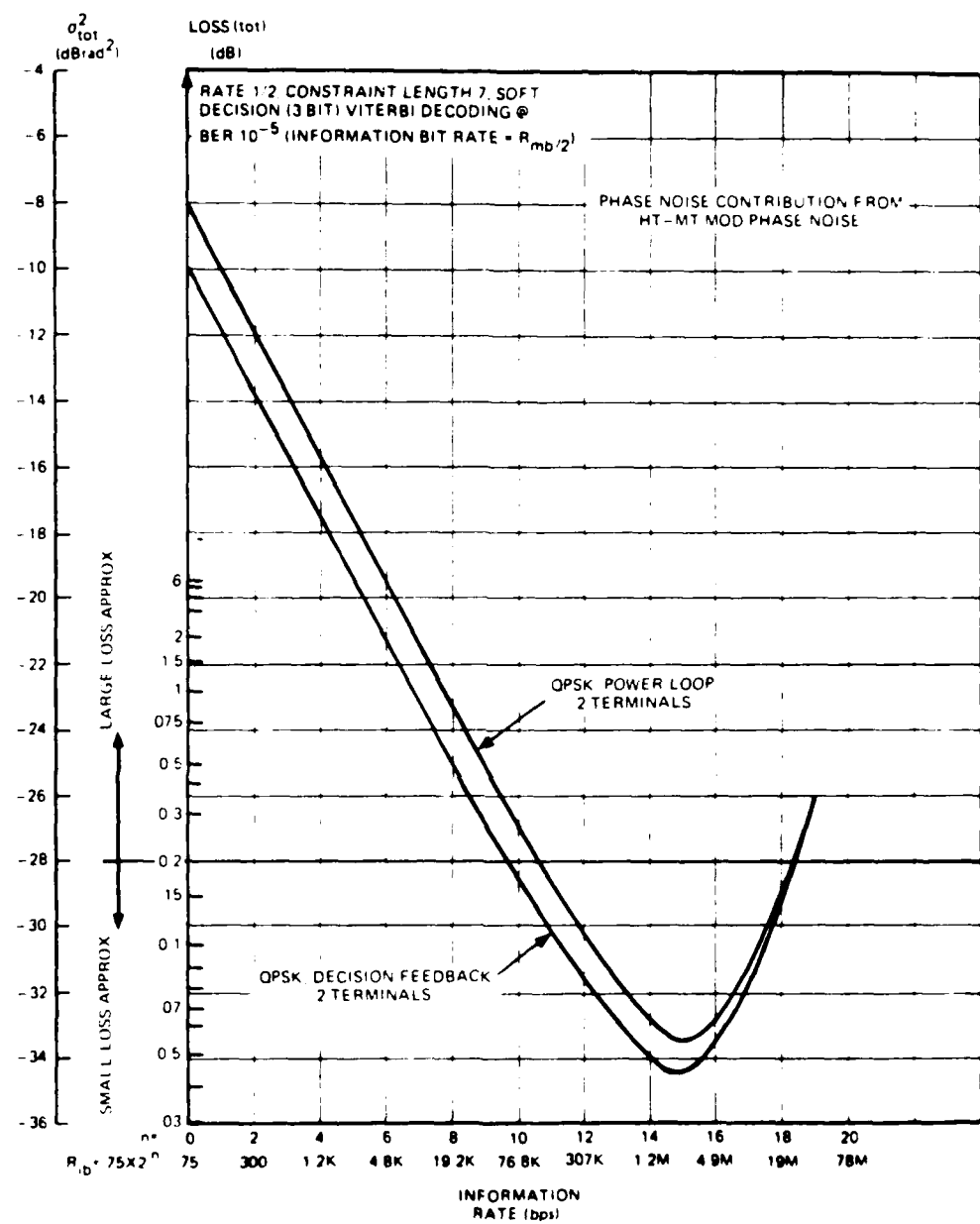


Figure 4-1. Demodulation Loss (dB),  $L_{\text{tot}}$ , and Total Phase Variance,  $\sigma_{\text{tot}}^2$ , versus Information Bit Rate,  $R_{\text{ib}}$  (bps), at Optimum BW

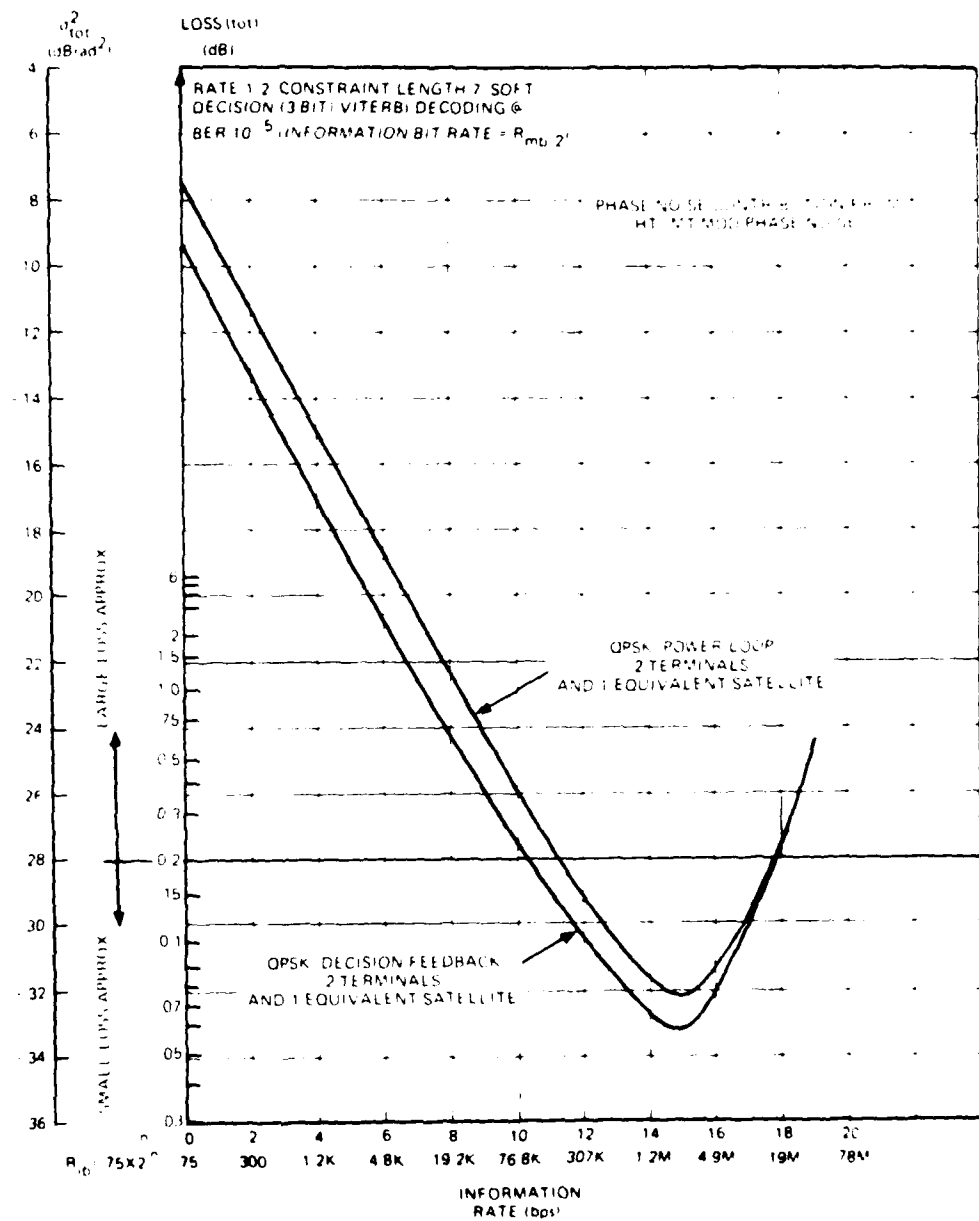


Figure 4-5. Demodulation Loss (dB),  $L_{tot}$ , and Total Phase Variance,  $\sigma_{tot}^2$ , versus Information Bit Rate,  $R_{ib}$  (bps) at Optimum BW

Tables D-1 through D-8 provide back-up data for the results shown in Figures 4-1 through 4-5. However, the tabulated results are expressed as a function of modulation bit rate  $R_{mb}$  as compared to information bit rate  $R_{ib}$  shown in the figures where the two parameters are related as:

$$R_{ib} = R_{mb} \cdot 2$$

In the tables the optimum bandwidth, total phase noise variance and its two components (thermally induced loop phase noise  $\sigma_{th}^2$  and the untracked portion of the composite oscillator phase noise spectrum  $\sigma_{pn}^2$ ) are given as a function of the modulation bit rate.

Also tabulated are the demodulation losses that would be experienced when using 8-level soft decision (3-bit), rate 1/2, constraint length  $K = 7$ , Viterbi decoding followed by differential decoding based upon two different approximations to the probability distribution of phase tracking error experienced in a PLL. \* Results based on a Gaussian approximation [8] are easily calculated but are only valid for small losses as shown in the tables while the results using a Tikhonov approximation [2] are valid when the losses are less than 6 dB.

#### 4.2 OPTIMUM PERFORMANCE WITH REALISTIC TERMINAL PHASE NOISE

##### 4.2.1 Phase Noise Synthesized Using Comtech Lab., Inc. L-Band Oscillator, Fluke Frequency Synthesizer and Selected Atomic and Crystal Standards

Figure 4-6 shows the general structure for deriving a 7800-MHz signal from a 5-MHz standard and Figure 4-7 shows their corresponding single sideband phase noise densities at 7800 MHz. \*\*

\*See Appendix A.

\*\*It should be noted that for straight frequency multiplication,  $10 \log M^2$  (dB) where  $M = \text{new frequency/old frequency}$  is added to original specifications when required.

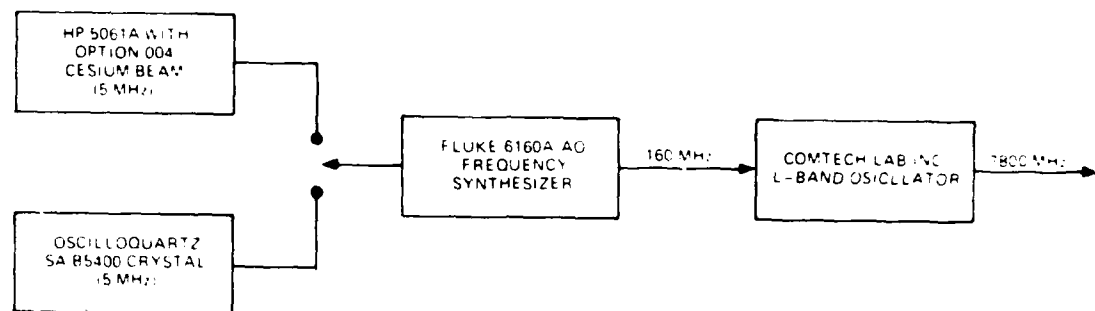


Figure 4-6. L-Band Reference Signal Generator

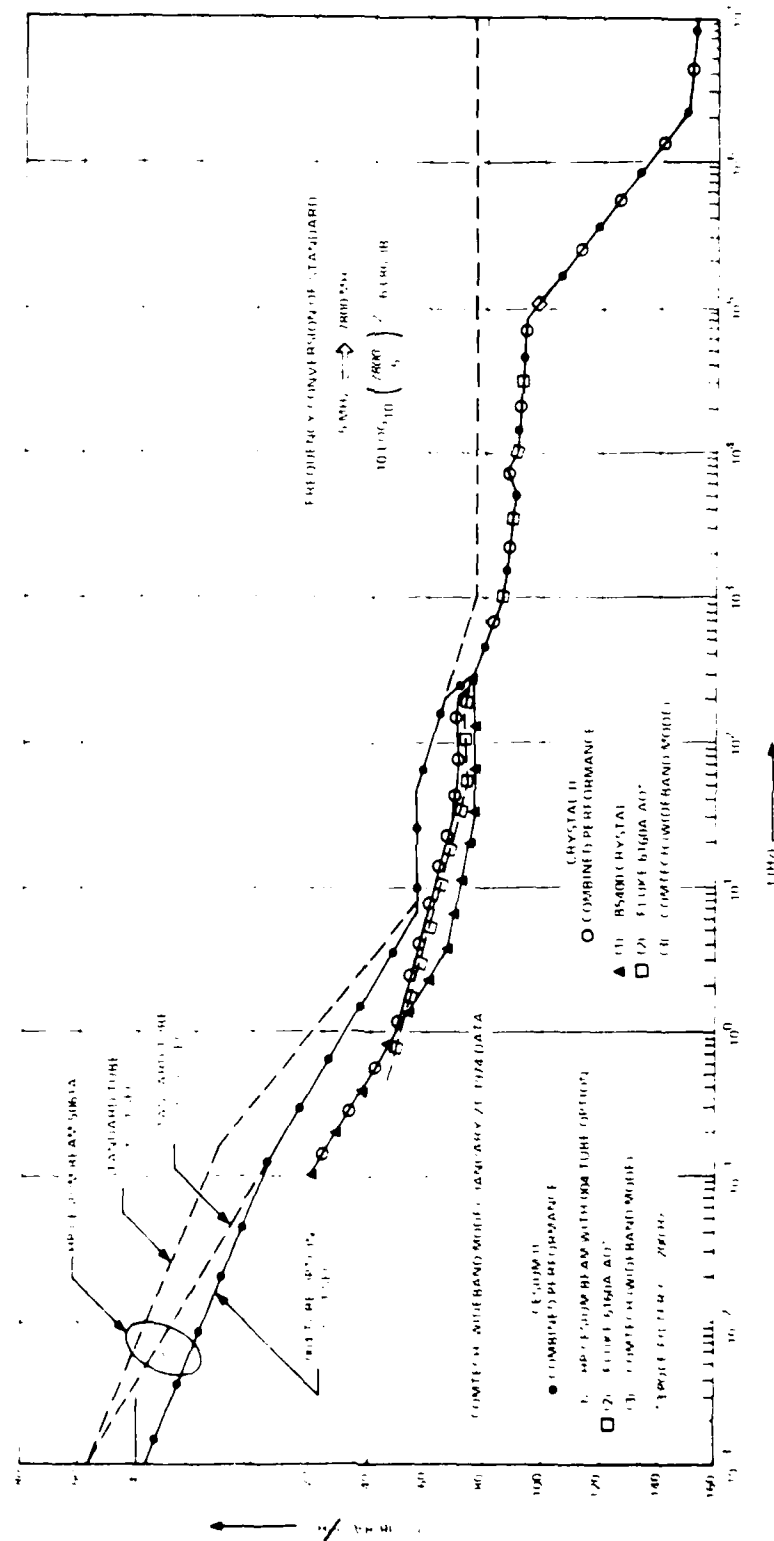


Figure 4-7. Synthesized Single Sideband Phase Noise Densities  $|f(t)|$  for "Cesium II" and "Crystal II" at 7800 MHz.

The Hewlett Packard HP 5061 A<sup>[14]</sup> and the Oscilloquartz SA B5400<sup>[15]</sup> have been chosen as representative of state of the art portable cesium beam standards and high quality crystal references, respectively.

As noted by Hewlett Packard, 60 second time constant operation (see Figure 4-5) requires a carefully controlled environment. Therefore, for field operations the 1 second time constant operation seems practical. Since it is expected that the optional (004) beam tube may be used in the Phase II DSCS, results obtained here will pertain only to the optional 004 beam tube with a 1 second time constant.

At this point in time it is not known whether the Oscilloquartz B5400 crystal could meet its specified performance (Figure 4-7) under field conditions, however, for the purpose of illustration it will be assumed that these conditions can be satisfied with adequate margin.

A Fluke 6160 A/AO frequency synthesizer has been chosen as representative of high quality synthesizers and provides the required flexibility with respect to frequency assignment. It is assumed that the standard drives the synthesizer and only wideband phase locking ( $\gtrsim$ 100 kHz) is involved within the synthesizer. In accord with discussions between CSC and a Fluke representative, and as verified by Comtech, a three-pole filter with 3-dB corner frequency at 200 Hz exists within the synthesizer.

Single sideband phase noise data for the Fluke synthesizer has not been shown directly in Figure 4-7. However, it is incorporated in the measured data<sup>[16]</sup> provided by measurements of a Comtech Lab. L-band oscillator driven by a Fluke 6160A, AO synthesizer and the measured data is shown by the dotted curve of Figure 4-7 designated here as Comtech (Wideband Mode).<sup>[16]</sup> Using [16] and Fluke data, the dotted curve below frequencies  $\sim$ 100 kHz is dominated by synthesizer noise and above 100 kHz is dominated by L-band oscillator noise.

---

\*This time constant refers to the bandwidth at which the internal 5-MHz crystal is locked to the cesium beam tube.

Measured data provided by Comtech Inc. is valid in the region 10 Hz - 10 MHz and since phase noise data is required beyond 10 MHz it has been assumed that as a worst case a phase noise floor exists at -153 dB rad<sup>2</sup>/Hz.

In summary, two synthesized phase noise curves (labelled "cesium II" and "crystal II" in Figure 4-7) will be evaluated for generation of 7800 MHz frequency up conversion or down conversion chains. The "cesium II" curve corresponds to a frequency conversion chain driven by the HP 5061 A with optional (004) cesium beam and with 1 second time constant. The resultant single sideband phase noise is shown in Figure 4-7 and consists of three sections with frequencies below 300 Hz dominated by the atomic standard frequencies from 300 Hz-10 MHz dominated by the synthesizer L-band oscillator combination and above 10 MHz given by the assumed phase noise floor.

The second phase noise curve (designated "crystal II" in Figure 4-7) corresponds to frequency conversion driven by the Oscilloquartz SA B5400 crystal as shown in Figure 4-6. The resultant single sideband "crystal II" phase noise curve consists of four sections with frequencies below 2 Hz dominated by the crystal standard, frequencies between 2 Hz-300 Hz being a composite of noise from Fluke 6160A AO synthesizer and crystal standard and frequencies above 300 Hz are as described for the "cesium II" curve.\*

#### 4.2.2 BPSK and QPSK System Performance Optimization With Synthesized Phase Noise Data

To our knowledge as of March 1974, single sideband phase noise curves "cesium II" and "crystal II" generated in Paragraph 4.2.1 represent the most current estimates of terminal phase noise at 7800 MHz which is expected for the best terminals currently under consideration for operation in the Phase II DSCS. Therefore an extensive set of data (Figures 4-8 through 4-11 and Tables

---

\*A roman numeral II has been used here to differentiate this most recent data from that which appeared in a prior memorandum.

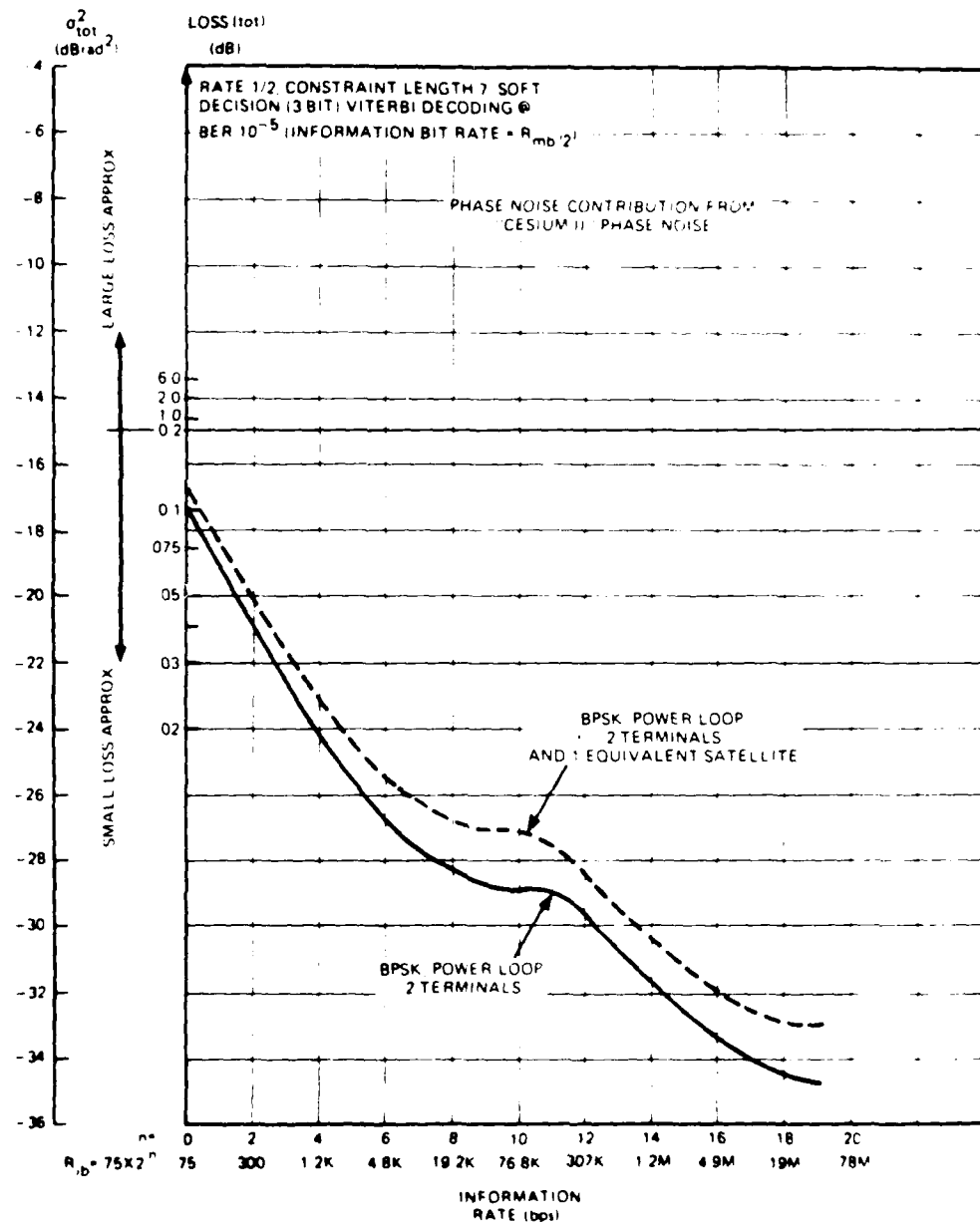


Figure 4-5. Demodulation Loss (dB),  $L_{\text{tot}}$ , and Total Phase Variance,  $\sigma_{\text{tot}}^2$ , versus Information Bit Rate,  $R_{\text{ib}}$  (bps), at Optimum BW

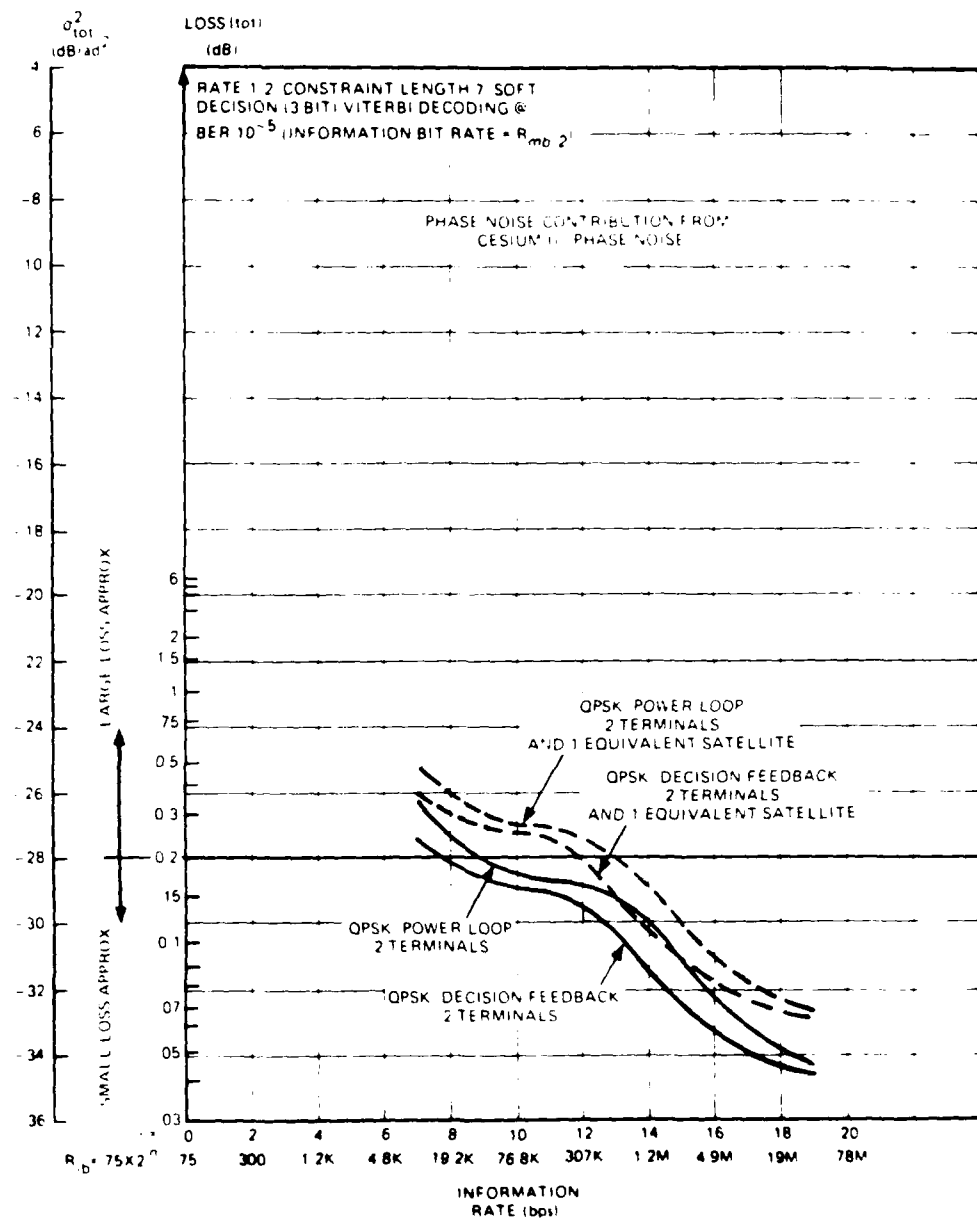


Figure 4-9. Demodulation Loss (dB),  $L_{tot}$ , and Total Phase Variance,  $\sigma_{tot}^2$ , versus Information Bit Rate,  $R_{ib}$  (bps) at Optimum BW

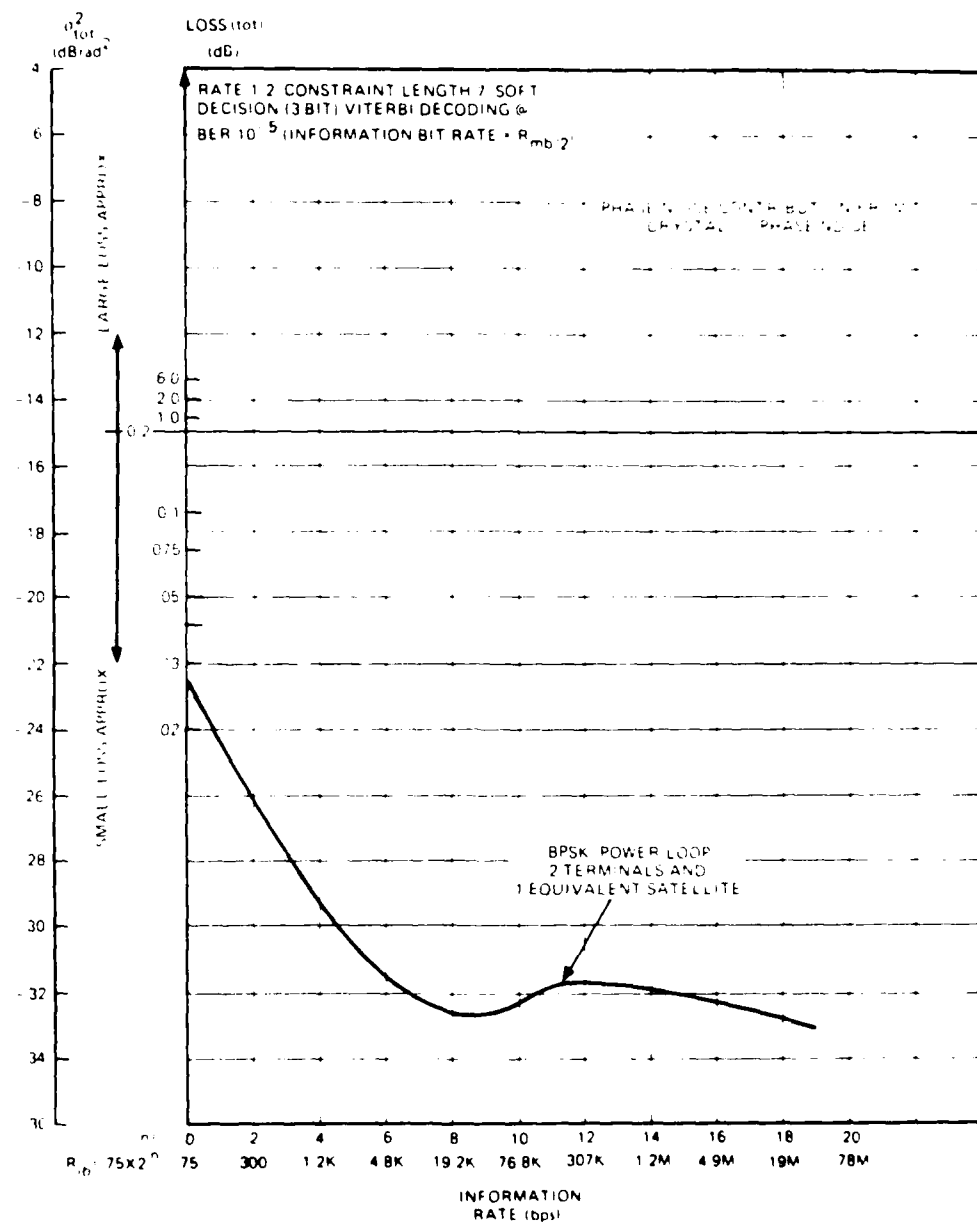


Figure 4-10. Demodulation Loss (dB),  $L_{tot}$ , and Total Phase Variance,  $\sigma_{tot}^2$ , versus Information Bit Rate,  $R_{ib}$  (bps), at Optimum BW

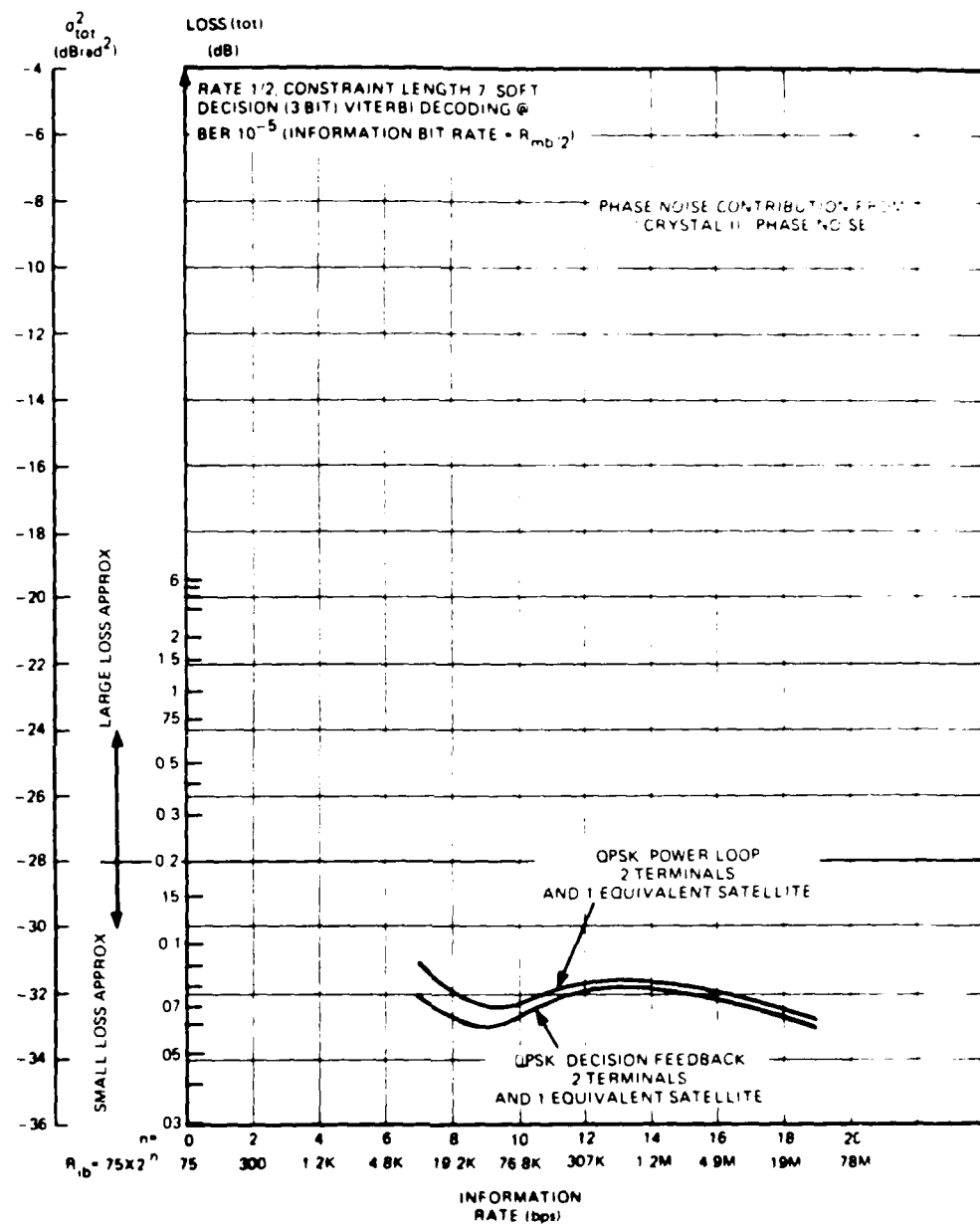


Figure 4-11. Demodulation Loss (dB),  $L_{tot}$ , and Total Phase Variance,  $\sigma_{tot}^2$ , versus Information Bit Rate,  $R_{ib}$  (bps), at Optimum BW

D-9 through D-17 has been generated to indicate possible demodulation performance for the Phase II DSCS.

Figures 4-8 through 4-11 illustrate demodulation losses as a function of information bit rate  $R_{ib}$  at the optimum bandwidth for two and three times the indicated phase noise ("cesium II" or "crystal II"), respectively.

As before it should be emphasized that the tabulated losses are a function of modulation bit rate  $R_{mb}$  while in the figures the losses are plotted as a function of information bit rate  $R_{ib}$  where  $R_{ib} = R_{mb}/2$  due to the rate 1/2 coding procedure.

Results using "crystal II" phase noise are presented only for the case of phase noise contributed by two terminals and one equivalent satellite since these results indicate that adequate performance (< 0.2 dB loss) is achieved with all configurations (see Figure 4-10 and 4-11) over the required range of data rates.

It should be noted that results in Figures 4-8 through 4-11 do not indicate a maximum information rate limitation within the indicated range as experienced for results obtained in Paragraph 4.1 (see Figures 4-4 and 4-5). This result is due to the reduced phase noise floor of  $-153 \text{ dB rad}^2/\text{Hz}$  (Figure 4-7) for "cesium II" and "crystal II" phase noise as compared to a phase noise floor of  $-105 \text{ dB rad}^2/\text{Hz}$  (Figure 4-1) assumed for the HT-MT modulation phase noise. Of course, if the  $-153 \text{ dB rad}^2/\text{Hz}$  floor persisted to higher frequencies and if signaling were required at higher data rates the same upward loss trend at high rates would be repeated.

Minimum and maximum data rates possible for the three terminal phase noise contribution either "cesium II" or "crystal II" have been summarized in Table S-1.

Finally, since the data in Figures 4-8 through 4-11 and Table S-1 represent demodulation losses for phase noise contributed by two terminals (no

satellite contribution) and two terminals plus one equivalent satellite, the data provides upper and lower bounds on expected losses. However, it is desirable to measure actual satellite phase noise to provide a more exact picture of expected demodulation performance losses in the Phase II DSCS.

SECTION 5 - DEMODULATION PERFORMANCE OF CURRENT  
MODULATION SYSTEMS OPERATING IN THE PRESENCE OF PHASE  
NOISE IN THE PHASE II DSCS

5.1 RADIATION INC. BPSK (MD-921 G)

Radiation Inc. has recently designed a BPSK modem which is expected to be operated with the following earth terminals of the Phase II DSCS:

1. MSC-46 "Upgrade"
2. HT-MT "Follow-on"
3. TSC-54.

Since each of the above earth terminals are expected to be operated with Comtech Lab. up- and down-converters or terminals meeting the HT-MT phase noise specifications, phase noise associated with each terminal may be adequately described by the curves labeled modified HT-MT of Figure 4-1 and "cesium II" or "crystal II" of Figure 4-7.

The Radiation BPSK modem has been designed with a power type carrier recovery PLL with a fixed bandwidth  $B_G = 175$  Hz and damping factor  $\zeta = 1.0$ .

Figures 5-1 through 5-3 have been generated to indicate expected performance of this modem operating in conjunction with soft\* Viterbi decoding in the presence of the modified HT-MT Type "cesium II" and "crystal II" oscillator phase noise densities. Tables D-18 through D-23 contain the numerical support for these figures.

As in the preceding sections, data rates listed in the tables are expressed as modulation bit rate  $R_{mb}$  while the data rates shown in the figures are information bit rate where  $R_{ib} = R_{mb}/2$  (see Figure 2-1).

\* See note 1 of Annex.

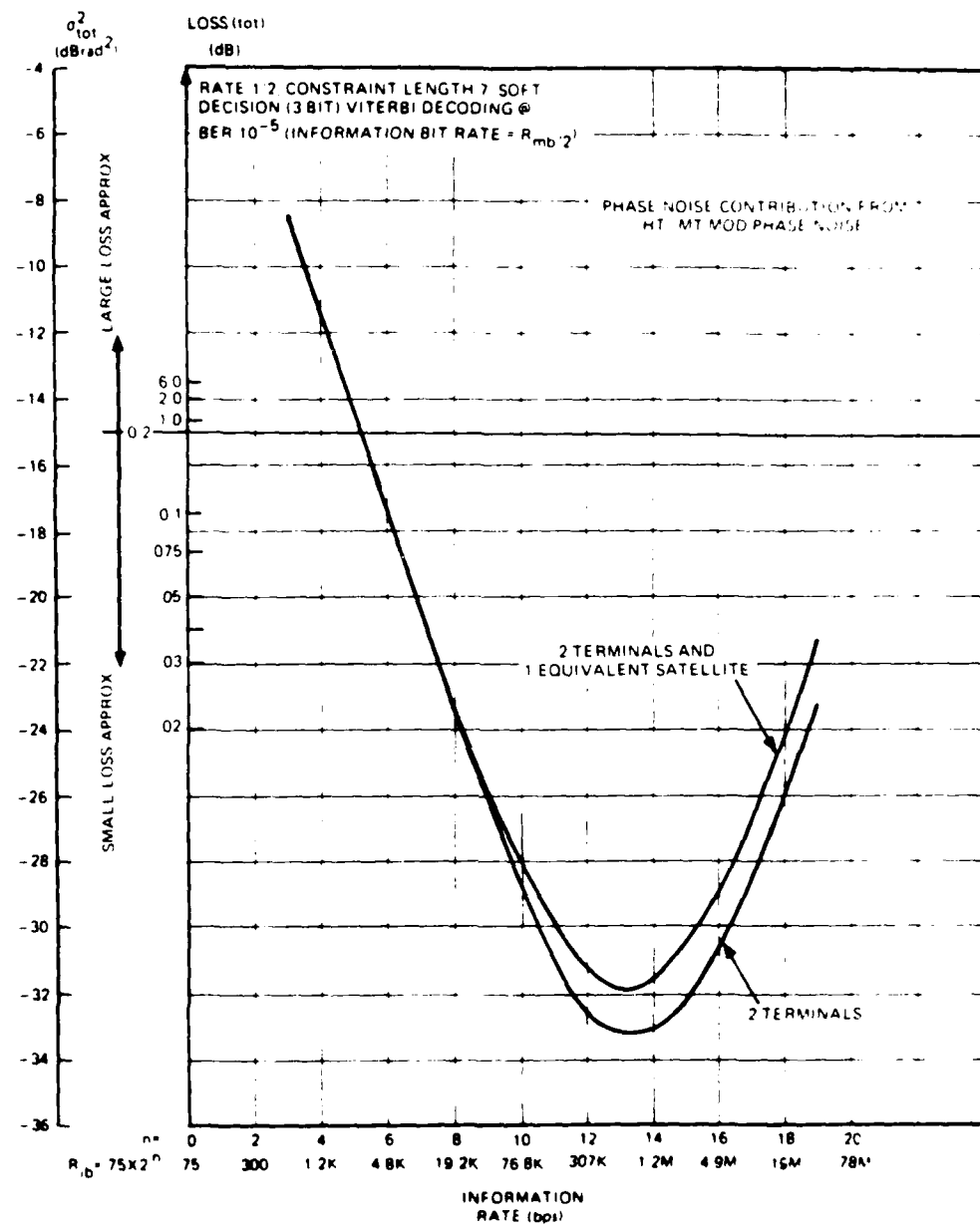


Figure 5-1. Radiation Inc. MD-921G BPSK Demodulation Loss (dB),  $L_{tot}$ , and Total Phase Variance,  $\sigma_{tot}^2$ , versus Information Bit Rate,  $R_{ib}$  (bps).  $B_\phi = 175$  Hz.

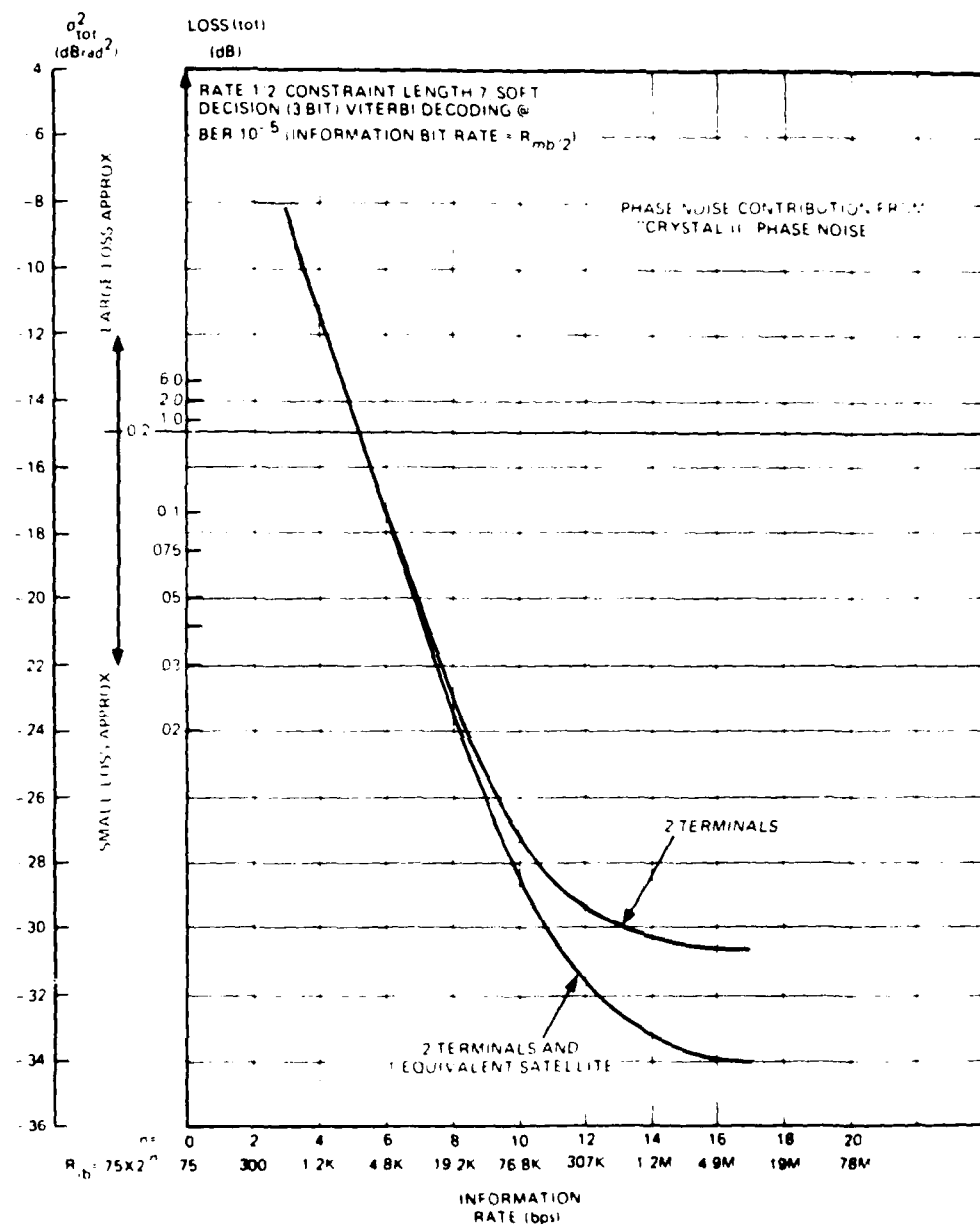


Figure 5-2. Radiation Inc. MD-921G BPSK Demodulation Loss (dB),  $L_{tot}$ , and Total Phase Variance,  $\sigma_{tot}^2$ , versus Information Bit Rate,  $R_{ib}$  (bps),  $B_\varphi = 175$  Hz

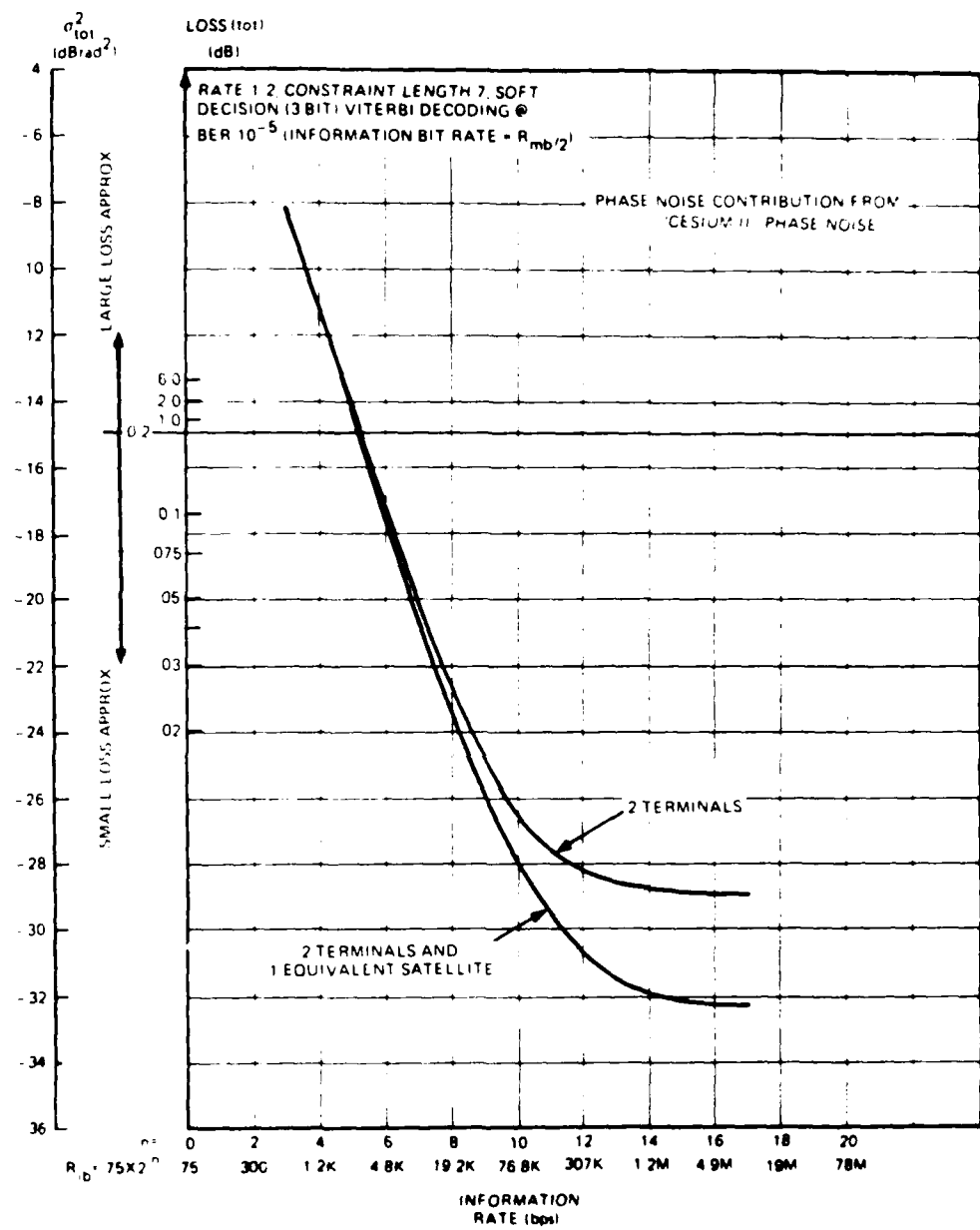


Figure 5-3. Radiation Inc. MD-921G BPSK Demodulation Loss (dB),  $L_{tot}$ , and Total Phase Variance,  $\sigma_{tot}^2$ , versus Information Bit Rate,  $R_{ib}$  (bps),  $B_\phi = 175$  Hz.

It may be noted in Figures 5-1 through 5-3 that a 0.707 PLL damping factor has been used to generate expected system performance data even though it has been stated that the Radiation modem has a PLL damping factor of 1.0. This change was effected here solely to reduce the costs associated with computer integration of Equation 3-10b. As stated in [11], a considerable increase in computation cost is required for PLL damping factors besides 0.707. A comparison of curves of Figures 5-2 and 5-4 (see also Tables D-22 and D-24) indicate that only a small improvement in demodulation performance is obtained with a PLL damping factor of 0.707 as compared to a PLL with damping factor of 1.0. Although differences in performance are small for loops with these two damping factors at the specified bandwidth, results are in accord with expected performance from a mean squared error criterion, that is, that optimum performance is obtained with a damping factor of 0.707.

Perusal of Figures 5-1 through 5-3 indicate that adequate demodulation performance (less than 0.2 dB loss) is achieved only when data rates are above 3600 bps.

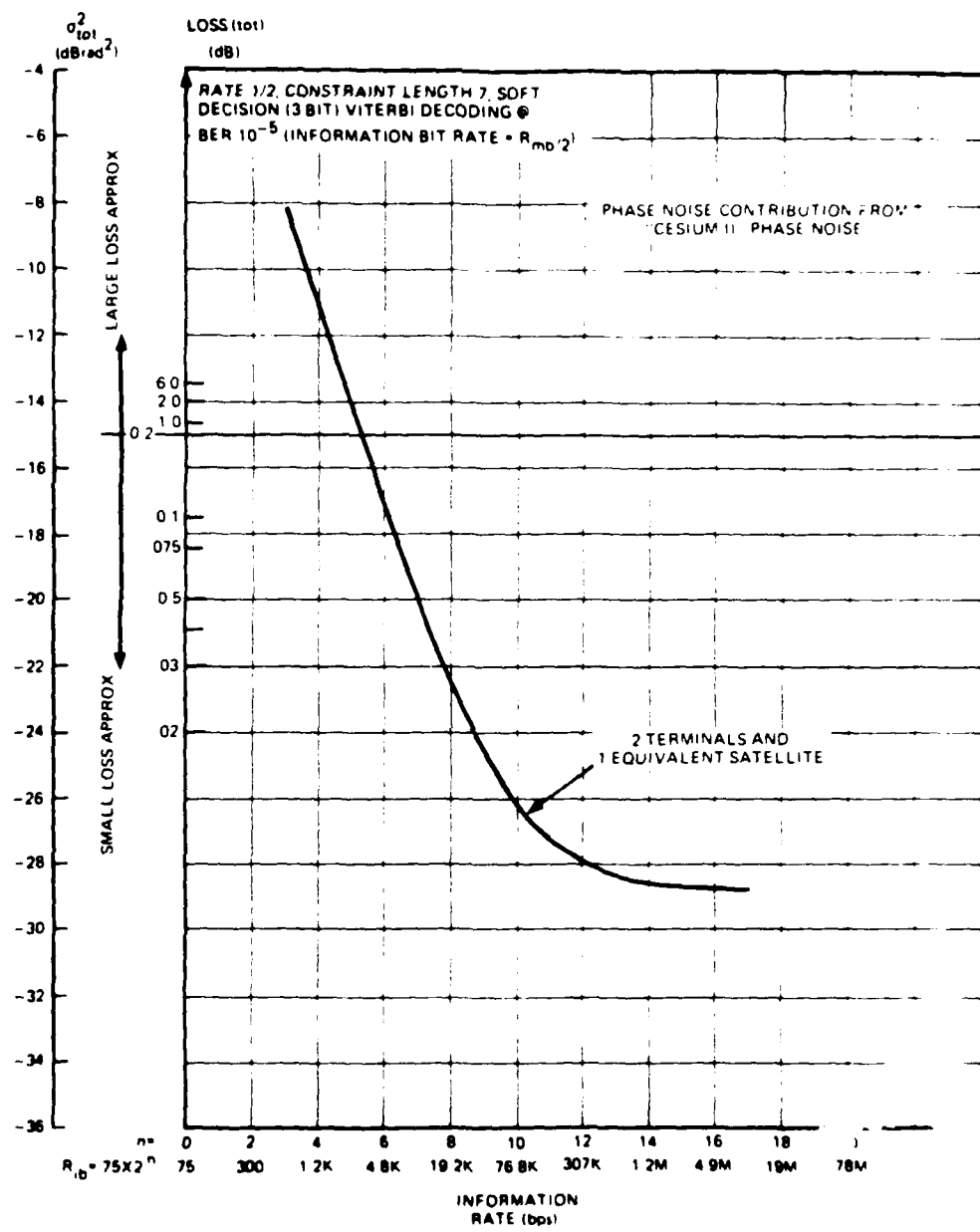


Figure 5-4. Radiation Inc. MD-921G BPSK Demodulation Loss (dB),  $L_{tot}$ , and and Total Phase Variance,  $\sigma_{tot}^2$ , versus Information Bit Rate,  $R_{ib}$  (bps),  $R_\varphi = 175$  Hz,  $\zeta = 1.0$

## 5.2 MAGNAVOX RESEARCH LAB., INC. (MRL) USC-28 BPSK SPREAD SPECTRUM SYSTEM

### 5.2.1 General

MRL's USC-28 is a BPSK spread spectrum system which consists of the following basic subsystems; Link Order Wire (LOW), Channel Data Receive Transmit (R/T), and a Critical Control Circuit (CCC).

Preceding analyses in this paper have neglected demodulation losses due to phenomenon other than imperfect carrier phase estimation. That is, losses such as those due to imperfect PSK symbol timing have been neglected. Therefore, as a continuation of this simplified analysis for the USC-28, losses due to improper PN code tracking will also be neglected and only those losses due to imperfect carrier phase estimation will be calculated.

Neglecting PN modulation, Figure 5-3 shows a simplified version of the time and power shared configuration of the LOW and R/T channels assumed in the analysis of the following sections. The CCC is a separate control circuit (not shown in Figure 5-5).

A complete analysis of the USC-28 from a phase noise point of view is provided in [1]. Our main purpose here will be to provide a simplified system analysis which will provide the basis for a USC-28 phase noise specification as discussed in the summary section and Section 6. We shall also briefly indicate expected system performance of the USC-28 operated with the HT-MT (AN MSC-60) terminal and the MSC-46 upgrade terminal as compared to the results described in [1] for an improved version of the AN ASC-18 terminal.

### 5.2.2 Phase Noise Effects in the USC-28

In Figure 5-5 it is shown that the LOW channel and R-T channel operate on a power shared basis and that carrier phase estimates are derived from the LOW and used for demodulation of data on the R-T channel. As indicated in the figure, two models of the USC-28 which are currently under discussion are the

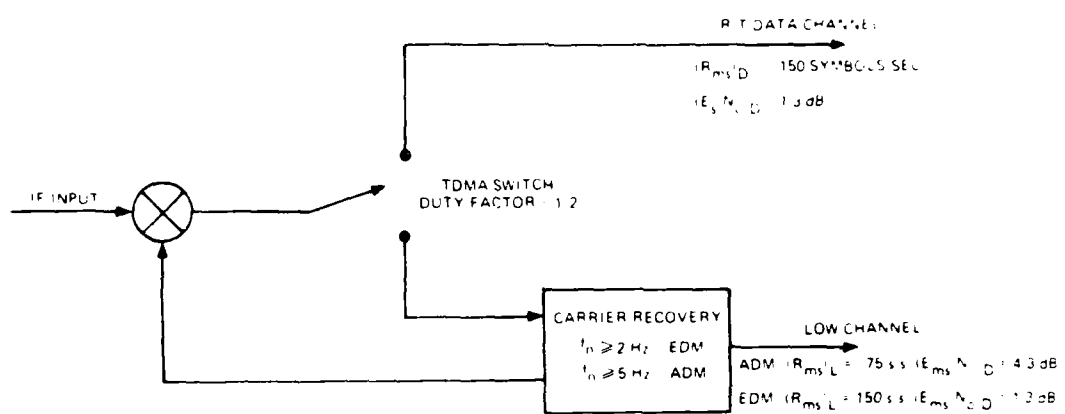


Figure 5-5. Worst Case LOW and R/T Configuration

Advanced Development Model (ADM) and the Engineering Development Model (FDM). For the purpose of our discussion, the difference between these two models is that the EDM LOW has Hamming (16, 11) coding for forward error control FEC and operates at a fixed BPSK symbol rate of 150 S/S while the ADM does not have FEC and operates at a fixed rate of 75 S/S (or equivalently 75 bps).

The R/T channel on both ADM and EDM is convolutionally encoded\* and has variable data rates, the lowest being 75 bps (or equivalent 150 S/S). The TDMA duty factor switch is adjusted to provide the best power tradeoff between LOW and R/T as a function of R/T data rate. As in preceding analyses, to determine demodulation performance, we must calculate carrier phase reference quality defined as the total phase error variance  $\sigma_{tot}^2$ . As before, the quantity  $\sigma_{tot}^2$  is the sum of a phase error variance  $\sigma_{th}^2$  due to thermal noise and a phase error variance  $\sigma_{pn}^2$  due to the untracked portion of the phase noise process on the received signal. Since carrier phase estimates are obtained from the LOW, the thermally induced phase error variance is easily calculated given the LOW energy per modulation symbol/noise density  $(E_{ms}/N_0)_L$ , LOW modulation symbol rate  $(R_{ms})_L$ , LOW carrier tracking bandwidth  $B_\varphi$ , and the appropriate modulation removal loss factor  $\eta_\varphi$ . Calculation of the phase error variance  $\sigma_{pn}^2$  is, however, not as obvious here as in prior analyses. For the purpose of demodulation on the R/T data channel, the phase error variance  $(\sigma_{pn})_D^2$  is due to phase noise in the frequency band  $\{f_n \text{ to } (R_{ms})_D/2\}$  when  $f_n$  is the LOW PLL corner frequency and  $(R_{ms})_D/2$  is one half the R/T PSK symbol rate. As discussed in Section 3, the upper frequency limitation is the result of using integrate and dump filtering which effectively suppresses high frequency phase reference estimation errors. On the other hand, the phase error variance  $(\sigma_{pn})_L^2$  due to phase noise on the LOW is the result of phase noise in the frequency band  $\{f_n \text{ to } (R_{ms})_L/2\}$ . Therefore, if  $(R_{ms})_L = (R_{ms})_D$  as in the lowest FDM

\* See Note 1 of the Annex.

R/T data rate then  $(\sigma_{pn}^2)_L = (\sigma_{pn}^2)_D$ . However, at higher R/T data rates  $(R_{ms})_D \geq (R_{ms})_L$  which gives  $(\sigma_{pn}^2)_D \geq (\sigma_{pn}^2)_L$  so that the total phase error variances for R/T data and LOW are such that  $(\sigma_{tot}^2)_D \geq (\sigma_{tot}^2)_L$ .

Thus, if one were to judge demodulation performance in the R/T channel, based solely upon carrier tracking performance on the LOW, severe errors could occur because of the failure to account for the additional phase noise in the frequency band  $\{(R_{ms}/2)_L \text{ to } (R_{ms}/2)_D\}$ .

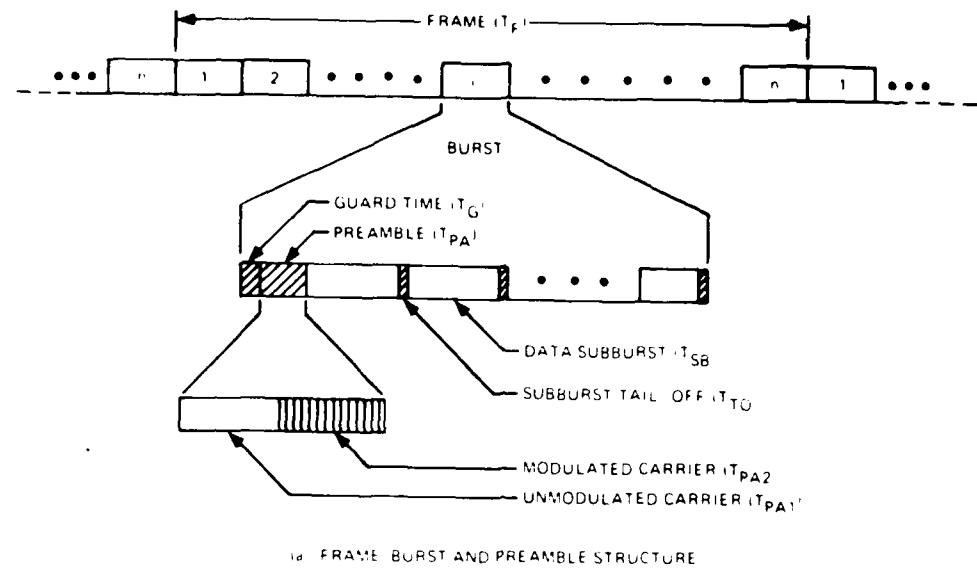
#### 5.2.3 Performance of the USC-28 Operating with Terminals of the Phase II DSCS

A complete analysis of the USC-28 operating with an airborne AN/ASC-18 terminal is given in [1]. The reference gives a complete description of demodulation performance assuming that phase noise improvements are made to the AN/ASC-18 terminal. It was shown that the most critical performance requirements on carrier phase estimation performance (and, therefore R/T demodulation performance) occurred at the lowest R/T data rates, where the phase noise of the improved AN/ASC-18 terminal is similar to that of the cesium II curve of Figure 4-7. Since the cesium II phase noise is expected for HT-MT (AN/MSC-60) and upgraded MSC-46 terminals, performance at low data rates with these terminals will be similar to that shown in [1] for the AN/ASC-18 terminal. At high data rates, the cesium II phase noise performance is better than that of the improved AN/ASC-18; therefore, at high data rates performance of the USC-28 with the HT-MT and upgraded MSC-46 will be better than that shown in [1].

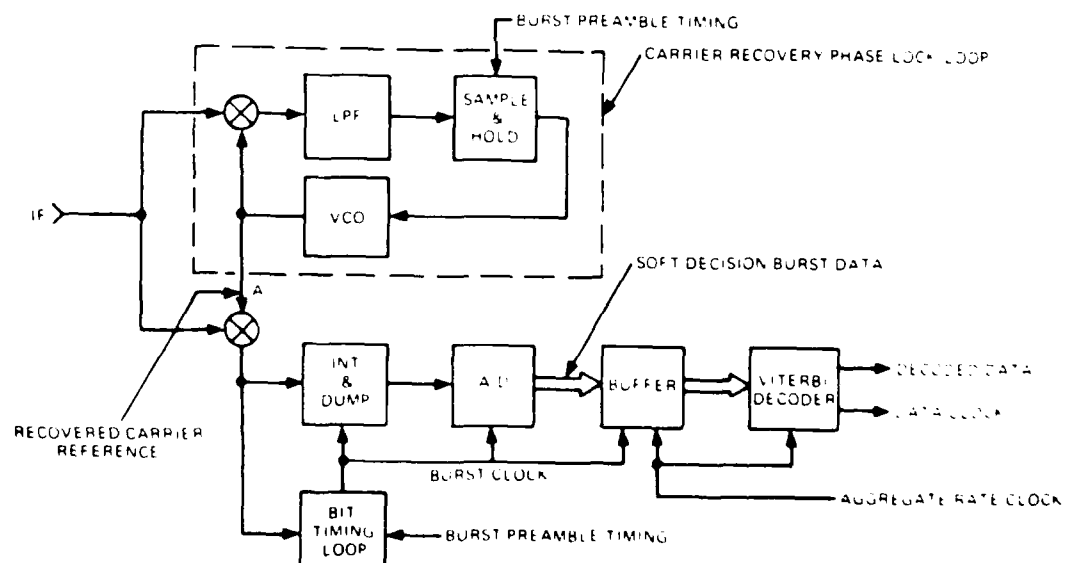
### 5.3 RAYTHEON INC. TDMA (EDM)

#### 5.3.1 General <sup>[17]</sup>

The Raytheon EDM TDMA currently being procured by USASATCOMA is a burst coherent form of TDMA with a preamble preceding each data burst transmission which contains the residual carrier and bit timing references to maintain gated carrier and bit timing tracking loops in appropriate synchronization, within a certain minimum mean square phase error criterion. The frame structure and the basic carrier tracking demodulation and decoding techniques are depicted in Figure 5-6. Figure 5-6(a) shows the TDMA frame composed of  $n$  bursts originating from a network of  $n$  earth terminals each transmitting a burst of data. Each burst includes guard time, preamble time, and subbursts representing individual basebands and subburst tail-off time. The subburst tail-off time results from the desire to share a single error encoder and error decoder with time sequential subbursts of data. The single encoder must be "flushed" and returned to a reference condition before encoding the next subburst of data bits. This results in time in the burst that is unusable for sending data. The preamble is composed of a subburst of unmodulated carrier for carrier reference recovery and a subburst of modulated (alternate "ones" and "zeros") carrier for bit timing reference recovery. The functional demodulator detail necessary for understanding the problem is shown in Figure 5-6(b). TDMA frame, burst and subburst timing are derived (by other circuits not shown in Figure 5-6(b)) and made to gate tracking loops at the appropriate times to permit "sampled data" burst coherent recovery of both carrier and bit timing references to enable efficient coherent demodulation of data subbursts. The recovered carrier reference multiplies the modulated carrier at the appropriate times to demodulate the desired subbursts. This operation is followed by matched filtering (integrate and dump) the noisy data and analog to digital conversion (for soft decision). The soft decision is then converted from burst rate down to an aggregate rate and decoded by a



(a) FRAME, BURST AND PREAMBLE STRUCTURE



(b) FUNCTIONAL DEMODULATOR BLOCK DIAGRAM

Figure 5-6. TDMA Frame and Demodulator Details

### 5.3.2 Impact of Phase Noise Upon TDMA System Performance

One of the most useful measures of system performance for a TDMA system is TDMA frame efficiency  $\eta$  given by the following equation:

$$\eta = 1 - \frac{T_{OH}}{T_F} \quad (5-1)$$

where  $T_{OH}$  = total frame overhead

$T_F$  = total frame duration

However, TDMA frame overhead is a function of many parameters as shown by the following equation:

$$T_{OH} = n T_g + \sum_{i=1}^n T_{PA}(i) + \sum_{i=1}^n T_{TO}(i) \quad (5-2)$$

where  $T_g$  = guard time between bursts

$T_{PA}(i)$  = preamble time for  $i^{\text{th}}$  burst

$T_{TO}(i)$  = subburst tail-off time for  $i^{\text{th}}$  burst.

It may easily be seen that network size  $n$  and connectivity will have a profound influence on frame efficiency. In addition, for networks with various size terminals required preambles  $T_{PA}(i)$  can be considerably different depending upon terminal G/T. Since the number of parameters which can be varied for this type of system is quite large and since our main interest in this paper is to indicate expected demodulation performance of a TDMA system operating in the presence of oscillator phase noise, the scope of the problem will be restricted by the following assumptions:

1. A maximum of 2-3 percent loss in frame efficiency is allocated to that part of preamble time reserved for residual carrier tracking.

2. The preceding frame efficiency loss is to be allocated **equally between 20-30 earth terminals.**
3. Demodulation losses will be based solely upon a 0.2-dB loss due to imperfect carrier phase tracking. All other demodulation losses including those due to symbol timing error are neglected as in the analysis of preceding sections.
4. Demodulation losses are based upon the assumption of soft decision (3 bit) rate 1/2, constraint length 7, Viterbi decoding followed by differential decoding. From the analysis of preceding sections and References 2 and 8, it is easily seen that carrier phase reference error variances of approximately -15 dB and ~ -28 dB are required for coded operation with BPSK and QPSK, respectively.
5. (F. R.) = 1200 frames per second

Assumptions 1 and 2 translate to a required duty factor of 0.001 for residual carrier tracking preamble time.

It has been shown<sup>[18]</sup> that a gated PLL will behave similar to a continuously tracking PLL if the effective loop time constant is much larger than the TDMA frame duration and if the gain in the gated PLL is increased by the duty factor  $d^{-1}$ . Mathematically this may be stated as:

$$\frac{(1-d)}{F.R.} \cdot \frac{\omega_n}{2\zeta} \ll 1 \quad (5-3)$$

where

$$d = \frac{T_{CPA}}{T_F} = \text{carrier preamble duty factor}$$

$T_{CPA}$  = carrier preamble time duration

and  $(\omega_n, \xi)$  are the equivalent continuous PLL (natural radian frequency damping factor).

Therefore, Equation 3-10 (a, b) may be used to calculate PLL carrier tracking error variance provided the energy per symbol to noise ( $E_s/N_0$ ) is replaced by its averaged value over the TDMA frame duration ( $E_s/N_0)_{AV}$  where  $(E_s/N_0)_{AV} = dT_s C/N_0$  where C is the received carrier power and  $T_s$  equals duration of each PSK symbol in the received burst.

Figures 5-7 through 5-12 (see also Tables D-25 through D-46) show expected demodulation performance for the Raytheon EDM TDMA system using a 100-Hz carrier tracking PLL bandwidth and optimum PLL bandwidth. Operation is assumed in the presence of oscillator phase noise contributed by two and three terminals of the following types:

1. Modified HT-MT (Figure 4-1)
2. "Cesium II" (Figure 4-7)
3. "Crystal II" (Figure 4-7).

The reader is reminded that all references to "bits" in the tables refer to "modulation bits" while in the figures the term "bits" refer to "information bits." Thus, due to the rate of 1/2 coding, the following relationships hold.

$$R_{ib} = R_{mb}/2$$

$$\text{and } E_{ib}/N_0 = E_{mb}/N_0 + 3 \text{ (dB)}$$

where

$R_{ib}$  = Information bit rate (information bps)

$R_{mb}$  = Modulation bit rate (modulation bps)

Tables S-3 (a) and (b) summarize the minimum and maximum allowable Raytheon TDMA data rates when used with possible phase noise contributions expected in the Phase II DSCS. Table S-3 (a) shows these results when a constant PLL noise bandwidth of 100 Hz (one sided) is used and Table S-3 (b) shows results when an optimum PLL bandwidth is chosen as a function of data rate. These tables (and Figures 5-7 through 5-12) show that dramatic improvements in performance are obtained when an optimum PLL noise bandwidth is used. They also show that the additional complexity of a variable bandwidth PLL is well justified based on demodulation improvements.

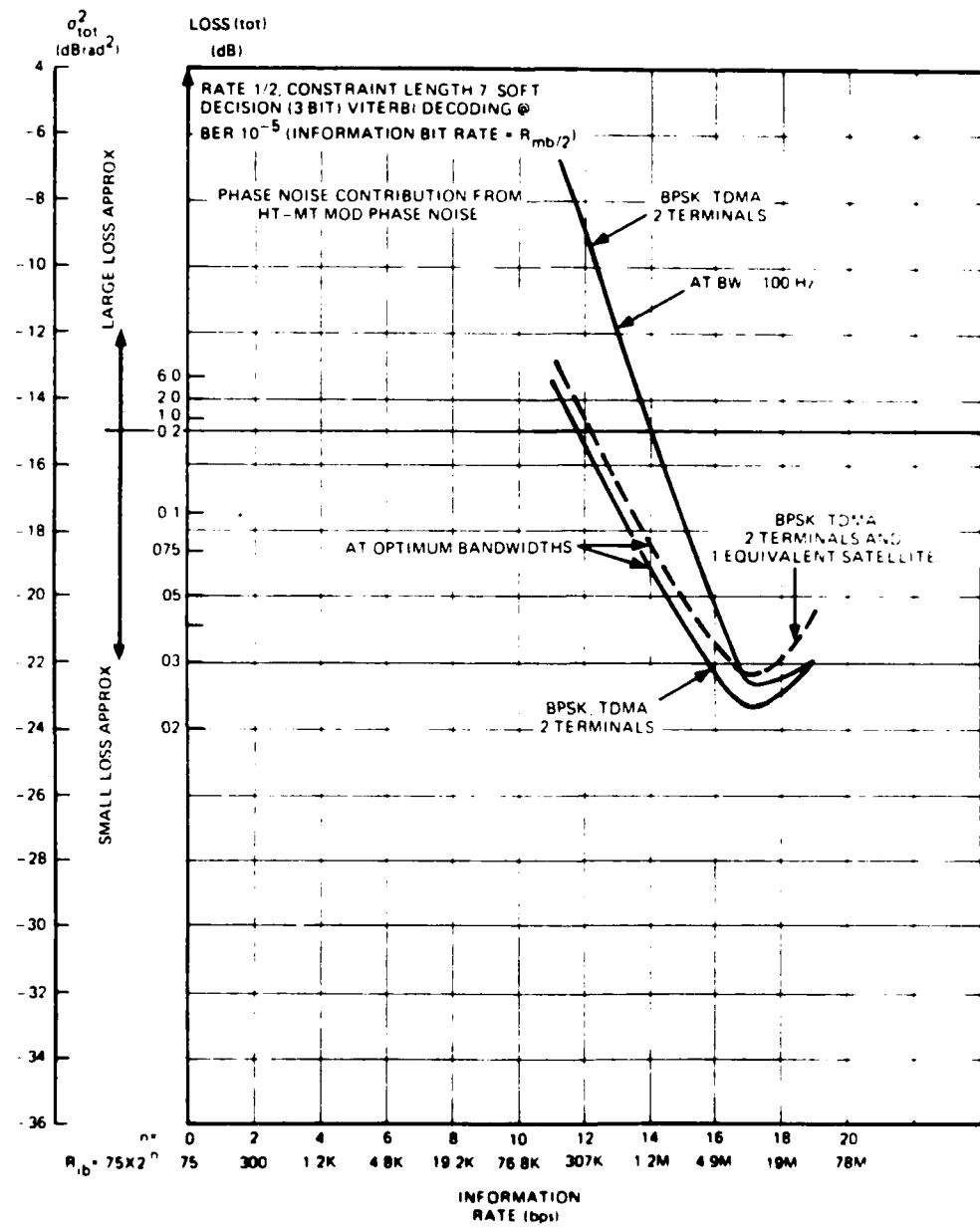


Figure 5-7. Raytheon Inc. BPSK TDMA Demodulation Loss (dB),  $L_{tot}$ , and Total Phase Variance,  $\sigma_{tot}^2$  versus Information Bit Rate,  $R_{ib}$ (bps)

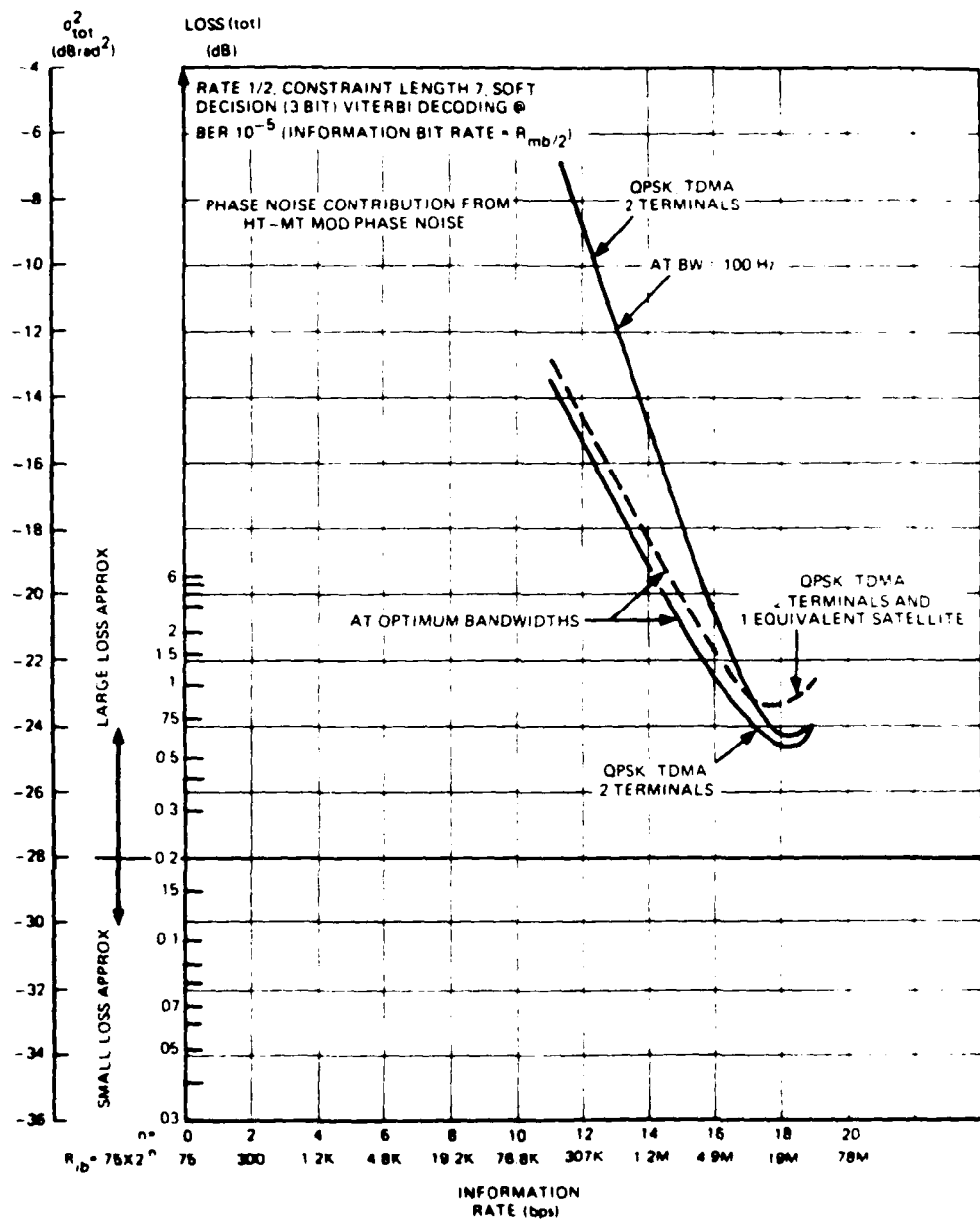


Figure 5-8. Raytheon Inc. QPSK TDMA Demodulation Loss (dB),  $L_{tot}$ , and Total Phase Variance,  $\sigma_{tot}^2$ , versus Information Bit Rate,  $R_{ib}$  (bps)

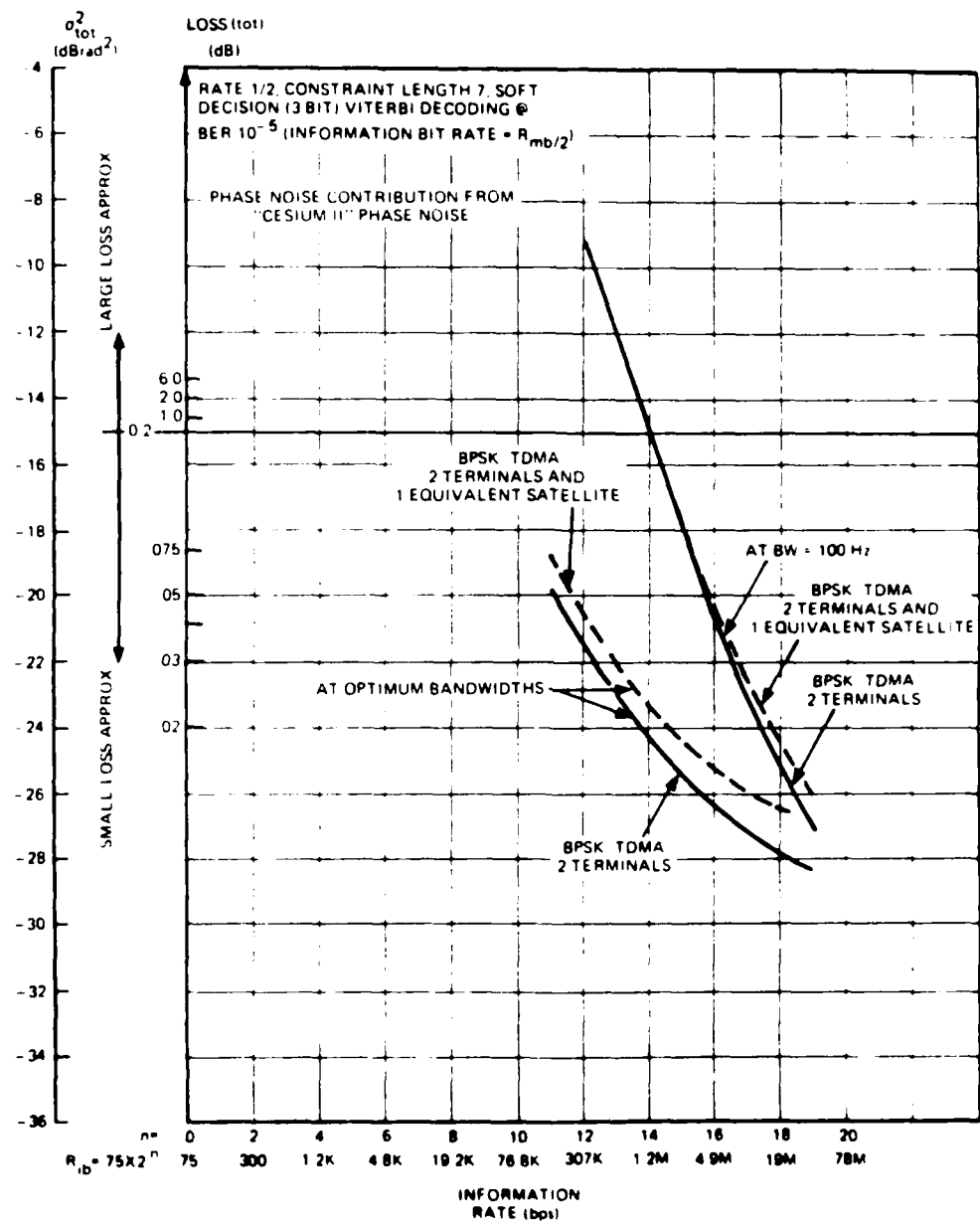


Figure 5-9. Raytheon Inc. BPSK TDMA Demodulation Loss (dB),  $L_{tot}$ , and Total Phase Variance,  $\sigma_{tot}^2$ , versus Information Bit Rate,  $R_{ib}$  (bps)

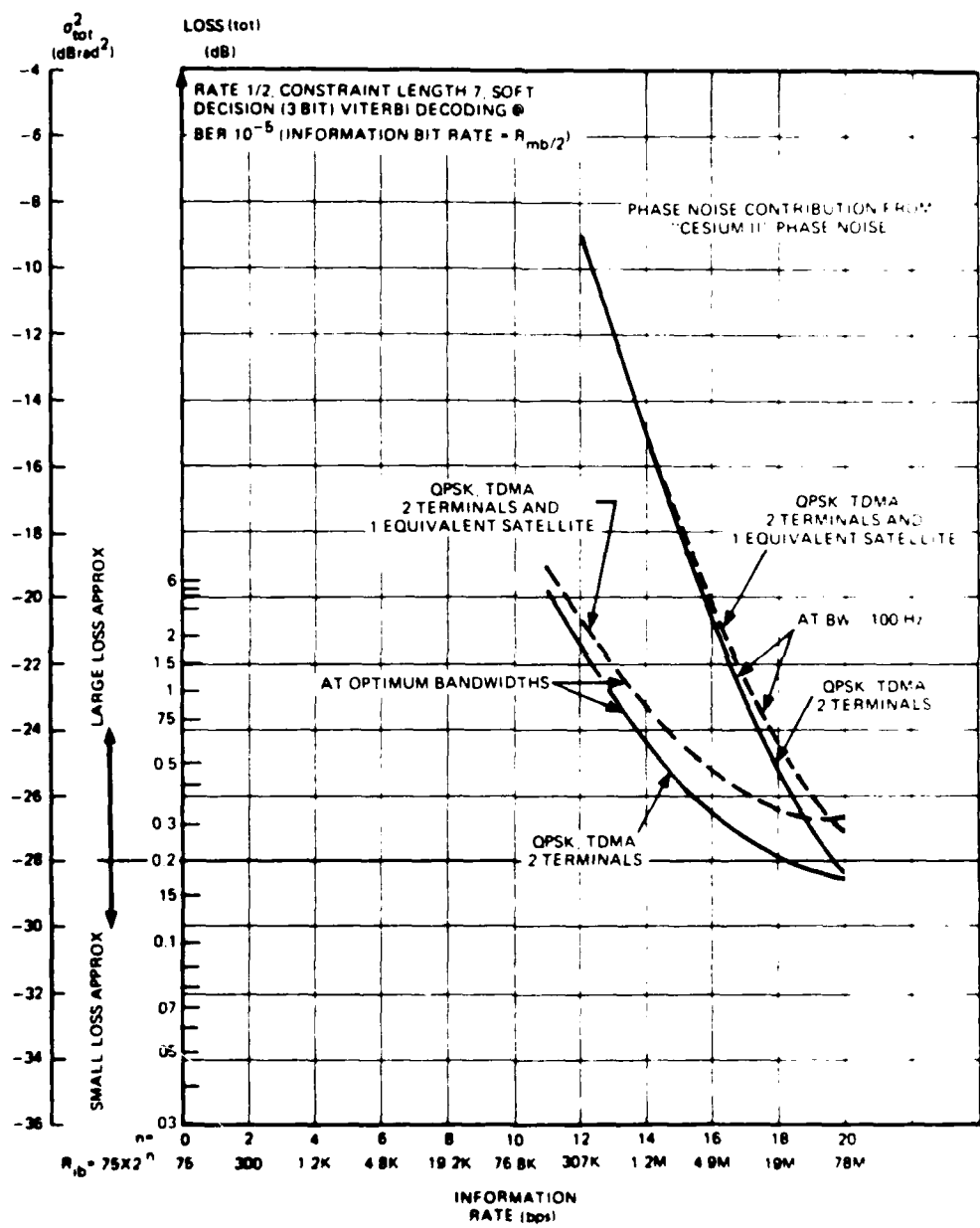


Figure 5-10. Raytheon Inc. QPSK TDMA Demodulation Loss (dB),  $L_{\text{tot}}$ , and Total Phase Variance,  $\sigma_{\text{tot}}^2$ , versus Information Bit Rate,  $R_{\text{ib}}$  (bps)

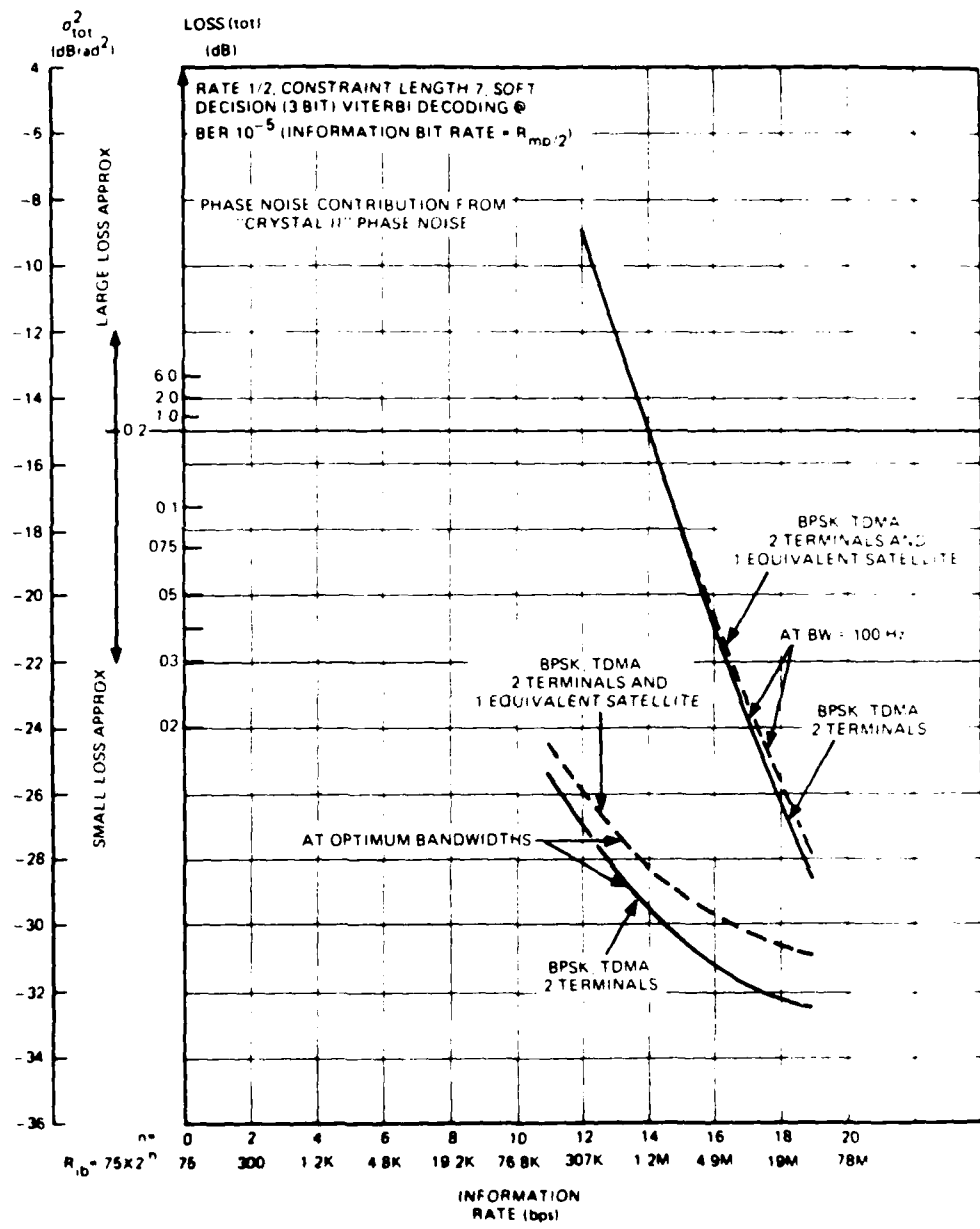


Figure 5-11. Raytheon Inc. BPSK TDMA Demodulation Loss (dB),  $L_{tot}$ , and Total Phase Variance,  $\sigma_{tot}^2$ , versus Information Bit Rate,  $R_{ib}$  (bps)

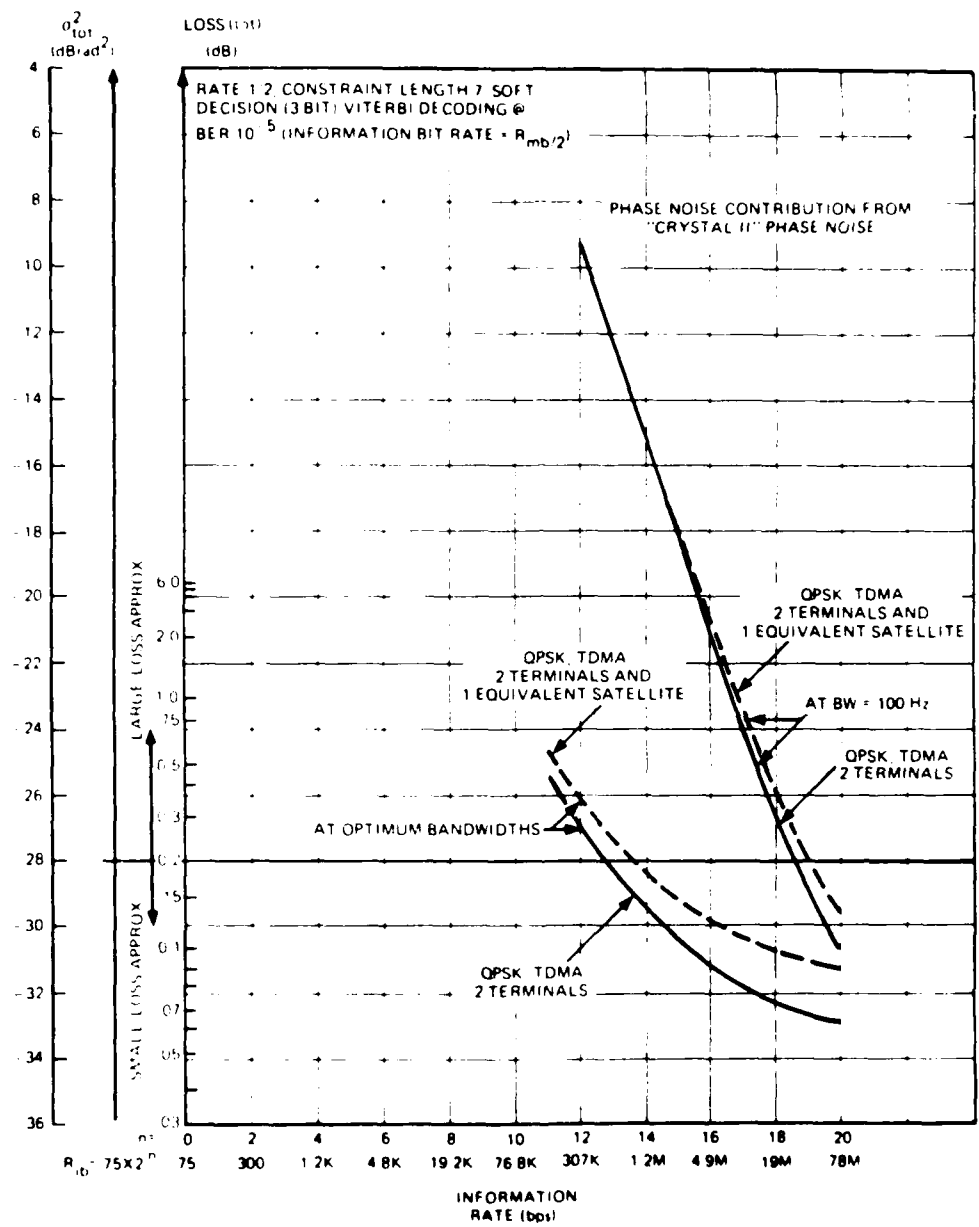


Figure 5-12. Raytheon Inc. QPSK TDMA Demodulation Loss (dB),  $L_{tot}$ , and Total Phase Variance,  $\sigma_{tot}^2$ , versus Information Bit Rate,  $R_{ib}$  (bps)

## SECTION 6 - PHASE NOISE SPECIFICATIONS FOR TERMINALS OF THE DSCS

### 6.1 ANALYTICAL STUDY

All of the preceding performance analyses were based on the assumption of a known or specified oscillator phase noise spectral density. Because system performance results depend primarily on the area under the phase noise density curve between the PLL corner frequency and the PSK symbol rate, it is possible to specify an infinite number of phase noise spectra which will meet certain performance criteria. On the other hand, if we are to devise a phase noise specification that will ensure stated system performance measure, it should be remembered that the particular shape has only secondary influence on the performance. Only the total phase noise power from the corner frequency of the loop to one-half the symbol rate is of concern. Therefore, it is logical and convenient to set standards for the maximum phase noise power in a given band. Since most frequency sources show phase noise characteristics  $f^{-s}$  with the exponent  $s$  ranging from 1 to 3, the most critical characteristic  $f^{-3}$  may be assumed in determining the frequency band to be specified. Then, whatever the actual phase noise characteristic may be, the total phase noise variance can be met.

Stated more explicitly, if the phase noise specification is based on an  $f^{-s_1}$  phase noise characteristic about the loop corner frequency  $f_n$  and if  $f^{-s_2}$  phase noise is actually experienced, the total phase noise variance can be lowered relative to its specified value, provided  $s_2 < s_1$ . (We will prove this for  $s$ -values larger than 1 since we can infer about  $s \leq 1$  by continuity.) It can be verified as follows. If the phase noise variance in the band specified by assuming  $f^{-s_1}$  phase noise equals the phase noise variance for  $f^{-s_2}$  phase noise then from Equation (3-31) we have

$$\frac{\frac{H_{s_1}}{s_1-1} + L x_{s_1}}{(s_1-1) x_{s_1}} = \frac{\frac{H_{s_2}}{s_2-1} + L x_{s_1}}{(s_2-1) x_{s_1}} \quad (s_1 > s_2 > 1) \quad (6-1)$$

so

$$H_{s_2} - \frac{s_2-1}{s_1-1} H_{s_1} - x_{s_1} \quad (s_1 > s_2 > 1) \quad (6-2)$$

Since the optimum x-value for an  $f^{-s_2}$  phase jitter characteristic is given by

$$x_{s_2} = \sqrt{\frac{H_{s_2}}{L}} - \sqrt{\frac{s_2-1}{s_1-1}} x_{s_1} \quad (s_1 > s_2 > 1) \quad (6-3)$$

the minimum total phase noise variance

$$\sigma_{s_2}^2 = \frac{s_2}{s_2-1} L x_{s_2} \quad (s_2 > 1)$$

$$\frac{s_2}{s_2-1} \sqrt{\frac{s_2-1}{s_1-1}} L x_{s_1} \quad (6-4)$$

is less than  $\sigma_{s_1}^2 = \frac{s_1}{s_1-1} L x_{s_1}$  for  $s_2 < s_1$  because the function

$$\frac{\sigma_s^2}{\sigma_{s_1}^2} = f(s) = \frac{s}{s_1} \left( \frac{s_1-1}{s-1} \right)^{1-\frac{1}{s}} \quad (s_1 > s > 1) \quad (6-5)$$

is monotone and increasing for  $s < s_1$ .\* Thus we can conclude that  $f^{-3}$  phase noise is more critical than for example  $f^{-1}$  or  $f^{-2}$ .

---

\* It follows that  $f(s)$  has these properties because the derivative of  $f(s)$  is positive for  $1 < s < s_1$  as shown in Appendix B.

AD-A100 722 COMPUTER SCIENCES CORP FALLS CHURCH VA  
EFFECTS OF PHASE NOISE AND THERMAL NOISE UPON COHERENT PSK DEMO-ETC(U)  
AUG 74 H I PAUL, P A KULLSTAM DCA100-73-C-0008  
NL

UNCLASSIFIED

2 of  
AD-A  
100-722

END  
DATE  
FILED  
8-81  
DTIC

Based on the assumption that we are faced with an  $f^{-3}$  phase noise characteristic, the resulting phase noise variance from the band  $f_0$  to  $\infty$  is given by

$$\frac{h_3}{2 f_0^2} \int_{f_0}^{\infty} \frac{h_3}{f^3} df \quad (6-6)$$

Equating this with the contribution due to  $f^{-3}$  phase noise in Equation (3-20), it implies that when using a PLL with a matched filter processor the lower band frequency should be set to

$$f_0 = \frac{B_\phi}{4.3} \quad (6-7)$$

Furthermore, if we set the upper band limit to  $R_s/2$ , the phase error variance, due to phase noise (power) in the band  $(f_0, R_s/2)$ , will give an upper bound to the minimum achievable phase noise variance according to Equation (3-20) (regardless of whether  $f^{-1}$ ,  $f^{-2}$ , or  $f^{-3}$  phase noise is dominating).

From [2] and [8] it is known that to prevent more than 0.2 dB in equivalent power loss, due to phase noise at the decision point, it will be necessary that phase noise variance  $\sigma_{tot}^2 \approx -15$  dB from BPSK and  $\sigma_{tot}^2 \approx -28$  dB for QPSK when coding is used. Assuming an  $f^{-3}$  phase noise characteristic, the system should be designed such that two-thirds of the total phase noise variance  $\sigma_{tot}^2$  is due to the phase-locked loop variance caused by the additive Gaussian noise. That is, the equivalent power loss requirement translates into the loop phase noise variances.

$$\sigma_{th}^2 = -16.77 \approx -17 \text{ dB for BPSK} \quad (6-8)$$

$$\sigma_{th}^2 = -29.77 \approx -30 \text{ dB for QPSK}$$

where according to Equation (3-9) we have

$$\sigma_{th}^2 = \frac{N_o B_\phi}{E_s R_s} \eta_\phi \quad (6-9)$$

At the operation point  $E_s/N_o = E_{mb}/N_o = 1.3$  dB for rate 1/2 coded BPSK and  $E_s/N_o = E_{mb}/N_o + 3 = 4.3$  dB for coded QPSK. Furthermore, from Table A-1 (taken from [8]) the values of the degradation factor  $\eta_\varphi$  are given both for decision-feedback (DF) and matched filter (MF power loop implementations).

Thus, given  $\sigma_{th}^2$ ,  $E_s/N_o$  and  $\eta_\varphi$  we can calculate the corresponding  $B_\varphi/R_s$  ratio using Equation (6-7) and, using  $f_0 = B_\varphi/4.3$ , determine the corresponding frequency specification band ( $f_0, R_s/2$ ) for a given PSK symbol rate  $R_s$ . This has been carried out and the general algorithmic structure has been presented in Table 6-1 and a specific set of frequency bands was given in Table S-4 and Figure S-1. Note that the power loop implementation will specify wider bands, which means that a prescribed phase noise variance (power) requirement will be harder to meet. (The last band for  $R_s = 80$  M symbols per second has been modified and extended down to 23 Hz since it refers to the TDMA operation. Use of a loop having a noise bandwidth of 100 Hz has been suggested.)<sup>[17]</sup>

Having determined the frequency bands that are related to the data rates, we must now determine the allowable phase noise power in these bands. In Table 1-5 the maximum phase noise power in a particular band is given for a set of equivalent power loss\* values using the Gaussian loss approximation.<sup>[8]</sup> The table also distributes the total phase noise contributions on two and three terminals. The two-terminal case is applicable when the satellite has a negligible phase noise contribution, and it is assumed that the transmitting and receiving terminals have equal contributions. The three-terminal case assumes the satellite has a contribution equal to one of the terminals.

An example of the use of the preceding techniques for generating a phase noise specification is given in Paragraph 6.2. Phase noise specifications for the AN/MSC-60 (HT) "follow-on" and the AN/MSC-46 "upgrade" are given in Tables 1-6 and 1-7, respectively.

\*A word of caution: It is impossible to satisfy demodulation loss criteria (minimum MSE) while simultaneously having inadequate carrier tracking loop cycle skipping performance. Criteria for these parameters must also be satisfied in any system analysis.

Table 6-1. Algorithm for Generating Frequency Specification Bands  $\{f_o, R_s/2\}$   
 $\{R_s - PSK \text{ symbol rate}\}$

$\frac{R_s}{2} / f_o$	
BPSK	QPSK
Matched Filter Power Loop	110
Decision Feedback	92
	1435

## 6.2. APPLICATIONS

### 6.2.1 General

Terminal phase noise specification designed for BPSK systems in the DSCS are derived using the following assumptions:

1. Rate 1/2, constraint length 7, convolutional encoding with soft decision (3-bit) Viterbi decoding is used (see Table 1-5).
2. Maximum allowable demodulation loss to the imperfect carrier phase estimation is < 0.2 dB (see Table 1-5).
3. Equal phase noise contribution from terminal transmitter, terminal receiver and satellite (see Table 1-5).
4. Conservative case; systems will use matched filter power loops for carrier phase estimation (see Table 6-1).

### 6.2.2 BPSK System Specifications

In addition to the assumptions listed in the preceding section, specific equipments notably the Radiation BPSK MD-921G modem have the following PSK symbol rate limitations:

32 Ksps - 10 Msps

Using Table 6-1 and the assumptions in Paragraph 6.2.1, the following two frequency bands may be derived using the lowest and highest BPSK symbol rates:

(145 Hz - 16 kHz)

and

(45.5 kHz - 5 MHz)

That is,  $\{ f_o, R_s/2 \}$  where  $\frac{R_s}{2} / f_o = 110$ .

Using Table 1-4 note that in each of the preceding bands the total phase noise added to any transmitted or received carrier should not exceed -24.5 dB rad<sup>2</sup> to keep demodulation losses, due to errors in carrier phase estimation,  $\leq 0.2$  dB. Since the above described modem may be used for any BPSK symbol rate within the stated limits, a complete specification would require additional overlapping specification bands. This composite phase noise specification (overlapping bands) may easily be satisfied by state of the art designs. Therefore a simplified, but slightly more stringent single band specification which is still easily achieved by state of the art techniques is given by the following:

#### BPSK Specification

The total spurious content added to any transmitted or received carrier, including phase noise and discrete spurious signals from both sides of the carrier, shall be at least 25 dB below the carrier level when measured in a band 145 Hz to 5 MHz from the carrier frequency.

In the preceding specification an attempt has been made to use language and style suited to actual equipment specifications.

#### 6.2.3 QPSK System Specifications

Techniques analogous to those used for BPSK are used to derive QPSK phase noise specifications.

For the DSCS, QPSK symbol rates are expected within the ranges:

(32 Ksps - 40 Msps)

From Table 6-1 and the assumptions of Paragraph 6.2.1 a series of overlapping specification bands ( $f_o$ ,  $R_s$ ) where  $\frac{R_s}{2} / f_o = 2850$  may be derived.

Then using Table 1-4 and the same set of assumptions, the following specifications may be derived for QPSK signaling.

#### QPSK Specification

The total spurious content added to any transmitted or received carrier, including phase noise and discrete spurious signals from both sides of the carrier shall be at least 37.5 dB below the carrier level when measured in the following bands:

- 5 Hz to 16 Hz from the carrier frequency
- 20 Hz to 76 kHz from the carrier frequency
- 200 Hz to 0.6 MHz from the carrier frequency
- 1.7 kHz to 5 MHz from the carrier frequency
- 7 kHz to 20 MHz from the carrier frequency.

#### 6.2.4 Phase Noise Specifications for MRL's USC-28 BPSK Spread Spectrum

The USC-28 may essentially be treated as a modified BPSK system after the PN sequence has been removed as discussed in Paragraph 5.2.3 of this report. Carrier phase estimates are derived from the LOW. Worst case operation (from a phase noise point of view) is a rate 1/2 coded LOW at 150 BPSK symbols per second and an  $E_s/N_0 = 1.3$  dB (energy per modulation symbol, noise density). If the R/T channel operates at 150 BPSK symbols per second with an  $E_s/N_0 = 1.3$  dB the carrier phase estimation problem is equivalent to that for an ordinary 150 BPSK symbol rate system.

Thus the following frequency band ( $f_o$ ,  $R_s/2$ ) derived as in Paragraph 6.2.2  
(.6 - 75 Hz) where  $\frac{R_s}{2} / f_o = 110$ .

Using Table 1-4 and the assumption of Paragraph 6.2.1, the total phase noise added to any transmitted or received carrier should not exceed -24.5 dB rad<sup>2</sup>  $\approx$  -25 dB rad<sup>2</sup> to keep demodulation losses due to errors in carrier phase estimation  $\leq$  0.2 dB.

As noted in Paragraph 5.2.3, even at high data rates the carrier phase estimate was derived from the LOW which was constrained (in rate 1/2 coded operation) to operate at a 150 BPSK symbol per second rate. Operation at the highest BPSK symbol rate (5 msps) means that the effective phase noise band is stretched to become (0.6 Hz-2.5 MHz). However, operation of the USC-28 is such that at the high data rates so much additional power is added to the LOW ( $E_s/N_0 \gg 1.3$  dB) that losses due to thermally induced errors in carrier phase estimation become negligible. Thus, from Table S-5 the total error variance  $\sigma_{tot}^2 = -15$  dB rad<sup>2</sup> for a 0.2 dB demodulation loss may be assumed to be caused by untracked oscillator phase noise and distributed equally (1/3 allocation or -4.77 dB) to give -19.77 rad<sup>2</sup> for each of the up- and down-converters and the satellite. Thus, the following terminal phase noise specification is generated for terminals operating with the USC-28 BPSK spread spectrum system.

#### Specification for USC-28

The total spurious content added to any transmitted or received carrier, including phase noise and discrete spurious signals, shall not exceed conditions specified in the following paragraphs.

1. Total spurious content from both sides of the carrier shall be at least 25 dB below the carrier level when measured in a band 0.6 Hz to 75 Hz from the carrier frequency.
2. Total spurious content from both sides of the carrier shall be at least 20 dB below the carrier level when measured in a band 0.6 Hz to 2.5 MHz from the carrier frequency.

#### 6.2.5 Phase Noise Specifications for Raytheon Inc.'s Burst Coherent TDMA

As discussed in Paragraph 5.3 of this report the 100 Hz carrier tracking PLL bandwidth for the TDMA system is constrained to much less than the TDMA frame rate independent of the actual BPSK or QPSK symbol rate. The

most critical (i.e., largest) frequency band may therefore be derived by using the highest QPSK symbol rate of 80 msps and Equation (6-7). The TDMA band is thus (23 Hz-40 MHz) or  $\{B_\phi/4.3, R_s/2\}$  where  $B_\phi = 100$  Hz.

Using Table S-4 the following specification is derived for QPSK TDMA where demodulation losses due to imperfect carrier phase estimation are  $\leq 0.2$  dB.

#### Phase Noise Specifications for Raytheon Inc. TDMA

The total spurious content added to any transmitted or received carrier including phase noise and discrete spurious signal from both sides of the carrier shall be at least 37.5 dB below the carrier level when measured in a band 23 Hz-40 MHz from the carrier frequency.

#### 6.2.6 Summary

In Paragraph 6.2 phase noise specifications have been presented for various equipment expected to be operational in the DSCS. Since the AN/MSC-60 (HT) follow-on earth terminal is expected to work with all or some modified version of the preceding equipment, all of the specifications of Paragraph 6.2 must be equalled or exceeded by this earth terminal.

Deleting all but the most stringent specifications gives the proposed specification on phase noise for the follow-on AN/MSC-60 (HT) earth terminal shown in Table S-6.

#### 6.3 PHASE NOISE SPECIFICATIONS FOR THE AN/MSC-46 "UPGRADE"

Preceding derivations of phase noise specifications for the AN/MSC-60 (HT) follow-on included all contributions to phase noise on the transmitted or received signal including the effects of the frequency standard which is the basic source of all frequencies in the terminal. However, the AN/MSC-46 upgrade will be based on terminal designs for which the frequency standard

will be government furnished equipment (GFE) procured under separate contract.

Therefore a sub-system phase noise specification must be generated for terminal designs excluding the effects of a frequency standard. Of course these subsystem phase noise specifications must be consistent with total phase noise specifications on terminals with a frequency standard.

Considerable difficulty is experienced when attempting to allocate phase noise between the terminal itself and its frequency standard. This difficulty occurs in spite of the fact that phase noise due to the standard dominates at very low frequencies while phase noise due to the terminal dominates at higher frequencies because the crossover frequency between these two phase noise sources is a function of very specific equipment designs.

However, discussions with both a Fluke representative and Comtech proved that Fluke's 6160 A/AO synthesizer has a 3-pole 200 Hz low pass filter which filters phase noise due to the frequency standard beyond this point. Since the Fluke synthesizer is an integral part of the AN MSC-46 upgrade design we can state that phase noise due to the standard will dominate at frequencies below 200 Hz while phase noise due to the terminal itself will dominate at frequencies above 200 Hz.

The terminal phase noise specifications for the AN MSC-46 upgrade shown in Table S-7 is seen to be a modification of the phase noise specifications for the AN MSC-60 (HT) follow-on (Table S-6) only within the region below 200 Hz. A comparison of these phase noise specifications in the frequency band (0.6 Hz-75 Hz) indicates that the phase noise contribution due to the "terminal only" must be 12 dB below that due to the frequency standard, i.e., less than 0.25 dB additional phase noise caused by the "terminal only." A second band has also been derived in the same manner to cover the frequency band (1.8 Hz-200 Hz).

In summary, phase noise specifications have been derived for terminal designs which do not include a frequency standard (as in Table S-7 for the upgraded AN/MSC-46). To meet total system phase noise specifications, frequency standards must be chosen that satisfy the total specification. At this time a complete set of phase noise specifications have not been derived for the frequency standard independent of the terminal design. Thus, for the present, frequency standards are best evaluated in conjunction with a specific terminal design.

## ANNEX

### NOTE 1:

In this paper the term Soft Viterbi decoding represents the following set of operational values.

It is assumed that rate 1/2, constraint length 7, convolutional encoding is preceded by a differential encoding process as shown in Figure 2-1. On the receiver side it is assumed that soft Viterbi (8-level) decoding is performed and then followed by differential decoding. The nominal BER at the system output is assumed to be  $10^{-5}$  required an energy per information bit/noise density  $E_{ib}/N_0 = 4.3$  dB. Due to the rate 1/2 structure of the encoding process this corresponds to an energy per modulation bit/noise density  $E_{mb}/N_0 = 1.3$  dB.

### NOTE 2:

An additional degradation factor<sup>[9]</sup> should also be included for decision feedback loops since the phase error at the symbol decision point causes an increase in the number of erroneous symbol decisions which directly change the loop gain by  $(1 - 2P_s \sin^2 \frac{\pi}{M})$  where  $P_s$  is the symbol error probability and  $M$  is the type of PSK modulation.

Loop corner frequency  $f_n'$  as defined by Equations (3-11) through (3-14) is proportional to the square root of loop gain and therefore  $f_n'$  should be modified as:

$$f_n' = f_n \sqrt{1 - 2P_s \sin^2 \frac{\pi}{M}}$$

For small values of  $P_s$  this effect on the corner frequency may be neglected.

### NOTE 3:

It is assumed that the B5400 crystal would eventually be phase-locked to an atomic standard to prevent long-term frequency drifts of the crystal.

oscillator. However, in this report it is assumed that the bandwidth at which the crystal is phase-locked to the atomic standard would be considerably smaller (< a factor of 10) than the optimum bandwidth of the receiver tracking loops. Under these conditions the effects of phase noise in the atomic standard may be neglected as in the curve labelled "crystal II" of Figure 4-7. Of course, the analysis in this report could easily be used to indicate expected performance should the appropriate data become available.

APPENDIX A - PARTIALLY COHERENT M-ARY  
PSK DEMODULATION LOSS FUNCTIONS

In [6] it is shown that the variance of the phase estimate obtained using a power loop tracking on M-ARY PSK signal in the presence of additive white Gaussian noise (AWGN) is given by:

$$\sigma^2 = \frac{N_o B}{E_s R_s} \eta_\varphi \quad (A-1)$$

where

$$\eta_\varphi = \eta_\varphi^{(P)} = \frac{1}{M^2} \sum_{k=1}^M \binom{M}{k}^2 k! \left( \frac{N_o}{E_s} \right)^{k-1} \quad (A-2)$$

In [8] it is shown that the variance of the phase estimate obtained using decision feedback (DF) tracking an M-ARY PSK signal in the presence of AWGN is also given by Equation (A-1) where:

$$\eta_\varphi = \eta_\varphi^{(d)} = \frac{1 + 2P_s \frac{E_s}{N_o} \left[ \sin^2\left(\frac{2\pi}{M}\right) - \frac{4N_o}{3E_s} \sin^2\left(\frac{\pi}{M}\right) \right]}{\left[ 1 - 2P_s \sin^2\left(\frac{\pi}{M}\right) \right]^2} \quad (A-3)$$

$P_s$  modulation symbol error probability (i.e., the probability that the symbol is received correctly is  $1 - P_s$ ) and all other parameters are as defined in Sections 2 and 3.

Evaluation of (A-2) and (A-3) is provided in Table A-1 for various configurations of interest. Also shown in Table A-1 are tabulated loss functions for symbol timing loops which have not been considered in this report.

---

\* This correction factor differs slightly from the one given in [9]. The difference lies in the precise definition of loop bandwidth. The above form is preferred.

Table A-1. Performance Comparison of Decision-Feedback and Power Loop Implementations for M-ary PSK Demodulation

DECISION FEEDBACK IMPLEMENTATION  
 ET<sub>A1</sub> = CARRIER PHASE ESTIMATION LOSS  
 ET<sub>A2</sub> = SYMBOL TIMING ESTIMATION LOSS

POWER LOOP IMPLEMENTATION  
 ET<sub>A3</sub> = CARRIER PHASE ESTIMATION LOSS  
 ET<sub>A4</sub> = SYMBOL TIMING ESTIMATION LOSS

M = 2	n	INT. TIME/SYM. DURATION = .5			
EP/N <sub>0</sub> (DBI)	ET <sub>A1</sub> (DBI)	ET <sub>A2</sub> (DBI)	ET <sub>A3</sub> (DBI)	ET <sub>A4</sub> (DBI)	
-1.7	1.64578	2.404719	1.66678	4.74661	
0	1.00541	1.74091	1.02541	2.52181	
.3	.904782	1.64732	.904782	1.29124	
1.3	.614955	1.34929	.614955	2.09129	
2	.454478	1.19046	.454478	2.74179	
4	.144925	.783384	.144925	2.16498	
6	2.77372E-2	.517919	2.77372E-2	1.76476	
8	2.21137E-2	.331199	2.21137E-2	1.48754	
10	4.47504E-3	.211893	4.47504E-3	1.30226	
12	9.70724E-4	.134924	9.70724E-4	1.18294	
14	0	.559925E-2	0	1.10506	
M = 3	n	INT. TIME/SYM. DURATION = .5			ET <sub>A4</sub> (DBI)
EP/N <sub>0</sub> (DBI)	ET <sub>A1</sub> (DBI)	ET <sub>A2</sub> (DBI)	ET <sub>A3</sub> (DBI)	ET <sub>A4</sub> (DBI)	
-1.7	2.05909	5.37244	1.48509	2.39206	
0	2.01728	4.02647	2.77427	2.74177	
.3	1.86647	3.81794	.479196	2.64570	
1.3	1.39662	3.18328	.411143	2.34951	
2	1.10049	2.79172	.272394	2.14491	
4	.437178	1.88764	5.41409E-2	1.76470	
6	9.42211E-2	1.25041	3.54841E-2	1.48751	
8	7.48936E-3	.815870	-2.24599E-4	1.30226	
10	1.21179E-4	.526223	-9.22198E-6	1.18294	
12	9.70724E-4	.336949	0	1.10506	
14	0	.214601	0	1.05556	
M = 4	n	INT. TIME/SYM. DURATION = .5			ET <sub>A4</sub> (DBI)
EP/N <sub>0</sub> (DBI)	ET <sub>A1</sub> (DBI)	ET <sub>A2</sub> (DBI)	ET <sub>A3</sub> (DBI)	ET <sub>A4</sub> (DBI)	
-1.7	3.97774	9.1468	1.54557	2.98756	
0	3.19446	6.9307	.961951	2.47078	
.3	2.36110	6.58134	.971136	2.34876	
1.3	2.50861	5.50502	.602147	2.09471	
2	2.17949	4.86274	.645584	1.94467	
4	1.12841	3.711449	.145997	1.61784	
6	.344725	2.20227	2.77207E-2	1.37804	
8	4.38679E-2	1.64582	2.21111E-3	1.23464	
10	1.38979E-3	.934873	4.47504E-5	1.17961	
12	4.95049E-4	.599352	9.70724E-6	1.02774	
14	0	.38208	0	1.02774	
M = 8	n	INT. TIME/SYM. DURATION = .5			ET <sub>A4</sub> (DBI)
EP/N <sub>0</sub> (DBI)	ET <sub>A1</sub> (DBI)	ET <sub>A2</sub> (DBI)	ET <sub>A3</sub> (DBI)	ET <sub>A4</sub> (DBI)	
-1.7	3.73902	29.9389	2.074	2.01727	
0	3.29227	23.5407	2.00001	1.99471	
.3	2.24053	22.5017	2.00227	1.97470	
1.3	3.47265	19.2408	2.004415	1.75061	
2	3.88705	17.1442	1.98197	1.64889	
4	3.64418	12.024	1.45917	1.40770	
6	2.546911	8.14126	1.17470	1.05068	
8	1.370377	5.35972	.566975	1.14488	
10	.381453	3.46141	.162894	1.08223	
12	7.98079E-2	.21051	1.41815E-2	1.04156	
14	4.61977E-3	1.40311	7.08278E-6	1.01691	

In Section 3 of this report we have shown how carrier phase estimation quality (MSE) could be described in terms of phase error variances which depend upon various system parameters (e.g.,  $E_{ib}/N_0$ ,  $S_{\delta\phi}(f)$ ,  $B_\phi$ ,  $\eta_\phi$ , etc.). In the preceding we have also summarized how the modulation removal loss factor  $\eta_\phi$  (required in the calculation of phase error variance) may be calculated for matched filter power loops and decision feedback loops. It remains, however, to indicate how these phase error variances may be translated into demodulation losses from ideal performance. In [8] it is shown that for small demodulation losses, the following equation will provide an accurate description of M-ary PSK demodulation loss  $L$  in dB versus phase error variance in radians.

$$L = 4.34 \sigma^2 \left\{ 1 + \frac{2E_{mb}}{N_0} \log_2 M \left[ \cos^2 \left( \frac{\pi}{M} \right) + \frac{\sigma^2}{2} \left( 1 - 3 \cos^2 \left( \frac{\pi}{M} \right) \right) \right] \right\} \quad (A-4)$$

where

$\frac{E_{mb}}{N_0}$  = energy per modulation bit / noise density expressed in a pure number.

For BPSK and QPSK this result simplifies to:

BPSK ( $M = 2$ )

$$L = 4.34 \sigma^2 \left( 1 - \sigma^2 \frac{E_{mb}}{N_0} \right) \text{ (dB)} \quad (A-5)$$

QPSK ( $M = 4$ )

$$L = 4.34 \sigma^2 \left( 1 - \frac{2E_b}{N_0} - \sigma^2 \frac{E_{mb}}{N_0} \right) \text{ (dB)} \quad (A-6)$$

and if  $\sigma^2 \ll 1$  the following familiar forms result:

BPSK (M = 2)

$$L = 4.34 \sigma^2 \text{ (dB)} \quad (A-7)$$

QPSK (M = 4)

$$L = 4.34 \sigma^2 \left( 1 + \frac{2E_b}{N_o} \right) \text{ (dB)} \quad (A-8)$$

Equations (A-4) through (A-8) will provide accurate loss estimates when the carrier phase estimation error variance  $\sigma^2$  is of sufficiently small magnitude. This accuracy limitation occurs because the preceding equations are based upon an assumption of a Gaussian phase error density as being an accurate characterization of the phase error process in a second order carrier phase estimator. Actually it is known from [5] that even for a first order simple PLL, the Gaussian assumption is only valid at small  $\sigma^2$  values (high signal-to-noise-ratios) and that a Tikhonov phase error density is exact for a first order loop in the presence of AWGN and is also a good approximation for a second order loop. The Tikhonov phase error density is given by the following

$$p(\varphi) = \exp(\alpha \cos \varphi) / 2\pi I_0(\alpha) \quad |\varphi| \leq \pi \quad (A-9)$$

where  $\alpha$  is the PLL signal-to-noise ratio.

Charles Wolfson has assumed that a modified form of the Tikhonov density may be used to describe the phase error process in various power loops (i.e., modulation removal loops such as squaring, quadrupling) to derive demodulation losses for BPSK and QPSK systems. This modified Tikhonov phase error density is given by the following:

$$p(M\varphi) = M \exp[\alpha_M \cos(M\varphi)] / 2\pi I_0(\alpha_M) \quad (A-10)$$

where

$$|\varphi| \leq \pi/M$$

$$M^2 \alpha_M \sim \sigma^{-2}$$

and  $M$  is the maximum number of signal phases.

Since the modified Tikhonov density will approach a Gaussian density for small  $\sigma^2$  (large  $\alpha$ ), losses based upon either technique are in good agreement when demodulation losses are small. In [8] it is shown that results based upon the Gaussian approximation are accurate to within 0.01 dB when

$$L < 0.66 \left( \frac{E_s}{N_0} \right)^{-2/3} \quad (\text{dB}) \quad M = 2 \quad (A-11)$$

and

$$L < 0.4 \quad (\text{dB}) \quad M = 4 \quad (A-12)$$

For the large loss case, it is obvious that neither the Gaussian nor modified Tikhonov density will accurately describe the phase error process in a modulation removal PLL. However, it is believed that the approximation based upon the Tikhonov density will provide the most accurate description of demodulation losses currently available. Due to the nature of the analyses used to derive demodulation losses in [8] and [2, 7] based, respectively, on the Gaussian or Tikhonov densities, it is believed that the former will provide the most accurate characterization for small losses (small  $\sigma^2$ ) while the latter

will provide the most accurate characterization for large losses (large  $\sigma^2$ ). Therefore, in this report a two part (large and small) loss approximation is used to indicate demodulation performance.

In the preceding we have limited our discussion of demodulation losses to PSK systems which are unencoded. To access the impact of convolutional encoding and Viterbi decoding (as described in Note 1 of the Annex to this report) we may use the coder functional as described in [19].

That is;

$$P_e \text{ (coding)} = \text{"const"} \Phi \left( -\sqrt{\frac{2E_b}{N_o}} d_{\min} \right) \quad (A-13)$$

where

$d_{\min} = 10$  is the minimum free distance of the rate 1/2, constraint 7 convolutional code.

Equation (A-13) implies that the net effect of coding is to increasing the effective signal-to-noise ratio by  $10 \log d_{\min}$  in the error function. Thus, in the Gaussian approximation to the loss function (Equations (A-4) through (A-7)) the equivalent losses for the coded case may be calculated with an effective  $E_b/N_o$

$$(E_b/N_o)_{\text{eff}} = E_b/N_o + 10 \text{ dB.}$$

For example, when using the Gaussian approximation and the system described in Note 1, and when  $L = 0.2$  dB

$$\sigma^2 = 14.9 \text{ dB BPSK}$$

$$\sigma^2 = 27.8 \text{ dB QPSK}$$

$$\Phi(x) = \frac{1}{\sqrt{2\pi}} \int_{-\infty}^x \exp(-t^2/2) dt$$

The "const" in Equation (A-13) is not strictly a constant with respect to  $E_b/N_o$  but is much less dependent than the error integral  $\Phi$ .

Results using the Tikhonov phase error density as described above and in [2] and [7] are summarized in Figure A-1.

The following convention has been adopted when plotting all of the (non-linear) demodulation loss scales shown in this report:

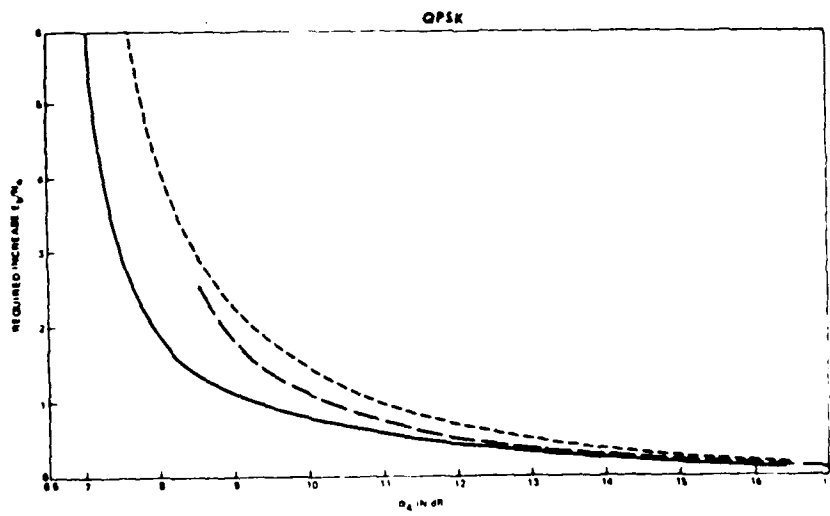
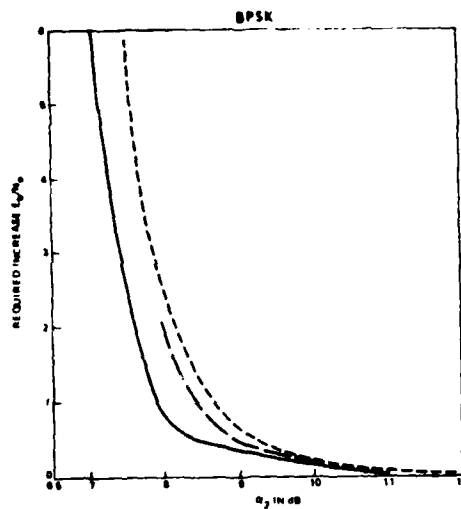
When demodulation losses are less than 0.2 dB, then losses are based upon the Gaussian approximation. When the losses are  $> 0.2$  dB then losses are based upon the Tikhonov approximation.

In our view this two part loss functional with a break point at 0.2 dB represents the best estimate of demodulation losses currently for the coded case.

More recently in [21], loss formulas were derived which indicate that the coded QPSK loss functional (both large and small loss approximation) used in this report may be too conservative. However, if new loss functionals are indeed proved to be more accurate than those used here (especially for QPSK), it is a simple matter to replot the loss ordinates of the demodulation performance curves of this report since the remainder of the analysis will remain affected.

SUPPRESSED CARRIER SYSTEMS

$$P(e) = 10^{-5}$$



————— UNCODED  
 - - - HARD DECISION DEMODULATION (Q=2)  
 - - - - SOFT DECISION DEMODULATION (Q=8)

Figure A-1. Comparison of Degradation Incurred for Auxiliary Carrier, Suppressed Carrier BPSK and QPSK Systems With and Without Viterbi Decoding

## APPENDIX B - VERIFICATION OF WORST CASE PHASE NOISE ASSUMPTION

Verify that Equation (6-5)

$$\frac{\sigma_s^2}{\sigma_{s_1}^2} = f(s) = \frac{s}{s_1} \left( \frac{s_1-1}{s-1} \right)^{1-\frac{1}{s}} \quad (s_1 \geq s > 1) \quad (6-5)$$

is monotone and increasing for  $(1 < s \leq s_1)$ . That is  $f(s) \leq f(s_1)$  when  $1 < s \leq s_1$ .

That  $f(s)$  is monotone and increasing may be seen from the positiveness of the derivative of  $\sigma^2 f(s)$  ( $s_1 \geq s > 1$ ). Now,

$$\sigma^2 f(s) = \sigma^2 \frac{s}{s_1} \left( \frac{s-1}{s} \right)^{1-\frac{1}{s}} \left( \frac{s_1-1}{s-1} \right) \quad s_1 \geq s > 1 \quad (B-1)$$

so

$$\frac{\partial \sigma^2 f(s)}{\partial s} = \frac{1}{2} \sigma^2 \frac{s_1-1}{s-1} \quad (B-2)$$

Since  $(s_1-1) > (s-1)$  when  $(s_1 \geq s > 1)$

$$\frac{\partial \sigma^2 f(s)}{\partial s} > 0 \quad (B-3)$$

and

$$\frac{\partial^2 f(s)}{\partial s^2} > 0 \quad (B-4)$$

Hence, we can conclude that  $f(s) \leq f(s_1)$  for  $1 < s \leq s_1$ .

APPENDIX C - EVALUATION OF INTEGRALS ASSOCIATED  
WITH PHASE NOISE INFLUENCE ON COHERENT PSK DEMODULATION

This appendix presents an evaluation of the integrals

$$I_k = \int_0^\infty \frac{x^k}{1+x^4} \left( \frac{\sin \alpha x}{\alpha x} \right)^2 dx ; \quad \text{for } k = 0, 1, 2, 3, 4; \quad (C-1)$$

associated with phase noise influence on coherent PSK demodulation.

Although these integrals are very similar for all  $k$ -values, a closed form solution can only be obtained for even  $k$ -values using complex integration or residue calculus. For odd  $k$ -values we must settle for approximate integral evaluations.

#### C.1 EVEN K-VALUES

For even  $k$ -values, i.e.,  $k = 0, 2, 4$ , we first rewrite  $I_k$  as

$$I_k = \frac{1}{\alpha^2} \int_0^\infty \frac{x^{k-2}}{1+x^4} \sin^2 \alpha x dx \quad (C-2)$$

For  $k = 0$ ,

$$I_0 = \frac{1}{\alpha^2} \int_0^\infty \left( \frac{1}{x^2} - \frac{x^2}{1+x^4} \right) \sin^2 \alpha x dx \quad (C-3)$$

$$\frac{1}{\alpha^2} \int_0^\infty \frac{\sin^2 \alpha x}{x^2} dx = \frac{1}{2\alpha^2} \int_0^\infty \frac{x^2}{1+x^4} (1-\cos 2\alpha x) dx \quad (C-4)$$

while for  $k = 2$  or  $4$ ,

$$I_k = \frac{1}{2\alpha^2} \int_0^\infty \frac{x^{k-2}}{1+x^4} (1-\cos 2\alpha x) dx \quad (C-5)$$

Since the integrands of all four integrals are even functions, we can evaluate them over the interval  $(-\infty, \infty)$  and obtain twice their values. This method makes it possible to determine the value of a particular integral as the residues of its integrand. Consequently, these integrals are also available in tables such as those published by [20], from which we directly obtain

$$\int_0^{\infty} \frac{\sin^2 \alpha x}{x^2} dx = \frac{\alpha \pi}{2} \quad (C-6)$$

$$\int_0^{\infty} \frac{\cos 2\alpha x}{1+x^4} dx = \frac{\pi \sqrt{2}}{4} e^{-\sqrt{2}\alpha} (\cos \sqrt{2}\alpha + \sin \sqrt{2}\alpha) \quad (C-7)$$

$$\int_0^{\infty} \frac{x^2}{1+x^4} \cos 2\alpha x dx = \frac{\pi \sqrt{2}}{4} e^{-\sqrt{2}\alpha} (\cos \sqrt{2}\alpha - \sin \sqrt{2}\alpha) \quad (C-8)$$

and, by letting  $\alpha \rightarrow 0$  in Equations (C-7) and (C-8),

$$\int_0^{\infty} \frac{dx}{1+x^4} = \int_0^{\infty} \frac{x^2}{1+x^4} dx = \frac{\pi \sqrt{2}}{4} \quad (C-9)$$

Thus we get

$$\begin{aligned} I_0 &= \frac{\alpha \pi}{2\alpha^2} - \frac{\pi \sqrt{2}}{8\alpha^2} + 1 - e^{-\sqrt{2}\alpha} (\cos \sqrt{2}\alpha + \sin \sqrt{2}\alpha) \\ &= \frac{\pi}{2\alpha} \left[ 1 - \frac{\sqrt{2}}{4\alpha} (2\sqrt{2}\alpha + 2\alpha^2 + \frac{2}{3}\alpha^4 + \dots) \right] \\ &= \frac{\pi}{2\alpha} \left( \frac{\sqrt{2}}{2}\alpha - \frac{\sqrt{2}}{6}\alpha^3 \dots \right) \\ &= \frac{\pi \sqrt{2}}{4} \left( 1 - \frac{1}{3}\alpha^2 \dots \right) \quad (C-10) \end{aligned}$$

$$\begin{aligned}
 I_2 &= \frac{1}{2\alpha^2} - \frac{\pi\sqrt{2}}{4} [1 - e^{-\sqrt{2}\alpha} (\cos \sqrt{2}\alpha + \sin \sqrt{2}\alpha)] \\
 &= \frac{1}{2\alpha^2} - \frac{\pi\sqrt{2}}{4} (2\alpha^2 - \frac{4}{3}\sqrt{2}\alpha^3 + \frac{2}{3}\alpha^4 + \dots) \\
 &= \frac{\pi\sqrt{2}}{4} (1 - \frac{2\sqrt{2}}{3}\alpha + \frac{1}{3}\alpha^2 + \dots)
 \end{aligned} \tag{C-11}$$

and

$$\begin{aligned}
 I_4 &= \frac{1}{2\alpha^2} - \frac{\pi\sqrt{2}}{4} [1 - e^{-\sqrt{2}\alpha} (\cos \sqrt{2}\alpha - \sin \sqrt{2}\alpha)] \\
 &= \frac{\pi\sqrt{2}}{8\alpha^2} (2\sqrt{2}\alpha - 2\alpha^2 + \frac{2}{3}\alpha^4 + \dots) \\
 &= \frac{\pi}{2} (\frac{1}{\alpha} - \frac{1}{\sqrt{2}} + \frac{1}{3\sqrt{2}}\alpha^2 + \dots)
 \end{aligned} \tag{C-12}$$

For  $\alpha < 1$ , e.g.,  $\alpha < 0.1$ , we can approximate

$$I_0 = \frac{\pi\sqrt{2}}{4} \tag{C-13}$$

$$I_2 = \frac{\pi\sqrt{2}}{4} (1 - \frac{2\sqrt{2}}{3}\alpha) \tag{C-14}$$

$$I_4 = \frac{\pi}{2} (\frac{1}{\alpha} - \frac{1}{\sqrt{2}}) \tag{C-15}$$

## C.2 ODD K-VALUES

For odd k-values, i.e.,  $k = 1, 3$ , we must settle for approximate evaluations of the values of  $I_k$ . Since we desire to evaluate  $I_k$  for small  $\alpha$ -values, we must first bound the integral

$$I_k = \int_0^\alpha \frac{x^k}{1+x^4} \left( \frac{\sin \alpha x}{\alpha x} \right)^2 dx \tag{C-16}$$

with an upper bound

$$I_k = \int_0^a \frac{x^k}{1+x^4} dx + \frac{1}{\alpha^2} \int_a^\infty \frac{\sin^2 \alpha x}{x^{6-k}} dx \quad (C-17)$$

and a lower bound ( $|\alpha a| < \pi$ )

$$I_k = \left( \frac{\sin \alpha a}{\alpha a} \right)^2 \int_0^a \frac{x^k}{1+x^4} dx - \frac{a^4}{1+a^4} - \frac{1}{\alpha^2} \int_a^\infty \frac{\sin^2 \alpha x}{x^{6-k}} dx \quad (C-18)$$

where the value of  $a$  will be chosen later to obtain tight bounds. The inequalities result from the observations that

$$\left( \frac{\sin \alpha a}{\alpha a} \right)^2 \leq \left( \frac{\sin \alpha x}{\alpha x} \right)^2 \leq 1 \quad \text{for } 0 \leq |\alpha x| \leq |\alpha a| \leq \pi$$

and

$$\frac{a^4}{1+a^4} \leq \frac{x^4}{1+x^4} \leq 1 \quad \text{for } x > a$$

Of the two remaining integrals, the first is elementary for  $k = 1, 3$ . We have

$$\int_0^a \frac{x dx}{1+x^4} = \frac{1}{2} \arctan a^2 \quad (C-19)$$

$$\int_0^a \frac{x^3 dx}{1+x^4} = \frac{1}{4} \ln(1+a^4) \quad (C-20)$$

The other integral can be reduced to a simpler form and expressed in terms of the cosine integral  $ci(x)$ . Since

$$\frac{1}{\alpha^2} \int_a^\infty \frac{\sin^2 \alpha x}{x^{6-k}} dx = \alpha^{3-k} \int_{\alpha a}^\infty \frac{\sin^2 u}{u^{6-k}} du \quad (C-21)$$

and using repeated partial integration with  $\beta = \alpha a$ ,

$$\int_B^\infty \frac{\sin^2 u}{u^5} du = \frac{1}{4} \left( \frac{\sin \beta}{\beta} \right)^2 + \frac{1}{3\beta^2} \frac{\sin 2\beta}{2\beta} + \frac{1}{6} \frac{1}{\beta^2} - \frac{2}{3} \int_B^\infty \frac{\sin^2 u}{u^3} du \quad (C-22)$$

we arrive at

$$\int_B^\infty \frac{\sin^2 u}{u^3} du = \frac{1}{2} \left( \frac{\sin \beta}{\beta} \right)^2 + \frac{\sin 2\beta}{2\beta} - \text{ci}(2\beta) \quad (C-23)$$

where

$$\text{ci}(2\beta) \Delta - \int_{2\beta}^\infty \frac{\cos u}{u} du = \gamma - \ln(2\beta) - \sum_{k=1}^\infty \frac{(-1)^k (2\beta)^{2k}}{2k (2k)!} \quad (C-24)$$

and  $\gamma = 0.577 215 \dots$  is Euler's constant. Thus, we have an upper bound for

$$\begin{aligned} I_1 &= \frac{1}{2} \arctan a^2 + \frac{1}{2} \left[ \frac{1}{4} \left( \frac{\sin \alpha a}{\alpha a} \right)^2 + \frac{1}{3} \frac{\sin 2\alpha a}{2\alpha a} + \frac{1}{6} \right] \\ &\quad - \frac{2}{3} \alpha^2 \left[ \frac{1}{2} \left( \frac{\sin \alpha a}{\alpha a} \right)^2 + \frac{\sin 2\alpha a}{2\alpha a} - \text{ci}(2\alpha a) \right] \end{aligned} \quad (C-25)$$

Keeping the dominating terms for small  $\alpha$ , we get

$$\begin{aligned} I_1 &= \frac{1}{2} \arctan a^2 + \frac{1}{2} \left( \frac{3}{4} - \frac{11}{36} \alpha^2 a^2 \right) - \left( 1 - \frac{2}{3} \gamma \right) \alpha^2 + \frac{2}{3} \alpha^2 \ln 2\alpha a \\ &= \frac{1}{2} \arctan a^2 + \frac{3}{4a^2} - \frac{2}{3} \alpha^2 \ln 2\alpha a - \left( \frac{47}{36} - \frac{2}{3} \gamma \right) \alpha^2 \end{aligned} \quad (C-26)$$

The corresponding lower bound for

$$I_1 = \frac{1}{2} \left( \frac{\sin \alpha a}{\alpha a} \right)^2 \arctan a^2 + \frac{a^4}{1 + a^4} \left( \frac{3}{4a^2} + \frac{2}{3} \alpha^2 \ln 2 \alpha a + \dots \right) \quad (C-27)$$

If we choose  $a = 2.5$ , the upper and lower bound for  $\alpha < 0.1$  will be within 2 percent of each other. Thus, the integral  $I_1$ , with good accuracy, is approximately equal to

$$I_1 = \frac{\pi}{4} + 0.04 + \frac{2}{3} \alpha^2 \ln \alpha + 0.15 \alpha^2 = 0.825 + \frac{2}{3} \alpha^2 \ln \alpha \quad (\alpha < 0.1) \quad (C-28)$$

For  $k = 3$  we have the upper bound

$$\begin{aligned} I_3 &\approx \frac{1}{4} \ln (1 + a^4) + \frac{1}{2} \left( \frac{\sin \alpha a}{\alpha a} \right)^2 + \frac{\sin 2 \alpha a}{2 \alpha a} - \text{ci}(2 \alpha a) \\ &= \frac{1}{4} \ln (1 + a^4) + \left( \frac{3}{2} - \gamma \right) - \ln 2 \alpha a + \frac{1}{6} \alpha^2 a^2 + \dots \end{aligned} \quad (C-29)$$

and the lower bound

$$I_3 \approx \frac{1}{4} \ln (1 + a^4) \left( \frac{\sin \alpha a}{\alpha a} \right)^2 + \frac{a^4}{1 + a^4} \left[ \left( \frac{3}{2} - \gamma \right) - \ln 2 \alpha a + \frac{1}{6} \alpha^2 a^2 + \dots \right] \quad (C-30)$$

Again, with  $a = 2.5$ , the upper bound is within 2 percent of the true value of  $I_3$  for  $\alpha$ -values less than 0.1. Thus we have the approximation

$$I_3 = \ln \frac{1}{\alpha} + 0.235 + 1.04 \alpha^2 \quad (\alpha < 1) \quad (C-31)$$

APPENDIX D - TABULATED RESULTS

Table D-1. BPSK Decision Feedback With HT-MT Mod Phase  
Noise (2 Terminals) (Losses-Soft Decision Viterbi Rate 1/2  
Decoding BER  $10^{-5}$ )

OPTIMUM LOOF BANDWIDTH AND THE COEFFICIENTING  
PHASE NOISE VARIANCE

OSCILLATOR SPECTRAL CHARACTERISTICS

$H_0 = 1.25E-10$  JAT/HZ       $H_1 = 0$  JAT       $H_2 = .01$  JAT\*HZ  
 $H_3 = .2$  JAT\*HZ $^2$

Mod. F11 RATE *	FE-CPT(IF)	PH-VAF(TD)	PH-VAF(TH)	PH-VAF(PN)
F/S	H2	IE	IF	IE
75	6.86532	-9.0945	-11.0654	-13.5151
150	8.64972	-11.067	-13.0782	-15.3874
300	10.8979	-13.0126	-15.0791	-17.2304
600	17.2985	-16.8563	-19.0931	-20.8085
1200	27.4543	-20.613	-23.1076	-24.2085
2400	43.5474	-24.2458	-27.1247	-27.3916
4800	68.91	-27.703	-31.1521	-30.3147
9600	107.913	-30.8574	-35.2848	-39.8358
19200	157.07	-33.0366	-39.6152	-44.1148
4915200	504.219	-33.2059	-40.5706	-44.0861
19641600	967.665	-28.7913	-43.7601	-28.9319
78643200	1900.59	-23.0145	-46.872	-23.0324
CODEC GAIN OF		10	IF	

DEMODULATION LOSSES USING GAUSSIAN  
APPROX. APPROXIMATE WHEN  $< \cdot 116469$

Mod. F11 RATE *	LOSS(TOT) (TE)	LOSS(TH) (TE)	IF	TIKHONOV APPROX. LOSS (TOT) (DB)	LOSS (TH) (DB)
75	1.41504	.698037	>6	>6	
150	.997623	.356174	>6	>6	
300	.363093	.191214	>6	.25	
600	.114408	.6.23682E-2	.12	.1	
1200	.6.81016E-2	.2.26185E-2			
2400	1.71557E-2	8.63430E-3			
4800	7.53394E-3	3.36315E-3			
9600	3.60192E-3	1.30847E-3			
19200	2.17138E-3	4.74904E-4			
38400	9.08781E-4	3.81019E-4			
76800	5.83489E-3	1.82694E-4			
153600	2.31798E-2	8.92096E-5			

\* Information bit rate  $\cdot \frac{1}{2}$  Modulation bit rate

Table D-2. QPSK Decision Feedback With HT-MT Phase Noise (2 Terminals; (Losses-Soft Decision Viterbi Rate 1/2 Decoding BER =  $10^{-5}$ )

OPTIMUM LOOP FANVILITM AND THE CORRESPONDING PHASE NOISE VARIANCE

OSCILLATOR SPECTRAL CHARACTERISTICS

$H_0 = 1.25E-10$  JAT/HZ       $H_1 = 0$  JAT  
 $H_2 = .01$  JAT\*H2       $H_3 = .2$  JAT\*H2\*H

M-ARY PSK      M = 4

FR/NC = 1.3      DF

Mod. EIT RATE *	FR-DET(DF)	FR-LAT(TC1)	FR-LAT(TH)	FR-DET(EN)
E/S	Hz	Hz	Hz	Hz
75	5.9201	-7.84914	-9.77871	-12.3015
150	7.44881	-9.81382	-11.7856	-14.1901
300	9.3975	-11.7668	-13.7925	-16.0584
1200	14.9171	-15.6382	-17.8063	-19.6789
2400	23.4766	-19.4803	-21.8206	-23.1405
4800	37.5757	-23.0976	-25.8365	-26.3974
76800	59.5156	-27.6198	-29.8589	-29.4128
307200	93.6815	-29.9088	-33.9091	-32.1113
1228800	145.5452	-35.6166	-38.1067	-34.1001
4915200	411.74	-34.3505	-39.5258	-35.9226
19660800	745.352	-31.1106	-42.7478	-31.7481
78643200	1503.55	-25.9719	-45.8804	-26.0165

CODING GAIN (dB)

10

DF

EMULATION: LOSSES USING GAUSSIAN APPROX ARE ACCURATE WHEN < .1

Mod. EIT RATE *	LOSS(TC1)	LOSS(TH)	IF	TIKHONOV APPROX.
E/S	(dB)	(dB)	LOSS(TOT)	LOSS(TH)
75	18.3492	18.1295	>6	>6
150	12.0386	7.79221	>6	>6
300	7.85491	4.96973	>6	>6
1200	3.17601	1.99672	>6	>6
2400	1.34001	.79595	>6	1.6
4800	.592674	.316383	.9	.35
76800	.261172	.125377	.26	<.1
307200	.123953	.493551E-2		
1228800	.044401	.187767E-2		
4915200	.01758E-2	.1.35E-31E-2		
19660800	.0077722	.6.4496E-3		
78643200	.001771	.3.12E-9E-3		

\* Information bit rate :  $\frac{1}{2}$  modulation bit rate

Table D-3. BPSK Power Loop With HT-MT Mod  
Phase Noise (2 Terminals) (Losses-Soft Decision  
Viterbi Rate 1/2 Decoding BER =  $10^{-3}$ )

OPTIMUM LOOP FANWIDTH AND THE COEFFICIENT INC  
PHASE NOISE VARIANCE

OSCILLATOR SPECTRAL CHARACTERISTICS  
H1 = 1.0E-10 RAD/HZ  
H2 = .01 RAD\*HZ  
H3 = .2 RAD\*HZ<sup>2</sup>

Mod. BIT RATE *	SI-OPTIMED	PH-VAE(TOT)	PH-VAE(TH)	PH-VAE(PN)
75	6.78007	-8.61978	-10.5129	-13.0447
150	8.15528	-10.5799	-12.5718	-14.9831
300	10.2878	-12.5987	-14.5787	-16.7738
600	14.3302	-16.3818	-18.5924	-20.3713
1200	25.9134	-20.1505	-22.6071	-23.7956
1900	41.1161	-23.801	-26.4236	-27.0074
76800	65.0959	-27.2824	-30.6488	-29.9637
307200	105.179	-30.4767	-34.7113	-32.533
1228800	158.217	-32.7906	-39.0009	-33.9786
1915000	175.634	-33.0638	-40.1657	-34.0053
1988000	891.113	-28.7663	-42.3674	-28.9194
7864000	1737.89	-23.0113	-46.4871	-23.0308
OPTIMUM GAIN OF		10	TP	
OSCILLATOR LOSSES USING GAUSSIAN			TP	
APPROX. ALL ACCURATE WHERE		+1164F9	TP	
Mod. BIT RATE *	LOSS(TOT)	LOSS(TH)	TIKHONOV APPROX.	
	(DB)	(DB)	LOSS(TOT)	LOSS(TH)
75	1.20184	.381063	>6	>6
150	.827981	.240054	>6	>6
300	.425119	.151223	>6	1.2
600	.120846	6.00106E-2	.13	<.02
1200	1.73843E-2	2.38114E-2		
1900	1.91051E-2	9.44341E-3		
76800	8.31883E-3	3.73775E-3		
307200	2.92483E-3	1.46676E-3		
1228800	2.29878E-3	5.16261E-4		
1915000	2.15772E-3	2.17754E-4		
1988000	5.91914E-3	1.99871E-4		
7864000	2.21581E-2	9.74493E-5		

\* Information bit rate =  $\frac{1}{2}$  modulation bit rate

Table D-4. QPSK Power Loop With HT-MT Mod Phase Noise (2 Terminals) (Losses-Soft Decision Viterbi Rate 1/2 Decoding BER =  $10^{-5}$ )

OPTIMUM LOOP LENGTH AND THE VITERBI DECISION PHASE NOISE VARIANCE

OPTIMUM LOOP LENGTH CHARACTERISTICS

BER =  $10^{-5}$  1/2 RATE/HZ

H1 = 0. FAI

H2 = 0.01 FAI+HZ

H3 = 0.2 FAI+HZ+Z

M-ARY FSK	M = 2	BER = 10 <sup>-5</sup>	IF	IF
Mod. FAI FAI *	FAI = 0.01	IF = 0.01	IF = 0.01	IF = 0.01
75	4.71103	-5.89877	-7.79442	-10.4124
150	5.02551	-7.8713	-9.8013	-12.3229
300	7.47556	-9.82527	-11.8088	-14.8115
600	11.4708	-13.7291	-15.828	-17.9041
1200	18.8456	-17.5591	-19.836	-21.4524
2400	29.9033	-21.2958	-23.8508	-24.8147
4800	47.4111	-24.8997	-27.8689	-27.9516
9600	74.9687	-28.7068	-31.9004	-30.8024
19200	116.868	-31.2964	-35.9928	-33.0953
38400	205.065	-33.3714	-37.8894	-35.2647
76800	467.891	-31.1543	-41.1683	-31.6103
78643200	1007.17	-25.9356	-44.3408	-25.9987

CODING GAIN OF  
DEMODULATION LOSSES USING GAUSSIAN  
AMPLITUDE AND ACCURATE VITERBI

10

IF

IF

IF

Mod. FAI FAI *	LOSS(TOT) (DB)	LOSS(TH) (DB)	LOSS(TOT) (DB)	LOSS(TH) (DB)
75	27.3409	18.5616	>6	>6
150	38.2639	15.0694	>6	>6
300	11.2809	7.75312	>6	>6
600	1.01019	3.13771	>6	>6
1200	0.11216	1.25471	>6	>6
2400	.897874	.499375	1.9	.7
4800	.392352	.198197	.5	.2
9600	.179213	.7.83704E-2	.13	.1
19200	9.00488E-2	3.05487E-2		
38400	5.58587E-2	1.97403E-2		
76800	9.30537E-2	9.87848E-3		
78643200	.309197	2.46974E-3		

\* Information bit rate =  $\frac{1}{2}$  modulation bit rate

Table D-5. BPSK Decision Feedback With HT-MT Mod  
Phase Noise (3 Terminals) (Losses-Soft Decision Viterbi  
Rate 1/2 Decoding BER =  $10^{-5}$ )

OPTIMUM LOSS FANVWITH AND THE CORRESPONDING  
PHASE NOISE VARIANCE

OSCILLATOR SPECTRAL CHARACTERISTICS

$H_0 = 1.89E-10$   $\text{Hz}^2/\text{Hz}$   
 $H_2 = .015$   $\text{Hz}^2/\text{Hz}$

$H_1 = 0$   $\text{Hz}^2$   
 $H_3 = .3$   $\text{Hz}^2/\text{Hz}^{1/2}$

M-ARY FSK  $M = 2$

FE/NO = 1.3  $\text{dB}$

Mod. BIT RATE * P/S	EV-OF(TOT)	PH-VAF(TOT)		PH-VAF(EN)
		Hz	FE	
75	7.85891	-8.49497	-10.4784	-12.8527
150	9.90142	-10.4458	-12.4853	-14.7084
300	18.4749	-12.3831	-14.4928	-16.532
1200	19.8012	-16.2047	-18.5062	-20.0623
4K00	31.4833	-19.9294	-22.5212	-23.4029
19200	49.8235	-23.5182	-26.54	-26.5169
76800	78.7113	-26.9146	-30.5745	-29.36
307200	122.587	-29.9649	-34.6818	-31.7532
1228800	322.904	-32.6829	-36.4868	-35.0225
4914800	608.708	-31.7458	-39.7527	-38.4939
19660800	1175.2	-27.0813	-42.9159	-27.1961
78643200	2305.02	-21.2602	-46.0112	-21.2747
COTING GAIN OF		10	FE	

DEMODULATION LOSSES USING GAUSSIAN  
APPROX ARE ACCURATE WHEN  $< .116469$

Mod. BIT RATE * P/S	LOSS(TOT) (FE)	LOSS(TH) (FE)	TIKHONOV APPROX.	
			LOSS(TOT) (DB)	LOSS(TH) (DB)
75	1.78159	.858422	>6	>6
150	.868145	.431279	>6	>6
300	.446045	.226235	>6	1.2
1200	.137615	7.28637E-2	.13	<.1
4K00	5.01591E-2	2.61199E-2		
19200	2.04635E-2	9.91499E-3		
76800	9.0738E-3	3.84718E-3		
307200	4.43173E-3	1.78355E-3		
1228800	2.35694E-3	9.77522E-4		
4914800	9.92961E-3	4.6009E-4		
19660800	8.7234E-3	2.21923E-4		
78643200	3.57463E-2	1.08771E-4		

\* Infor: 'n' bit rate =  $\frac{1}{2}$  modulation bit rate

Table D-6. QPSK Decision Feedback With HT-Mt Mod  
 Phase Noise (3 Terminals) (Losses-Soft Decision  
 Viterbi Rate 1/2 Decoding BER =  $10^{-5}$ )

OPTIMUM LOOP FANWIDTH AND THE CORRESPONDING  
 PHASE NOISE VARIANCE

OSCILLATOR SPECTRAL CHARACTERISTICS  
 HO = 1.89E-10 RAD/HZ      HI = 0 RAD  
 H2 = .015 RAD\*HZ      H3 = .3 RAD\*HZ\*2

M-ARY PSK	M = 4	EP/NO = 1.3	IF
Mod. F/B	EV-OPT(IF)	PH-VAF(TOT)	PH-VAF(TH)
F/S	Hz	DE	Hz
75	6.7768E	-7.23829	-9.19174
150	8.5382E	-9.19649	-11.1986
300	10.7574	-11.1428	-13.2055
1200	17.0755	-14.9886	-17.2195
4800	27.1007	-18.7482	-21.234
19200	48.9877	-28.3856	-25.251
76800	68.0387	-28.8537	-29.2778
307200	106.6	-29.0617	-33.348
1228800	156.149	-31.5718	-37.7108
4915200	495.241	-33.0989	-38.718
19660800	979.847	-29.768	-41.9109
78643200	1855.04	-24.2273	-45.0245

COFFING GAIN OF      10      IF

TEMPERATURE LOSSES USING GAUSSIAN  
 APPROX ATE ACCURATE WHEN  $< -4$

Mod. F/B	LOSS(TOT) (DB)	LOSS(TH) (DB)	IF	TIKHONOV APPROX. LOSS(TOT) (DB)	LOSS(TH) (DB)
75	20.8464	13.7774	>6	>6	>6
150	13.7433	8.87722	>6	>6	>6
300	8.98764	5.67084	>6	>6	>6
1200	3.79123	2.82239	>6	>6	>6
4800	1.60956	.910642	>6	1.9	.4
19200	.499124	.361914	1.25	.4	.1
76800	.315078	.143317	.35	.1	
307200	.150622	5.61599E-2			
1228800	8.45876E-2	8.05688E-2			
4915200	5.94753E-2	1.63093E-2			
19660800	.128028	7.82035E-3			
78643200	.457931	3.81833E-3			

\* Information bit rate =  $\frac{1}{2} \cdot$  modulation bit rate

Table D-7. BPSK Power Loop With HT-MT Mod Phase Noise (3 Terminals) (Losses-Soft Decision Viterbi Rate 1/2 Decoding BER =  $10^{-5}$ )

OPTIMUM LOOP BANDWIDTH AND THE CORRESPONDING PHASE NOISE VARIANCE

OSCILLATOR SPECTRAL CHARACTERISTICS

$H_0 = 1.89F^{-1C}$  FAI/HZ  
 $H_2 = 0.01F$  FAI\*HZ

$H_1 = 0$  FAI  
 $H_3 = .3$  FAI\*HZ $^{1/2}$

M-PSK	M=2	EF/NO = 1.3	EE	PH-VAF(FN)
Mod. EIT FATE*	EF-OPT(MF)	PH-VAF(TOT)	PH-VAF(TH)	PH-VAF(FN)
T/S	Hz	DP	DP	DP
75	7.41887	-8.00671	-9.97797	-12.3855
150	9.34711	-9.96054	-11.9849	-14.2485
300	11.7765	-11.9015	-13.9918	-16.0806
600	18.6929	-15.7328	-18.0058	-19.6317
1200	29.6659	-19.4715	-22.0206	-22.998
2400	47.0457	-23.0795	-26.0385	-26.1417
4800	74.3827	-26.5025	-30.0696	-29.0194
9600	116.0118	-29.5993	-34.1599	-31.4694
19200	153.6486	-31.418	-38.9592	-32.2595
38400	561.606	-31.623	-39.3518	-32.4254
76800	1081.65	-27.0408	-42.5259	-27.186
153600	2118.06	-21.2575	-45.628	-21.2734
COTING GAIN OF DEMODULATION LOSSES USING CAUSIAN APPROX ARE ACCURATE WHEN	10	EE	EE	EE

DEMODULATION LOSSES USING CAUSIAN  
APPROX ARE ACCURATE WHEN

$116479$

Mod. IIT FATE*	LOSS(TOT)	LOSS(TH)	TIKHONOV APPROX.	
(F/EE)	(EE)	(EE)	LOSS(TOT)	LOSS(TH)
75	2.15283	2.36207	>6	>6
150	1.03415	2.74792	>6	>6
300	.524004	1.73106	>6	.75
600	.157711	6.86931E-2	.25	<.1
1200	5.64837E-2	9.72543E-2	<.1	<.1
2400	2.87766E-2	1.08053E-1		
4800	1.00025E-2	4.27099E-3		
9600	4.8993E-3	1.66532E-3		
19200	3.1615E-3	5.51533E-4		
38400	2.01411E-3	5.03858E-4		
76800	8.76567E-4	2.45607E-4		
153600	3.57609E-4	1.18767E-4		

\* Information bit rate =  $\frac{1}{2}$  · modulation bit rate

Table D-8. QPSK Power Loop With HT-MT Mod Phase  
Noise (3 Terminals) (Losses-Soft Decision Viterbi Rate  
1/2 Decoding BER =  $10^{-3}$ )

OPTIMUM LOOP LENGTH AND THE CORRESPONDING  
PHASE NOISE VARIANCE

OSCILLATOR EFFECTIVE CHARACTERISTICS

$H_1 = 1.89E-10$  FAD/HZ

$H_1 = 0$  FAD

$H_2 = -0.15$  FAD/HZ

$H_3 = +0.2$  FAD\*H2+2

$N_{eff} = 1.3$  dB

$BER = 1.3 \times 10^{-3}$

Mod. IT	ITF *	EV-OEF(MF)	EV-LAF(TOT)	EV-LAF(TH)	EV-LAF(PN)
	E/S	H2	IE	IE	IE
7E		5.29278	-5.29278	-7.20746	-9.77158
1E0		6.79428	-7.26039	-9.21433	-11.6695
200		8.55045	-9.21846	-11.22118	-13.543
1200		12.5886	-13.0968	-15.235	-17.1978
2400		21.5684	-16.9083	-19.2498	-20.696
19200		34.6225	-20.605	-23.2645	-23.9969
76800		54.2471	-24.162	-27.2848	-27.0627
307200		85.5762	-27.5014	-31.3256	-29.8265
1228800		131.912	-30.3539	-35.4669	-31.9535
4915200		362.234	-38.2076	-37.1005	-33.909
19660800		585.472	-39.5544	-40.3447	-39.9324
78643200		1330.06	-24.1977	-43.4929	-24.2491

CODING GAIN OF

10

IE

EMULATIION LOSSES USING GAUSSIAN

APPROX ACCURATE WHEN

•4

IE

Mod. IT	ITF *	LOSS(TOT)	LOSS(TH)	TIKHONOV APPROX.	
	E/S	(IE)	(IE)	LOSS(TOT)	LOSS(TH)
7E		30.7819	20.98	>6	>6
1E0		20.7511	13.7103	>6	>6
200		13.4981	8.8329	>6	>6
1200		5.81193	3.58511	>6	>6
2400		8.45358	1.4358	>6	>6
19200		1.05196	•571385	2.6	.95
76800		•462857	•886701	.6	.25
307200		•215681	•945548-2	.2	.1
1228800		•111878	•248048-2		
4915200		7.30192E-2	•023672		
19660800		•13468	1.12158E-2		
78643200		•161543	•643887E-2		

\* Information bit rate =  $\frac{1}{2}$  modulation bit rate

Table D-9. Demodulation Performance - BPSK, Power Loop,  
"Cesium II" Phase Noise (2 Terminals)

{Losses - Soft Decision (3 bits), R=½, K=7, Viterbi Decoding @ BER=10<sup>-5</sup>}

\* Information bit rate =  $\frac{1}{2}$  · modulation bit rate

PHASE VARIANCES VS. DATA RATE \*  
AT OPTIMUM BER (BER=10<sup>-5</sup>)

M-ARY PSK      M = 2

PHASE = 1.2 ms

POWER LOOP IMPLEMENTATION

SAMPLING FACTOR = .717107

DMR (MPS. BPS/SEC)	bit	PH-VAL (TOT) (PH-VAL(002))	PH-VAL (TH) (PH-VAL(002))	PH-VAL (DP) (PH-VAL(002))
75.	1.4 7	-14.3244	-17.1174	-19.4422
300.	2.272	-14.1454	-11.1344	-23.2473
1200.	3.454	-22.5042	-25.5444	-25.4487
4800.	5.845	-25.6411	-24.0744	-24.0446
19200.	9.274	-27.5444	-23.0440	-29.0227
76800.	14.807	-28.6140	-31.0434	-29.2477
307200.	56.222	-28.7451	-77.2124	-29.4441
1228800.	284.101	-29.2074	-34.4411	-32.5741
4915200.	757.037	-29.6264	-34.0441	-34.0447
19660800.	1146.174	-33.0344	-42.5424	-34.8441
78667200.	1984.044	-34.5741	-46.1344	-34.4447

DEMODULATION LOSS VS. DATA RATE  
AT OPTIMUM BER (BER=10<sup>-5</sup>)

Sensitivity Gate (DP) = 10.00  
DEMODULATION LOSS = 100% (BER=10<sup>-5</sup>)  
APPROX. A/D ACCURATE WHEN < .116464 DB

POWER LOOP IMPLEMENTATION

SAMPLING FACTOR = .717107

DMR (MPS. BPS/SEC)	bit	LOSS(TOT)	LOSS(TH)
75.	1.407	.1774E+00	.1040E+00
300.	2.272	.4248E-01	.2686E-01
1200.	3.454	.2620E-01	.1349E-01
4800.	5.845	.1275E-01	.5407E-02
19200.	9.272	.7742E-02	.2145E-02
76800.	14.807	.6040E-02	.4576E-02
307200.	56.222	.5485E-02	.2041E-03
1228800.	284.101	.3821E-02	.1344E-02
4915200.	757.037	.2288E-02	.8608E-03
19660800.	1146.174	.1767E-02	.2643E-03
78667200.	1984.044	.1521E-02	.1057E-03

Table D-10. Demodulation Performance - QPSK, Power Loop,  
"Cesium II" Phase Noise (2 Terminals)

{Losses - Soft Decision (3bit), R=1/2, K=7, Viterbi Decoding at  $BER = 10^{-5}$ }/  
\*Information bit rate =  $1/2 \times$  modulation bit rate.

PHASE VARIANCES VS. DATA RATE \*  
AT OPTIMUM BANDWIDTH:

M-ADJ. ODR = 4

SNR/NOI = 1.7 dB

POWER LOOP IMPLEMENTATION:

DAMPING FACTOR = .707107

DMR (MOD. RATE/SEC)	-I (+7)	DH-VAR (THT)	DH-VAR (TH)	DH-VAR (DM) (DH-VA(882))
14200.	6.794	-24.2324	-24.2431	-24.2400
76800.	10.674	-27.4844	-24.7436	-24.1319
307200.	17.534	-24.4611	-32.2104	-24.1132
1224000.	145.204	-24.1614	-33.4432	-30.8623
6016000.	404.372	-21.2674	-35.7142	-33.20112
10660400.	240.662	-22.1202	-34.2157	-34.2420
74667200.	1772.342	-24.1544	-34.7442	-34.7462

DEMODULATION LOSS VS. DATA RATE  
AT OPTIMUM BANDWIDTH:

Sensitivity Gain (dB) = 15.00

DEMODULATION LOSSES USING GAUSSIAN  
APPROX. AND ACCURATE (BER < .4000000 DR)

POWER LOOP IMPLEMENTATION:

DAMPING FACTOR = .707107

DMR (MOD. RATE/SEC)	-I (+7)	1155(THT)	1155(TH)
14200.	6.794	.24-14.00	.11.35-0.01
76800.	10.674	.1024-0.01	.44-0.01-0.1
307200.	17.534	.14.74-0.01	.1-1.31-0.1
1224000.	145.204	.14.72-0.01	.4541-0.01
6016000.	404.372	.20.64-0.01	.42-75-0.1
10660400.	240.662	.64-1.6E-01	.14-64-0.01
74667200.	1772.342	.64-2.6E-01	.54-64-0.01

Table D-11. Demodulation Performance - QPSK, Decision Feedback,  
"Cesium II" Phase Noise (2 Terminals)

{Losses - Soft Decision (3 bit), R=1/2, K=7, Viterbi Decoding at  $BER = 10^{-5}$ }

\*Information bit rate =  $1/2 \cdot$  modulation bit rate.

PHASE VARIANCES vs. DATA RATE \*  
AT OPTIMUM BANDWIDTH

BER = 0.001

FRAMES = 1, 3, 7, 15

DETECTION FEEDBACK IMPLEMENTATION

DAMPING FACTOR = .717167

DMR (MHz, BITS/SEC)	SI	DH-VAR (TOT)	DH-VAR (TH)	DH-VAR (DH)
(DH=2.8E+02)				
14200.	8.400	-21.2463	-19.2466	-24.4700
74000.	13.630	-28.5420	-36.2410	-29.3468
307200.	25.840	-28.4427	-34.4447	-24.2740
1224000.	222.740	-30.2147	-34.5631	-32.2114
4014200.	427.641	-32.4777	-37.2424	-33.4817
19660810.	1028.911	-37.7426	-41.4174	-34.5771
78647210.	1703.514	-36.4454	-45.7466	-34.6624

DEMODULATION LOSS vs. DATA RATE  
AT OPTIMUM BANDWIDTH

Sensitivity Rate (DMR = 14.00)  
Demodulation Loss (dB) vs. Data Rate  
Approx. ARIE Attenuation (MHz) < .407210 dB

DETECTION FEEDBACK IMPLEMENTATION

DAMPING FACTOR = .717167

DMR (MHz, BITS/SEC)	SI	LOSS (T: T)	LOSS (T: H)
10200.	8.400	.22475+00	.7175E+01
74000.	13.630	.1642E+00	.2873E+01
307200.	25.840	.1544E+00	.1473E+01
1224000.	222.740	.1174E+01	.4244E+01
4014200.	427.641	.1145E+01	.1255E+01
19660810.	1028.911	.4124E+01	.4665E+02
78647210.	1703.514	.6722E+01	.3506E+02

Table D-12. Demodulation Performance - BPSK, Power Loop,  
"Cesium II" Phase Noise (2 Terminals and 1 Equivalent Satellite)

{Losses - Soft Decision (3 bit),  $R=\frac{1}{2}$ ,  $K=7$ , Viterbi Decoding @ BER=10<sup>-5</sup>}

\*Information bit rate =  $\frac{1}{2}$  • modulation bit rate

PHASE VARIANCES VS. DATA RATE \*

AT OPTIMUM HANWORTHY:

N-BEHY PSK      M=2

F-H/2 = 1.2 DH

POWER LOOP IMPLEMENTATION

DAMPING FACTOR = .707107

PHN (MOD. RATE/SEC)	M	PH-VAL(TOT) (DH-PSK) <sup>0.02</sup>	PH-VAL(TH) (DH-PSK) <sup>0.02</sup>	CH-VAL(PSK) (DH-PSK) <sup>0.02</sup>
75.	1.614	-14.1013	-14.5444	-14.2444
300.	2.627	-14.2766	-20.4040	-22.4400
1200.	4.193	-21.6964	-24.4444	-24.4234
4800.	6.776	-24.4443	-28.4543	-28.4644
19200.	10.602	-26.2769	-32.5044	-27.4474
76800.	17.409	-27.0742	-36.3766	-27.4140
307200.	142.520	-27.4744	-38.1414	-24.2441
1228800.	442.842	-26.4612	-33.8444	-31.4144
4915200.	949.117	-21.3264	-27.4552	-32.4410
19660800.	1347.820	-22.4040	-41.5342	-32.4702
78643200.	2230.116	-22.9122	-45.4041	-33.1441

{DEMODULATION LOSSES VS. DATA RATE  
AT OPTIMUM HANWORTHY:

SENSITIVITY GAIN (DH) = 10.00  
DEMODULATION LOSSES USING GAUSSIAN  
APPROX. APE ACCURATE WHEN  $< 1.154E-04$

POWER LOOP IMPLEMENTATION

DAMPING FACTOR = .707107

PHN (MOD. RATE/SEC)	M	LOSS(TH)	LOSS(TH)
75.	1.614	.2174E+00	.1237E+00
300.	2.627	.7E44E-01	.4714E-01
1200.	4.193	.7204E-01	.1E15E-01
4800.	6.776	.1E34E-01	.6307E-02
19200.	10.602	.1055E-01	.2454E-02
76800.	17.409	.8774E-02	.1007E-02
307200.	142.520	.7442E-02	.2641E-02
1228800.	442.842	.6446E-02	.1774E-02
4915200.	949.117	.7224E-02	.7H14E-03
19660800.	1347.820	.7E14E-02	.7114E-02
78643200.	2230.116	.2234E-02	.1241E-02

Table D-13. Demodulation Performance - QPSK, Power Loop,  
"Cesium II" Phase Noise (2 Terminals and 1 Equivalent Satellite)

{Losses - Soft Decision (3 bit),  $R=\frac{1}{2}$ ,  $K=7$ , Viterbi Decoding @ BER=10<sup>-5</sup>}

\* Information bit rate =  $\frac{1}{2} \cdot$  modulation bit rate

PHASE VARIANCES VS. DATA RATE\*  
AT OPTIMUM DATA RATE:

M-ARY PSK      M= 4

FH/N0= 1.7 dB

POWER LOOP IMPLEMENTATION

DAMPING FACTOR= .707107

DMR (MOD. BITS/SEC)	-1 (-7)	PHASE VARIANCE (dB-LEVELS@2)	PH-VAR (TH) (dB-LEVELS@2)	PH-VAR (-1) (dB-LEVELS@2)
19200.	7.762	-26.114	-24.717	-24.441
76800.	12.202	-26.546	-33.764	-27.414
307200.	21.046	-27.007	-37.617	-27.421
1228800.	263.244	-28.007	-32.604	-29.434
4915200.	407.177	-29.117	-34.467	-31.444
19660800.	1001.217	-31.742	-39.705	-32.714
78643200.	1547.347	-32.602	-42.741	-33.034

DEMODULATION LOSSES VS. DATA RATE  
AT OPTIMUM DATA RATE:

Sensitivity Gain (dB) = 14.00

DEMODULATION LOSSES USING GAUSSIAN

APPROX. AFR ACCURATE WHEN  $< .4000000$  FH

POWER LOOP IMPLEMENTATION

DAMPING FACTOR= .707107

DMR (MOD. BITS/SEC)	-1 (-7)	LOSS (TH)	LOSS (TH)
19200.	7.762	.77776+00	.12944+00
76800.	12.202	.24574+00	.51073+01
307200.	21.046	.26144+00	.42014+01
1228800.	263.244	.14206+00	.44414+01
4915200.	407.177	.11426+00	.34684+01
19660800.	1001.217	.61274+01	.16348+01
78643200.	1547.347	.46524+01	.53204+02

Table D-14. Demodulation Performance - QPSK, Decision Feedback, "Cesium II" Phase Noise (2 Terminals and 1 Equivalent Satellite)

{Losses - Soft Decision (3 bit), R=1, K=7, Viterbi Decoding @ BER=10<sup>-5</sup>}

\* Information bit rate =  $\frac{1}{2}$  · modulation bit rate

PHASE VARIANCE VS. DATA RATE \*  
AT OPTIMUM RAKE RATIO (TH):

M-ARY PSK      M= 4

FH/NCF = 1.3 dB

DECISION FEEDBACK IMPLEMENTATION

DAMPING FACTOR = .707107

DMP (MOP, HTS/FFC)	RI	PH-VAR (TOT)	PH-VAR (TH)	PH-VAR (PN)
	(H-7)	(H-7-VAR*0.2)	(H-7-VAR*0.2)	(H-7-VAR*0.2)
19200.	9.701	-26.0317	-31.7163	-27.3491
76800.	15.575	-27.0447	-35.6419	-27.7300
707200.	119.460	-27.7647	-32.4434	-28.8084
1228800.	425.066	-24.1872	-23.7414	-21.1517
4915200.	729.148	-27.0272	-24.6412	-22.4215
19660800.	1252.242	-22.2504	-40.7104	-32.4144
78663200.	1474.066	-22.8416	-44.7444	-37.1376

DEMODULATION LOSS VS. DATA RATE  
AT OPTIMUM RAKE RATIO:

SENSITIVITY RATE (DR) = 10.00  
DEMODULATION LOSS (dB) LISTED FOLLOWING  
APPROX. BER ACCURATE WHEN < .400000 DR

DECISION FEEDBACK IMPLEMENTATION

DAMPING FACTOR = .707107

DMP (MOP, HTS/FFC)	RI	LOSS (TOT)	LOSS (TH)
	(H-7)	(H-7)	(H-7)
19200.	6.701	.3026F+00	.4174F-01
76800.	15.575	.2776F+00	.3242F-01
707200.	119.460	.2222F+00	.4247F-01
1228800.	425.066	.1491F+01	.5544F-01
4915200.	729.148	.4542F-01	.2A12F-01
19660800.	1252.242	.7230F-01	.1031F-01
78663200.	1474.066	.4210F-01	.4063F-02

Table D-15. Demodulation Performance - BPSK, Power Loop,  
"Crystal II" Phase Noise (2 Terminals and 1 Equivalent Satellite)

{Losses - Soft Decision (3 bit), R=2, K=7, Viterbi Decoding @ BER=10<sup>-5</sup>}

\* Information bit rate =  $\frac{1}{2}$  \* modulation bit rate

PHASE VBF-TA1-SFC VS. DATA RATE \*  
AT OPTIMUM SNR = 10.0 dB

M-BPSK BPSK N=2

PHASE T-1.175

POWER LOOP IMPLEMENTATION

RAMMING FACTOR = .717177

DRH (MOD. RATE/SFC)	4	DRH-VBF (T-1.175) (10.0 dB - 0.2)	DRH-VBF (T-1) (10.0 dB - 0.2)	DRH-VBF (T-1) (10.0 dB - 0.2)
75.	.614	-21.5146	-22.4476	-24.0041
300.	.641	-24.2289	-26.2236	-28.2468
1200.	1.171	-27.6131	-29.2940	-30.5644
4800.	1.741	-30.4784	-34.2114	-37.7444
19200.	2.041	-32.1612	-37.6432	-43.4126
76800.	2.542	-33.6174	-40.6004	-47.2401
307200.	3.447	-37.4327	-42.0464	-49.0327
1228800.	4.674	-39.6887	-43.4617	-51.0674
4915200.	5.812	-42.0016	-46.1014	-52.0774
19660800.	6.824	-42.5744	-48.0203	-52.0163
78643200.	14.46723	-42.6428	-47.2471	-53.1501

DEMODULATION LOSS VS. DATA RATE  
AT OPTIMUM SNR = 10.0 dB

SENSITIVITY GATE (T-1) = 10.0 dB  
DEMODULATION LOSSES (VBF, VBF-1)  
APPROX. ALF ACCURATE SNR < .7174617 dB

POWER LOOP IMPLEMENTATION

RAMMING FACTOR = .717177

DRH (MOD. RATE/SFC)	4	LOSS (T-1.175) (1.0)	LOSS (T-1) (1.0)
75.	.614	.414141-01	.26341-01
300.	.641	.12141-01	.101121-01
1200.	1.171	.74461-02	.614461-02
4800.	1.741	.460111-02	.365461-02
19200.	2.041	.26571-02	.200001-03
76800.	2.542	.26471-02	.224461-02
307200.	3.447	.21341-02	.264061-02
1228800.	4.674	.26411-02	.16661-02
4915200.	5.812	.27811-02	.16461-02
19660800.	6.824	.26571-02	.214661-02
78643200.	14.46723	.22241-02	.11141-02

Table D-16. Demodulation Performance - QPSK, Power Loop,  
 "Crystal II" Phase Noise (2 Terminals and 1 Equivalent Satellite)

• Losses - Soft Decision (3 bit),  $R=\frac{1}{2}$ ,  $K=7$ , Viterbi Decoding @  $BER=10^{-5}$   
 • Information bit rate =  $\frac{1}{2}$  · modulation bit rate

• Information bit rate =  $\frac{1}{2}$  • modulation bit rate

UNIVERSITY OF TORONTO LIBRARY  
AT TORONTO, ONTARIO, CANADA

READY DCB 115 11

EE/EE = 1.3

PO. #FL 1000 THE LENDER'S TEL

DAMPING FACTOR = .707117

ITEM	20	ITEM 20 (CONT'D)	ITEM 20 (CONT'D)	ITEM 20 (CONT'D)
(MOP. 2115/446)	(-7)	ITEM 20 (CONT'D)	ITEM 20 (CONT'D)	ITEM 20 (CONT'D)
192000.	20100	-21.0504	-24.0411	-22.0134
762000.	20.675	-20.244	-20.0174	-22.0246
2072000.	20.021	-21.0414	-21.0377	-22.0414
12298000.	20.011	-21.0474	-20.011	-21.0041
60152000.	20.025	-21.0764	-20.0007	-22.0364
196608000.	20.100	-22.0186	-20.0010	-22.0041
766432000.	1221.720	-22.0644	-22.0011	-22.0111

PERIODIC ATTACHMENT OF THE CROWN  
AT OPTIMUM VIBRATION

Sensitivity data, such as those  
described above, collected by the  
people, are accurate and reliable.

## DRUGS FOR TREATMENT OF TBC

1 AND THE FACTORY .7 7187

NAME	1	110018-71	110007-71
EDWARD J. TAYLOR	1-71	(000)	(000)
122100	2-00-2	0-00-00-00	0-00-00-00
746100	2-0-0-2	0-0-00-00	0-0-00-00
207200	2-0-0-1	0-0-00-00	0-0-00-00
122400	2-0-0-1	0-0-00-00	0-0-00-00
6015200	2-0-0-2	0-0-00-00	0-0-00-00
1966000	2-0-0-2	0-0-00-00	0-0-00-00
74667210	2-0-0-2	0-0-00-00	0-0-00-00

Table D-17. Demodulation Performance - QPSK, Decision Feedback, "Crystal II" Phase Noise (2 Terminals and 1 Equivalent Satellite)

{Losses - Soft Decision (3 bit), R=1, K=7, Viterbi Decoding @ BER=10<sup>-5</sup> }  
 \* Information bit rate =  $\frac{1}{2}$  · modulation bit rate

PHASE VARIANCES VS. DATA RATE \*  
 AT OPTIMUM DATA RATE:

MARY PSK      N = 4

BER/NO = 1.2 · 10<sup>-5</sup>

DECISION FEEDBACK IMPLEMENTATION

DAMPING FACTOR = .707107

DMR (MOD. BITS/SEC)	41 (-7)	PH-VAR(TOT) (PH-LOS(0.02))	PH-VAR (TH) (PH-LOS(0.02))	PH-VAR (DL) (PH-LOS(0.02))
14200.	2.721	-32.0450	-37.2474	-33.6097
74800.	5.442	-32.4467	-40.2155	-33.7756
307200.	15.114	-32.2424	-41.4206	-32.7494
1228800.	44.146	-31.6421	-43.1424	-32.0110
4915200.	141.041	-31.4379	-44.1781	-32.2156
19660800.	412.452	-32.4012	-42.5494	-32.5346
78643200.	1721.651	-32.8616	-45.3274	-33.1152

DEMODULATION LOSSES VS. DATA RATE  
 AT OPTIMUM BANDWIDTH:

SENSITIVITY GATE (DMR) = 10.00  
 DEMODULATION LOSSES (LISTING GAUSSIAN)  
 APPROX. ARF ACCURATE WHEN < .4000000 DM

DECISION FEEDBACK IMPLEMENTATION

DAMPING FACTOR = .707107

DMR (MOD. BITS/SEC)	41 (-7)	LOSS(TOT) (DMR)	LOSS(TH) (DMR)
14200.	2.721	.7440E-01	.2204E-01
74800.	5.442	.6245E-01	.1155E-01
307200.	15.114	.7243E-01	.7456E-02
1228800.	44.146	.4222E-01	.5422E-02
4915200.	141.041	.7770E-01	.4466E-02
19660800.	412.452	.8944E-01	.6884E-02
78643200.	1721.651	.6241E-01	.2444E-02

Table D-18. Demodulation Performance - Radiation, Inc.  
BPSK With Modified HT-MT Phase Noise (2 Terminals)

(Losses - Soft Decision (3 bit), R = 1/2, K = 7, Viterbi Decoding at BER  $10^{-5}$ ,

LOOP BANDWIDTH AND THE CORRESPONDING  
PHASE NOISE VARIANCE

OSCILLATOR SPECTRAL CHARACTERISTICS  
H0 = 1.26E-10 RAD/HZ H1 = 0 RAD  
H2 = .01 RAD/HZ H3 = .2 RAD\*HZ<sup>1/2</sup>

M-ARY PSK M = 2 EPN/NO = 1.3 dB

MOD. BIT RATE * B/S	BW (MF) HZ	PH-VAR(TOT) DE	PH-VAR(TH) DE	PH-VAR(FN) DE
------------------------	---------------	-------------------	------------------	------------------

1200	175	-8.28419	-8.29215	-35.6584
4800	175	-14.281	-14.3127	-35.6552
19200	175	-20.2072	-20.3333	-35.6498
76800	175	-25.864	-26.3539	-35.5834
307200	175	-30.6057	-32.3745	-35.3612
1228800	175	-33.0648	-38.3951	-34.5711
4915200	175	-32.0938	-44.4157	-32.356
19660800	175	-28.1835	-54.4363	-28.2895
78643200	175	-22.8163	-56.4569	-22.8182

CODING SENSITIVITY GAIN = 1V DE

DEMODULATION LOSSES USING GAUSSIAN  
APPROX ARE ACCURATE WHEN < .116469 DE

MOD. BIT RATE * (B/S)	LOSS(TOT) (DE)	LOSS(TH) (DE)	Tikhonov Loss (tot) (dB)	Approx. Loss (Th) (dB)
--------------------------	-------------------	------------------	--------------------------------	------------------------------

1200	1.93446	.643094	>6	>6
4800	.243479	.160774	1.65	1.65
19200	4.66991E-2	4.01934E-2	<.1	<.1
76800	1.16415E-2	1.00483E-2	.	.
307200	3.8193E-3	2.51269E-3	.	.
1228800	2.15719E-3	6.28022E-4	.	.
4915200	2.70216E-3	1.57005E-4	.	.
19660800	6.78097E-3	3.92514E-5	.	.
78643200	2.42918E-2	9.81284E-6	.	.

\* Information bit rate =  $\frac{1}{2}$  · modulation bit rate

Table D-19. Demodulation Performance - Radiation Inc.  
 BPSK With Modified HT-MT Phase Noise (2 Terminals + 1  
 Equivalent Satellite) (Losses - Soft Decision (3 bit),  $R = 1/2$ ,  
 $K = 7$ , Viterbi Decoding at  $BER = 10^{-5}$ )

LOOP BANDWIDTH AND THE CORRESPONDING  
 PHASE NOISE VARIANCE

OSCILLATOR SPECTRAL CHARACTERISTICS  
 $H_0 = 1.89F \cdot 10^{-10}$  RAD/HZ       $H_1 = P \cdot FAD$   
 $H_2 = .015$  RAD $\cdot$ HZ $^{1/2}$        $H_3 = .3$  RAD $\cdot$ HZ $^{1/2}$

M-ARY FSK       $M = 2$        $FP/N_0 = 1.3$  dB  
 MOD. BIT RATE \*      BW (MF)  
 $P/S$        $H_2$       PH-VAR(TOT)      PH-VAR(TH)      PH-VAR(FN)  
 $DF$        $LF$        $DF$

1200	175	-8.28022	-8.29215	-33.8979
4800	175	-14.2652	-14.3127	-33.8943
19200	175	-20.1455	-20.3333	-33.8798
76800	175	-25.6384	-26.3539	-33.8825
307200	175	-29.934	-32.3745	-33.6882
1228800	175	-31.7504	-38.3951	-32.6101
4915200	175	-39.4185	-44.4157	-30.5951
19660800	175	-26.4312	-50.4363	-26.4485
78643200	175	-21.056	-56.4569	-21.0573

COILING SENSIVITY GAIN = 10 LF

DEMODULATION LOSSES USING GAUSSIAN  
 APPROX ARE ACCURATE WHEN  $< .116469$  DF

MOD. BIT RATE *	LOSS(TOT) (P/S)	LOSS(TH) (DP)	Tikhonov Loss (tot)	Approx. Loss (Th)
-----------------	--------------------	------------------	------------------------	----------------------

1200	1.93741	.643094	>6	>6
4800	.244664	.160774	1.65	1.65
19200	4.74446E-2	4.01934E-2	<.1	<.1
76800	1.02846E-2	1.00483E-2	.	.
307200	4.46681E-3	2.51209E-3	.	.
1228800	2.92652E-3	6.28722E-4	.	.
4915200	3.98954E-3	1.57005E-4	.	.
19660800	.010174	3.92514E-5	.	.
78643200	.037632	9.81284E-6	.	.

\* Information bit rate =  $\frac{1}{2}$  modulation bit rate

Table D-20. Demodulation Performance - Radiation Inc.  
BPSK with "Crystal II" Phase Noise (2 Terminals)

{Losses - Soft Decision (3 bit),  $R = 1/2$ ,  $K = 7$ , Viterbi Decoding at  $BER = 10^{-5}$ }

PHASE VARIANCE VS. DATA RATE \*

M-ARY PSK      M = ?

ER/N0 = 1.3 dB

POWER LOOP IMPLEMENTATION

DAMPING FACTOR = .707107

RMB (MOD. BITS/SEC)	BL (Hz)	PH-VAR (TOT) (DB-RAD**2)	PH-VAR (TH) (DB-RAD**2)	PH-VAR (PN) (DB-RAD**2)
1200.	175.000	-8.2772	-8.2922	-32.9209
4800.	175.000	-14.2495	-14.3128	-32.6462
19200.	175.000	-20.0714	-20.3334	-32.3965
76800.	175.000	-25.2754	-26.3540	-31.8531
307200.	175.000	-28.5923	-32.3745	-30.9474
1228800.	175.000	-30.0330	-38.3952	-30.7174
4915200.	175.000	-30.5170	-44.4157	-30.6977
19660800.	175.000	-30.6504	-50.4363	-30.6963

DEMODULATION LOSS VS. DATA RATE

MINIMUM-FREQ DISTANCE OF CODE=10.0  
DEMODULATION LOSSES USING GAUSSIAN  
APPROX. ARE ACCURATE WHEN  $< .116469$  dB

TIKHONOV APPROX.

RMA (MOD. BITS/SEC)	BL (Hz)	LOSS(TOT) (DB)	LOSS(TH) (DB)	LOSS(TOT) (DB)	LOSS(TH) (DB)
1200.	175.000	.2036E+01	.2024E+01	>6.	>6.
4800.	175.000	.2520E+00	.2471E+00	1.69	1.55
19200.	175.000	.4878E-01	.4559E-01	<.1	<.1
76800.	175.000	.1343E-01	.1039E-01	<.1	<.1
307200.	175.000	.6122E-02	.2533E-02	<.1	<.1
1228800.	175.000	.4369E-02	.6293E-03	<.1	<.1
4915200.	175.000	.3902E-02	.1571E-03	<.1	<.1
19660800.	175.000	.3783E-02	.3926E-04	<.1	<.1

\* Information bit rate = 1/2 • modulation bit rate

Table D-21. Demodulation Performance - Radiation Inc.  
BPSK with "Cesium II" Phase Noise (2 Terminals)

{Losses - Soft Decision (3 bit), R = 1/2, K = 7, Viterbi Decoding at B.E.R. =  $10^{-5}$

PHASE VARIANCES VS. DATA RATE \*

M-ARY PSK      M = 2

E<sub>H</sub>/N<sub>0</sub> = 1.3 dB

POWER LOOP IMPLEMENTATION

DAMPING FACTOR = .707107

PMR (MOD. BITS/SEC)	RL (Hz)	PH-VAR (TOT) (DB-RAD**2)	PH-VAR (TH) (DB-RAD**2)	PH-VAR (PN) (DB-RAD**2)
1200.	175.000	-8.2697	-8.2922	-31.1509
4800.	175.000	-14.2180	-14.3128	-30.8762
19200.	175.000	-19.9454	-20.3334	-30.6276
76800.	175.000	-24.8201	-26.3540	-30.0845
307200.	175.000	-27.4778	-32.3745	-29.1773
1228800.	175.000	-28.4793	-38.3952	-28.9464
4915200.	175.000	-28.8055	-44.4157	-28.9265
19660800.	175.000	-28.8946	-50.4363	-28.9252

DEMODULATION LOSS VS. DATA RATE

MINIMUM-FREE DISTANCE OF CODE=10.0  
DEMODULATION LOSSES USING GAUSSIAN  
APPROX. ARE ACCURATE WHEN < .116469 dB

TIKHONOV APPROX.

PMR (MOD. BITS/SEC)	RL (Hz)	LOSS (TOT) (DB)	LOSS (TH) (DB)	LOSS (TOT) (DB)	LOSS (TH) (DB)
1200.	175.000	.2042E+01	.2024E+01	>6.	>6.
4800.	175.000	.2545E+00	.2471E+00	1.76	1.55
19200.	175.000	.5040E-01	.4559E-01	<.1	<.1
76800.	175.000	.1499E-01	.1039E-01	<.1	<.1
307200.	175.000	.7958E-02	.2533E-02	<.1	<.1
1228800.	175.000	.6286E-02	.6293E-03	<.1	<.1
4915200.	175.000	.5823E-02	.1571E-03	<.1	<.1
19660800.	175.000	.5703E-02	.7926E-04	<.1	<.1

\* Information bit rate = 1/2 \* modulation bit rate

Table D-22. Demodulation Performance - Radiation Inc.  
BPSK With "Crystal II" Phase Noise (2 Terminals and 1  
Equivalent Satellite)

(Losses - Soft Decision (3 bit),  $R = 1/2$ ,  $K = 7$ , Viterbi Decoding at BER =  $10^{-5}$ )

PHASE VARIANCE VS. DATA RATE \*

M=AWV PSK      M = 2

FB/N<sub>0</sub> = 1.3 dB

POWER LOOP IMPLEMENTATION

DAMPING FACTOR = .707107

PMR (MOD. BITS/SEC)	RL (HZ)	PH-VAR (TOT) (DB-RAD**2)	PH-VAR (TH) (DB-RAD**2)	PH-VAR (PN) (DB-RAD**2)
1200.	175.000	-8.2902	-8.2922	-41.6820
4800.	175.000	-14.3024	-14.3128	-40.5349
19200.	175.000	-20.2775	-20.3334	-39.2157
76800.	175.000	-26.0001	-26.3540	-37.0660
307200.	175.000	-30.3307	-32.3745	-34.5860
1228800.	175.000	-32.7061	-38.3952	-34.0719
4915200.	175.000	-33.6490	-44.4157	-34.0292
19660800.	175.000	-33.9281	-50.4363	-34.0262

DEMODULATION LOSS VS. DATA RATE

MINIMUM-FREE DISTANCE OF CODE=10.0  
DEMODULATION LOSSES USING GAUSSIAN  
APPROX. ARE ACCURATE WHEN < .116469 DH

TIKHONOV APPROX.

PMR (MOD. BITS/SEC)	RL (HZ)	LOSS (TOT) (DB)	LOSS (TH) (DB)	LOSS (TOT) (DB)	LOSS (TH) (DB)
1200.	175.000	.2025E+01	.2024E+01	>6.	>6.
4800.	175.000	.2479E+00	.2471E+00	1.57	1.55
19200.	175.000	.4625E-01	.4559E-01	<.1	<.1
76800.	175.000	.1130E-01	.1039E-01	<.1	<.1
307200.	175.000	.4076E-02	.2533E-02	<.1	<.1
1228800.	175.000	.2346E-02	.6293E-03	<.1	<.1
4915200.	175.000	.1885E-02	.1571E-03	<.1	<.1
19660800.	175.000	.1767E-02	.3926E-04	<.1	<.1

\* Information bit rate = 1/2 · modulation bit rate

Table D-23. Demodulation Performance - Radiation Inc.  
BPSK with "Cesium II" Phase Noise (2 Terminals and 1  
Equivalent Satellite)

Losses - Soft Decision (3 bits),  $R = 1/2$ ,  $K = 7$ , Viterbi Decoding at  $BFR = 10^{-5}$

PHASE VARIANCES VS. DATA RATE\*

M-ARY PSK      M = 2

EH/ND = 1.3 DR

POWER LOOP IMPLEMENTATION

DAMPING FACTOR = .707107

DR	RL	PH-VAR (TOT)	PH-VAR (TH)	PH-VAR (PN)
(MOD. BITS/SEC)	(HZ)	(DB-RAD**2)	(DB-RAD**2)	(DB-RAD**2)
1200.	175.000	-8.2892	-8.2922	-39.9120
4800.	175.000	-14.2972	-14.3128	-38.7649
19200.	175.000	-20.2498	-20.3334	-37.4509
76800.	175.000	-25.8330	-26.3540	-35.3008
307200.	175.000	-29.5792	-32.3745	-32.8157
1228800.	175.000	-31.3454	-38.3952	-32.2996
4915200.	175.000	-32.0003	-44.4157	-32.2567
19660800.	175.000	-32.1883	-50.4363	-32.2538

DEMODULATION LOSS VS. DATA RATE

MINIMUM-FREE DISTANCE OF CODE=10.0  
DEMODULATION LOSSES USING GAUSSIAN  
APPROX. ARE ACCURATE WHEN < .16469 DR

TIKHONOV APPROX.

DR	RL	LOSS (TOT)	LOSS (TH)	LOSS (TOT)	LOSS (TH)
(MOD. BITS/SEC)	(HZ)	(DB)	(DB)	(DB)	(DB)
1200.	175.000	.2026E+01	.2024E+01	>6.	>6.
4800.	175.000	.2483E+00	.2471E+00	1.59	1.55
19200.	175.000	.4658E-01	.4559E-01	<.1	<.1
76800.	175.000	.1176E-01	.1039E-01	<.1	<.1
307200.	175.000	.4858E-02	.2533E-02	<.1	<.1
1228800.	175.000	.3218E-02	.6293E-03	<.1	<.1
4915200.	175.000	.2763E-02	.1571E-03	<.1	<.1
19660800.	175.000	.2645E-02	.3926E-04	<.1	<.1

\* Information bit rate = 1/2 • modulation bit rate

Table D-24. Demodulation Performance - Radiation Inc.  
BPSK with "Cesium II" Phase Noise (2 Terminals and 1  
Equivalent Satellite), PLL Damping  $\xi = 1.0$

{Losses - Soft Decision (3 bit), R = 1/2, K = 7, Viterbi Decoding at BER =  $10^{-5}$

PHASE VARIANCES VS. DATA RATE \*

M-ARY PSK      M = 2

EH/NO = 1.3 dB

POWER LOOP IMPLEMENTATION

DAMPING FACTOR = 1.000000

RBH (MOD. BITS/SEC)	RL (Hz)	PH-VAR (TOT) (DB-RA0002)	PH-VAR (TH) (DB-RA0002)	PH-VAR (PN) (DB-RA0002)
1200.	175.000	-8.2669	-8.2922	-30.6414
4800.	175.000	-14.2070	-14.3128	-30.3932
19200.	175.000	-19.9043	-20.3334	-30.1698
76800.	175.000	-24.6951	-26.3540	-29.6780
307200.	175.000	-27.2500	-32.3745	-28.8465
1228800.	175.000	-28.1944	-38.3952	-28.6303
4915200.	175.000	-28.4991	-44.4157	-28.6118
19660800.	175.000	-28.5821	-50.4363	-28.6105

DEMODULATION LOSS VS. DATA RATE

MINIMUM-FREE DISTANCE OF CODE=10.0  
DEMODULATION LOSSES USING GAUSSIAN  
APPROX. APF ACCURATE WHEN  $< .116469$  dB

TIKHONOV APPROX.

RBH (MOD. BITS/SEC)	RL (Hz)	LOSS (TOT) (DB)	LOSS (TH) (DB)	LOSS (TOT) (DB)	LOSS (TH) (DB)
1200.	175.000	.2044E+01	.2024E+01	>6.	>6.
4800.	175.000	.2553E+00	.2471E+00	1.78	1.55
19200.	175.000	.5094E-01	.4559E-01	<.1	<.1
76800.	175.000	.1545E-01	.1039E-01	<.1	<.1
307200.	175.000	.8398E-02	.2533E-02	<.1	<.1
1228800.	175.000	.6722E-02	.6293E-03	<.1	<.1
4915200.	175.000	.6257E-02	.1571E-03	<.1	<.1
19660800.	175.000	.6136E-02	.3926E-04	<.1	<.1

\* Information bit rate = 1/2 \* modulation bit rate

Table D-25. Demodulation Performance - Raytheon Inc.  
BPSK TDMA With HT-MT Mod Phase Noise (2 Terminals)

{Losses - Soft Decision (3 bit), R=1/2, K=7, Viterbi Decoding <sup>(a)</sup>  
BER=10<sup>-5</sup>

AUXILIARY CARRIER SYSTEM  
TDMA DUTY FACTOR = .001

BIT FANWIDTH AND THE CHANNEL INTEGRAL  
PHASE NOISE VARIANCE

OSCILLATOR SPECTRAL CHARACTERISTICS

HP= 1.26E-10 RAD/RZ      H1= 0 RAD  
HP= .01 RAD/RZ      H2= .2 RAD+HET<sup>2</sup>

N-ARY PSK      N= 2

FE/NP= 1.3 DB

Mod. HT1 RATE *	HT-1 FE(NP)	HT-VAR(TH)	PH-VAR(TH)	PH-VAR(CH)
H/S	H <sup>2</sup>	H	H	H
3072PP	100	-4.1E39	-6.11E21	-32.41E7
12288PP	100	-12.1E46	-12.19E9	-31.94E1
49152PP	100	-17.97E55	-14.21E4	-30.63E1
19664PP	100	-22.54E55	-24.23E4	-27.42E1
786432PP	100	-21.90E52	-30.25E4	-22.55E1

CODING SENSITIVITY (AIN = 10 DB  
DEMODULATOR LOSSES USEN GAUSSIAN  
APPROX ARF ACCURATE WHEN < +11.6469 DB

Mod. HT1 RATE *	LOSS(TH) (DB)	LOSS(TH) (DB)	Turbulence Approx	
			Loss(Tot) (DB)	Loss (TH) (DB)
3072PP	4.67517	1.60724	>6	>6
12288PP	.482124	.261923	>6	>6
49152PP	9.20425E-2	6.50559E-2	<.1	<.1
19664PP	2.59579E-2	.016364	.	.
786432PP	7.642365E-2	4.09699E-2	.	.

\* Information bit rate =  $\frac{1}{2}$  modulation bit rate

Table D-26. Demodulation Performance - Raytheon Inc. QPSK  
TDMA With HT-MT Mod Phase Noise (2 Terminals)

(Losses - Soft Decision (3 bit), R=1/2, K=7, Viterbi Decoding  $\Rightarrow$  BFR  $\cdot 10^{-5}$ )

AUXILIARY CARRIER SYSTEM  
TDMA DUTY FACTOR = .001

LINK BANDWIDTH AND THE UNRESOLVED  
PHASE NOISE VARIANCE

150MHz SPECTRAL CHARACTERISTICS

$H_0 = 1.26E-10$  RAD/Hz  $H_1 = 0$  RAD  
 $H_2 = .01$  RAD/Hz  $H_3 = .2$  RAD\*Hz $^{1/2}$

M-ARY PSK  $M = 4$

FB/TH = 1.3 DB

Mod. BIT RATE *	FB- H <sub>2</sub>	FB-VAR(T <sub>1</sub> )	FB-VAR(TH)	FB-VAR(EN)
387200	100	-6.16421	-6.17421	-32.4266
1228800	100	-12.1503	-12.1424	-32.2747
4915200	100	-18.0153	-18.2144	-31.4921
19660800	100	-23.8959	-24.231	-29.3126
78643200	100	-24.0074	-24.0561	-24.1842

CIRCUIT SENSITIVITY AT N = 10 DB  
DEMODULATION LOSSES USING GAUSSIAN  
APPROX ARE ACCURATE WHEN  $\leq .4$  DB

Mod. BIT RATE *	Tikhonov Approx.			
	LOSS(T <sub>1</sub> ) (DB)	LOSS(TH) (DB)	Loss(Tot) (DB)	Loss (TH) (DB)
387200	25.9159	25.8933	> 6	> 6
1228800	7.13036	7.11255	> 6	> 6
4915200	1.90293	1.81809	> 6	> 6
19660800	.594945	.457017	1.0	.65
78643200	.481673	.114111	.95	< .15

\* Information bit rate =  $\frac{1}{2}$  modulation bit rate

Table D-27. Demodulation Performance - Raytheon Inc. BPSK  
TDMA With "Cesium II" Phase Noise (2 Terminals)

{Losses - Soft Decision (3 bit), R=1/2, K=7, Viterbi Decoding @ BER=10<sup>-5</sup>}

PHASE VARIANCE (dB) = DATA RATE \*

MEAN PHASE NOISE

PHASE = 1.0000

AUXILIARY VARIOLOGUE SYSTEM  
TIME DILUTION FACTOR = 2.000000  
DAMPING FACTOR = 1.707107

DATA (1000.0 BIT/SEC)	0	PH-VAR (TOT) (PH-281002)	PH-VAR (TH) (PH-281002)	PH-VAR (PN) (PH-281002)
307670.	100.000	-26.154	-6.1742	-29.9737
122440.	100.000	-12.0114	-12.1448	-29.7890
49152.	100.000	-12.4241	-14.2154	-29.7730
1964080.	100.000	-22.1645	-24.2360	-29.7719
7846220.	100.000	-26.3470	-30.2566	-29.7716

DEMODULATION LOSS (dB) = DATA RATE

SENSEITIVITY DATA RATE = 10.00  
DEMODULATION LOSSES DUE TO GAIN/LOSS  
ABERRATION AND ACCURACY = < .1% < 0.04

DAMPING FACTOR = 1.707107

DATA (1000.0 BIT/SEC)	0	LOSS(TOT)	LOSS(TH)
307670.	100.000	.4444E+01	.4444E+01
122440.	100.000	.4559E+00	.4744E+00
49152.	100.000	.4527E+01	.7477E+01
1964080.	100.000	.2270E+01	.1720E+01
7846220.	100.000	.4549E+02	.4147E+02

\* Information bit rate =  $\frac{1}{2}$  \* modulation bit rate

Table D-28. Demodulation Performance - Raytheon Inc. BPSK  
TDMA With "Cesium II" Phase Noise (2 Terminals and 1 Equivalent Satellite)

PHASE VARIANCE VS. DATA RATE \*

N-BRDY DSF      N= 2

FRZD= 1.2 TH

AUXILIARY CARRIER SYSTEM  
TDMA DUTY FACTOR = .00100000  
DAMPING FACTOR= .707107

DMR (MOD. 41TS/SEC)	H1 (Hz)	PH-VAR (TOT) (DB-DBE1002)	PH-VAR (TH) (DB-DBE1002)	PH-VAR (P*) (DB-DBE1002)
307200.	100.000	-6.1471	-6.1762	-24.2126
1224800.	100.000	-12.0827	-12.1042	-24.0181
4915200.	100.000	-17.7617	-18.2150	-28.0121
19660800.	100.000	-22.7124	-24.2260	-28.0111
78643200.	100.000	-25.9725	-30.2566	-28.0107

DEMODULATION LOSSES VS. DATA RATE

SENSITIVITY GAIN (DB) = 10.00  
DEMODULATION LOSSES USING GAUSSIAN  
APPROX. APF ACCURATE WHEN  $\leq .116462$  DB

DAMPING FACTOR= .707107

DMR (MOD. 21TS/SEC)	H1 (Hz)	LOSS (TOT) (DB)	LOSS (TH) (DB)
307200.	100.000	.4506F+01	.4446F+01
1224800.	100.000	.4920F+00	.4749F+00
4915200.	100.000	.4859F-01	.7477F-01
19660800.	100.000	.2692F-01	.1720F-01
78643200.	100.000	.1134F-01	.6163F-02

\* Information bit rate =  $\frac{1}{2} \cdot$  modulation bit rate

{Losses - Soft Decision (3 bit), R=1/2, K=7, Viterbi Decoding @ BER = 10<sup>-5</sup>}

Table D-29. Demodulation Performance - Raytheon Inc. QPSK  
TDMA With "Cesium II" Phase Noise (2 Terminals)

PHASE VARIANCE (PSK) VS. DATA RATE \*

M-ARY PSK      M= 4

PH/NO= 1.3 dB

ANALYTICAL CALCULATIONS  
TDMA DUTY FACTOR = .200100000  
DAMPING FACTOR = .707107

DMR (M00. RTTS/SEC)	R (-2)	PH-VAR (TOT) (DR-RAD*0.2)	PH-VAR (TH) (DR-RAD*0.2)	PH-VAR (PN) (DR-RAD*0.2)
307200.	100.000	-6.1574	-6.1742	-30.2971
1228800.	100.000	-12.1247	-12.1448	-29.8338
4915200.	100.000	-17.9224	-18.2154	-29.7764
19660800.	100.000	-23.1666	-24.2360	-29.7721
78643200.	100.000	-28.9471	-30.2566	-29.7718
31457200.	100.000	-34.8450	-36.2772	-29.7717

DEMODULATION LOSS VS. DATA RATE

SENSITIVITY GATE (DMR) = 10.00  
DEMODULATION LOSSES USING GAUSSIAN  
APPROX. ADF ACCURATE WHEN  $\leq 0.000001$  dB

DAMPING FACTOR = .707107

DMR (M00. RTTS/SEC)	I (-2)	LOSS(TOT) (DMR)	LOSS(TH) (DMR)
307200.	100.000	.2444E+02	.2449E+02
1228800.	100.000	.7231E+01	.7113E+01
4915200.	100.000	.1444E+01	.1414E+01
19660800.	100.000	.3855E+00	.4470E+00
78643200.	100.000	.2622E+00	.1144E+00
31457200.	100.000	.1565E+00	.2561E-01

\* Information bit rate =  $\frac{1}{2} \cdot$  modulation bit rate

{Losses - Soft Decision (3 bit), R=1/2, K=7, Viterbi Decoding @ BER=10<sup>-5</sup>}

Table D-30. Demodulation Performance - Raytheon Inc. QPSK  
TDMA With "Cesium II" Phase Noise (2 Terminals and 1 Equivalent Satellite)

PHASE VARIANCES VS. DATA RATE \*

M-BIT QPSK      M=4

FR/NR = 1.7 NR

ARMED FORCES CARRIER SYSTEM  
TDMA DUTY FACTOR = .00100000  
DAMPING FACTOR = .707107

DMR (M00, BITS/SEC)	R1 (Hz)	DH-VAR (THT)	DH-VAR (TH)	DH-VAR (T)
		(DH-PA1)0021	(DH-PA1)0021	(DH-PA1)0021
307200.	100.000	-6.1400	-6.1742	-24.5276
1228800.	100.000	-12.0478	-12.1444	-24.0152
4915200.	100.000	-17.7420	-18.2164	-24.0143
19660800.	100.000	-22.7125	-24.2360	-24.0012
78643200.	100.000	-26.9726	-30.2464	-24.0002
31457200.	100.000	-27.3983	-36.2772	-24.0000

DEMODULATION LOSS VS. DATA RATE

SENSITIVITY GAIN (DH) = 10.00  
DEMODULATION LOSSES USING GAUSSIAN  
APPROX. ARE ACCURATE WHEN < .400000 NR

DAMPING FACTOR = .707107

DMR (M00, BITS/SEC)	R1 (Hz)	LOSS (THT)	LOSS (TH)
		(DH)	(DH)
307200.	100.000	.2602F+02	.2649F+02
1228800.	100.000	.7291F+01	.7117F+01
4915200.	100.000	.2007F+01	.1818F+01
19660800.	100.000	.6486F+00	.6570F+00
78643200.	100.000	.3165F+00	.3144F+00
31457200.	100.000	.2209F+00	.2204F-01

\* Information bit rate =  $\frac{1}{2}$  modulation bit rate

{Losses - Soft Decision (3 bit), R=1/2, K=7, Viterbi Decoding @ BER=10<sup>-5</sup>}

Table D-31. Demodulation Performance - Raytheon Inc. BPSK TDMA With "Crystal II" Phase Noise (2 Terminals)

PHASE VARIANCES VS. DATA RATE \*

M-ARY PCK  $\times = ?$

FR/AN = 1.3 FR

ANNUAL DUTY CYCLE SYSTEM  
TOMA DUTY FACTOR = .60160000  
DAMPING FACTOR = .707107

DMR (M00, M1TC/SEC)	M1 (-7)	PH-VAR (TOT) (PH-PAD002)	PH-VAR (TH) (PH-PAD002)	PH-VAR (PM) (PH-PAD002)
307200.	100.000	-6.1677	-6.1742	-34.4105
1228800.	100.000	-12.1657	-12.1948	-37.9155
4915200.	100.000	-14.0490	-14.2154	-33.8744
19660800.	100.000	-22.7677	-24.2301	-33.8715
78643200.	100.000	-24.6578	-30.2566	-33.8704

DEMONSTRATION LOSS VS. POTS LTF

SELECTIVITY DATA FOR 1.000  
DEMONSTRATION MODELS SELECTED  
APPROX. ARE APPROXIMATE AND 1.000

FADING FACT  $\alpha = .77117$

DMH	T	1045 (TH)	1045 (TH)
1000, 11175 (SEC)	-71	-1-01	-1-01
307210,	1-01-01-01	-417555-01	-442655-01
1224800,	1-01-01-01	-474855-01	-374955-01
4015200,	1-01-01-01	-121155-01	-767755-01
184600001,	1-01-01-01	-1-0175-01	-172055-01
78643270,	1-01-01-01	-557555-01	-414355-01

- Information bit rate =  $\frac{1}{2} \cdot$  modulation bit rate

Losses - Soft Decision (3 bit),  $R=\frac{1}{2}$ ,  $K=7$ , Viterbi Decoding @  $BER=10^{-5}$

Table D-32. Demodulation Performance - Raytheon Inc. BPSK  
TDMA With "Crystal II" Phase Noise (2 Terminals and 1 Equivalent  
Satellite)

PHASE VARIANCES VS. DATA RATE \*

M=8RY BPSK      M= 2

FH/Δf = 1.2 FR

MILITARY CARRIER SYSTEM  
TDMA DUTY FACTOR = .00100000  
DAMPING FACTOR = .707107

RMR (MM. BITS/SEC)	R <sub>I</sub> (Hz)	PH-VAR (TOT) (PH-PAD*#2)	PH-VAR (TH) (PH-PAD*#2)	PH-VAR (DAM) (PH-PAD * #2)
307200.	100.000	-6.1644	-6.1742	-32.6412
1228800.	100.000	-12.1511	-12.1448	-32.1422
4915200.	100.000	-18.0415	-18.2154	-32.1020
19660800.	100.000	-23.5781	-24.2360	-32.1462
78643200.	100.000	-28.0703	-30.2566	-32.0484

DEMODULATION LOSS VS. DATA RATE

SENSITIVITY GAIN (DR) = 10.00  
DEMODULATION LOSSES USING GAUSSIAN  
APPROX. ARE ACCURATE WHEN < .116460 DR

DAMPING FACTOR = .707107

RMR (MM. BITS/SEC)	R <sub>I</sub> (Hz)	LOSS (TOT) (DR)	LOSS (TH) (DR)
307200.	100.000	.4474E+01	.4474E+01
1228800.	100.000	.4819E+00	.4749E+00
4915200.	100.000	.8746E-01	.7477E-01
19660800.	100.000	.2017E-01	.1720E-01
78643200.	100.000	.6910E-02	.4147E-02

\* Information bit rate =  $\frac{1}{2} \cdot$  modulation bit rate

{Losses - Soft Decision (3 bit), R=1/2, K=7, Viterbi Decoding @ BER=10<sup>-5</sup>}

Table D-33. Demodulation Performance - Raytheon Inc. QPSK TDMA With "Crystal II" Phase Noise (2 Terminals)

### PHASE VARIANCES VS. DATA RATE \*

MARY DSK N= 4

ER/NO = 1.3 54

AUXILIARY CARRIER CYCLE  
TDMA DUTY FACTOR = .00100010  
DAMPING FACTOR = .707107

PRMR (MMD. BITS/SEC)	PI (HZ)	CH-1 AL (TOP)	PH-VAR (TH)	PH-VAR (DN)
307200.	100.000	-4.1460	-6.1742	-35.3759
1228800.	100.000	-12.1445	-12.1445	-34.0325
4915200.	100.000	-15.0462	-15.0462	-33.8430
19660800.	100.000	-22.7417	-24.2360	-33.6722
78643200.	100.000	-24.6270	-30.2466	-33.8712
314572800.	100.000	-31.8446	-37.2772	-33.8700

### DEMODULATION LOSS VS. DATA RATE

DAMPING FACTOR = .707107

DMA (MOD. RTTS/SEC)	-1 (-1)	LOC(S(TH)) (-1)	LOC(S(TH)) (-1)
307200.	100.000	.2444E+012	.2444E+012
1228800.	100.000	.7144E+011	.7144E+011
4915200.	100.000	.1E+011	.1E+011
19660800.	100.000	.4570E+010	.4570E+010
78643200.	100.000	.1E+010	.1E+010
314572000.	100.000	.7E+009	.7E+009

- Information bit rate =  $\frac{1}{2} \cdot$  modulation bit rate

Losses - Soft Decision (3 bit), R=1/2, K=7, Viterbi Decoding @ BER=10<sup>-5</sup>

Table D-34. Demodulation Performance - Raytheon Inc. QPSK  
TDMA With "Crystal II" Phase Noise (2 Terminals and 1 Equivalent  
Satellite)

PHASE VARIANCES VS. DATA RATE \*

M-ARY PSK      M= 4

FR/NO= 1.3 DR

AUXILIARY CARRIER SYSTEM  
TDMA DUTY FACTOR = .00100000  
DAMPING FACTOR= .707107

DR	H1	PH-VAR(TOT)	PH-VAR(TH)	PH-VAR(TH)
(MOD. BITS/SEC)	(Hz)	(DR-PAD*#?)	(DR-PA#*#?)	(DR-PA#*#?)
307200.	100.000	-6.1664	-6.1742	-22.01 -14
1228800.	100.000	-12.1522	-12.1448	-22.24 -17
4915200.	100.000	-1F.0418	-14.2154	-22.11 -17
19660800.	100.000	-23.5742	-24.2340	-22.14 -14
78643200.	100.000	-28.0705	-30.2648	-22.14 -14
314572800.	100.000	-30.6926	-36.2772	-22.14 -14

DEMODULATION LOSSES VS. DATA RATE

Sensitivity Gain (DR) = 10.00  
DEMODULATION LOSSES USING GAUSSIAN  
APPROX. ARE ACCURATE WHEN < .400000 DR

DAMPING FACTOR= .707107

DR	H1	LOSS(TOT)	LOSS(TH)
(MOD. BITS/SEC)	(Hz)	(DR)	(DR)
307200.	100.000	.2543F+02	.2544F+02
1228800.	100.000	.7140F+01	.7117F+01
4915200.	100.000	.1F99F+01	.1E14F+01
19660800.	100.000	.5216F+00	.4570F+00
78643200.	100.000	.1F99F+00	.1144F+00
314572800.	100.000	.1075F+00	.2461F-01

\* Information bit rate =  $\frac{1}{2} \cdot$  modulation bit rate

{Losses - Soft Decision (3 bit), R=3, K=7, Viterbi Decoding @ BER=10<sup>-5</sup>}

Table D-35. Demodulation Performance - Raytheon Inc. BPSK  
TDMA With HT-MT Mod Phase Noise (2 Terminals)

AUXILLIARY CARRIER SYSTEM\*  
TDMA DUTY FACTOR = .991

OPTIMUM LOOP BANDWIDTH AND THE CORRESPONDING  
PHASE NOISE VARIANCE

OSCILLATOR SPECTRAL CHARACTERISTICS

$H0 = 1.2AF - 1P$   $H0L/H7$        $H1 = 0$   $PAD$   
 $H2 = .01$   $HAL*H7$        $H3 = .2$   $FAE*H7 + P$

M-ARY PSK    $M = 2$        $ER/NP = 1.3$   $DE$

BIT RATE B/S	EW-OPT(MP) H7	ER-VAH(TOT) DE	ER-VAH(1H) DE	ER-VAH(F) DE
307200	11.5185	-13.4751	-15.5693	-17.6624
1228800	18.2K34	-17.2938	-19.5742	-21.1819
4915200	29.8166	-20.8878	-23.589	-26.2309
19668800	46.0189	-23.3268	-27.6867	-30.356
78643200	72.7784	-21.8728	-31.6366	-32.3574

CODING SENSITIVITY GAIN = 10  $DE$

DEMODULATION LOSSES USING GAUSSIAN  
APPROX ARE ACCURATE WHEN  $< .116469$   $DE$

BIT RATE (B/S)	LOSS(101) (DE)	LOSS(1H) (DE)
307200	.313139	.124632
1228800	.1V12H7	4.7K7P3F-P
4915200	.K39266	.F1K993
19668800	8.14397E-2	7.53K51F-3
78643200	3.06686E-2	2.97736E-3

\*Information bit rate  $\frac{1}{2}$  modulation bit rate

(Losses - Soft Decision (3 bits),  $R = \frac{1}{2}$ ,  $K = 7$ , Viterbi Decoding w BER  $= 10^{-5}$ )

Table D-36. Demodulation Performance - Raytheon Inc. BPSK TDMA  
With HT-MT Mod Phase Noise (2 Terminals and 1 Equivalent Satellite)

AUXILIARY CARRIER SYSTEM  
TDMA DUTY FACTOR = .001

OPTIMUM CODES WITH AND THE CORRESPONDING  
PHASE NOISE VARIANCE

OSCILLATOR SPECTRAL CHARACTERISTICS

$H_1 = 1.89E-14$  RAD/HZ       $H_1 = E$  RAD  
 $H_2 = .015$  RAD\*HZ       $H_3 = .3$  RAD\*HZ<sup>1/2</sup>

MARY FSR       $N = 2$        $E_H/N_R = 1.3$  DF

FIT RATE	EW-OPT(MHz)	PH-VAR(TOT)	PH-VAR(TH)	PH-VAR(FD)
E/S	$H_2$	DF	DF	DF
3872000	13.1853	-12.8428	-14.9733	-16.9576
12288000	20.9285	-16.6336	-18.9874	-24.4177
49152000	33.2166	-20.1537	-23.0826	-23.2316
196600000	52.6462	-22.2951	-27.0823	-24.0751
786432000	83.2975	-26.3229	-31.0607	-29.7857

CODING SENSITIVITY GAIN = 10 DF

DEMODULATION LOSSES USING GAUSSIAN

APPROX AFE ACCURATE WHEN  $< .116469$  DF

FIT RATE (P/S)	LOSS(TOT) (DF)	LOSS(TH) (DF)
3872000	.383432	.138488
12288000	.121467	5.47958E-2
49152000	4.73454E-2	2.17383E-2
196600000	2.76195E-2	.888615
786432000	4.53362E-2	3.39951E-3

\*Information bit rate  $\frac{1}{2}$  modulation bit rate

(Losses - Soft Decision (3 bit),  $R = \frac{1}{2}$ , K 7, Viterbi Decoding @ BER  $10^{-5}$ )

Table D-37. Demodulation Performance - Raytheon Inc. QPSK  
TDMA With HT-MT Mod Phase Noise (2 Terminals)

AUXILIARY CARRIER SYSTEM\*  
TDMA DUTY FACTOR = .001

OPTIMUM LOOF BANDWIDTH AND THE CORRESPONDING  
PHASE NOISE VARIANCE

OSCILLATOR SPECTRAL CHARACTERISTICS

HP = 1.26E-16 RAD/HZ  
HR = .01 RAD/HZ

HI = 1 RAD  
H3 = .2 RAD = H7/2

R=ANY FSK R=4

FF/NV= 1.3 LF

BIT RATE	FW-CF7(MHz)	FW-VAH(101)	FW-VAH(1H)	FF-LAH(101)
3072000	11.5185	-13.474	-15.5663	-17.6644
12288000	18.2834	-17.3624	-19.5747	-21.2841
49152000	29.0166	-24.9711	-23.589	-24.4127
196640000	46.0189	-23.9474	-27.6487	-26.3434
786432000	72.7784	-23.9579	-31.6366	-24.7766

CODING SENSITIVITY GAIN = 1V LF

DEMODULATION LOSSES USING GAUSSIAN  
APPROX AVE ACCURATE WHERE < .4 LF

BIT RATE	LOSS(101)	LOSS(1H)
3072000	5.33613	3.38494
12288000	2.13934	1.33225
49152000	.467755	.53424
196640000	.448317	.219522
786432000	.447181	.327671-2

\*Information bit rate  $\frac{1}{2}$  modulation bit rate

(Losses - Soft Decision (3 bit), R  $\frac{1}{2}$ , K 7, Viterbi Decoding @ BER  $10^{-5}$ ).

Table D-35. Demodulation Performance - Raytheon Inc. QPSK TDMA  
With HT-MT Mod Phase Noise (2 Terminals and 1 Equivalent Satellite)

AUXILIARY CARRIER SYSTEM\*  
TDMA DUTY FACTOR = .001

OPTIMUM LOOF BANDWIDTH AND THE CORRESPONDING  
PHASE NOISE VARIANCE

OSCILLATOR SPECTRAL CHARACTERISTICS

$H_1 = 1.09E-10$  HAL/H<sub>2</sub>       $H_1 = 0$  HAL  
 $H_2 = .015$  HAL\*H<sub>2</sub>       $H_3 = .3$  HAL\*H<sub>2</sub>H<sub>3</sub>

R-AHY FSK      R = 4

EF/N<sub>0</sub>R = 1.3   DF

FR1 RATE (R/S)	FW-CF(MF)	FR-VAF(1CT)	FR-VAF(TH)	FR-VAF(FC)
F/S	H <sub>2</sub>	LF	LF	LF
3672K	13.1853	-12.944	-14.9733	-16.9887
1228K	20.4985	-16.6453	-18.9874	-20.4455
49152K	33.2106	-20.2595	-23.0026	-23.5544
19660K	52.6462	-23.0394	-27.0223	-25.2562
786432K	83.0975	-22.5433	-31.0897	-23.0818

CODING SENSITIVITY GAIN = 1K   DF  
DEMODULATION LOSSES USING GAUSSIAN  
APPROX ARE ACCURATE WHEN  $\epsilon = .4$    DF

FR1 RATE (R/S)	LOSS(1CT)	LOSS(TH)
3672K	6.15E44	3.00E434
1228K	2.601E	1.523E1
49152K	1.13E6K	.696753
19660K	.6615E4	.240811
786432K	.6742E4	9.5679E-2

\*Information bit rate  $\frac{1}{2}$  modulation bit rate

{Losses - Soft Decision (3 bit), R  $\frac{1}{2}$ , K 7, Viterbi Decoding @ BER  $10^{-5}$

Table D-39. Demodulation Performance - Raytheon Inc. BPSK  
TDMA with "Cesium II" Phase Noise (2 Terminals)

Phase Variances vs. Data Rate\*  
at Optimum PLL Bandwidth:

WAVELENGTH = 1.3

PHASE = 1.6

DEMODULATOR LOSSES = 0.0  
TDMA GAIN FACTOR = 1.0  
DATA RATE FACTOR = 1.0

DATA RATE (MPS, BITS/SEC)	1	PH-VR (TH)	PH-VR (TH)	PH-VR (PS)
	(1.0E-02)	(1.0E-02)	(1.0E-02)	(1.0E-02)
20.72E0	1.0E-02	-19.71E1	-22.61E1	-23.57E0
122.44E0	4.0E-02	-19.01E1	-20.81E1	-26.00E1
64.15E0	5.0E-02	-19.51E1	-30.02E0	-27.51E1
16.00E0	1.0E-01	-21.21E1	-34.07E1	-28.24E1
7.8643E0	1.8E-01	-21.11E1	-37.04E1	-29.68E1

DEMODULATOR LOSSES = 0.01  
at Optimum PLL Bandwidth:

DEMODULATOR LOSSES = 0.01  
TDMA GAIN FACTOR = 1.0  
DATA RATE FACTOR = 1.0

DATA RATE FACTOR = 1.0

DATA RATE (MPS, BITS/SEC)	1	LOSS (TH)	LOSS (TH)
	(1.0E-02)	(1.0E-02)	(1.0E-02)
20.72E0	1.0E-02	0.5E-01	0.2415E-01
122.44E0	4.0E-02	0.1E-01	0.1122E-01
64.15E0	5.0E-02	0.1E-01	0.4369E-02
16.00E0	1.0E-01	0.1E-01	0.1700E-02
7.8643E0	1.8E-01	0.1E-01	0.8839E-03

\*Information bit rate =  $\frac{1}{2}$  modulation bit rate

{Losses - Soft Decision (3 bit),  $R = \frac{1}{2}$ ,  $K = 7$ , Viterbi Decoding @  $BER = 10^{-5}$ }

Table D-40. Demodulation Performance - Raytheon Inc. BPSK TDMA with "Cesium II" Phase Noise (2 Terminals and 1 Equivalent Satellite)

### Phase Variances vs. Data Rate at Optimum PLL Bandwidth:

8 - 844 Y 255

$$k_{\infty}(t,0) = 1, \quad t \in \mathbb{R}$$

AUXILIARY CARRIER SYSTEM  
TUNA DUTY FACTOR = .90100000  
CAMPING FACTOR = .777107

PHW (MM). PITS/SEC	PL (Hz)	PH-VAR(TOT) (DH-RAD#2)	PH-VAR(TH) (DH-RAD#2)	PH-VAR(PN) (DH-RAD#2)
307200.	2.975	-18.49E5	-21.64E5	-22.5871
1228800.	4.684	-22.07E5	-25.46E5	-24.7259
4915200.	7.526	-24.40E6	-24.64E4	-26.0406
196604800.	11.046	-24.84E7	-33.50E3	-26.6658
78643200.	10.134	-24.54E9	-37.21E4	-26.4847

### DEMODULATION LOSS VS. DATA RATE AT OPTIMUM BANDWIDTH:

WAMPUM FACTORY - 707107

RHM (MM)	LI (H <sub>2</sub> )	LOSS(T-T <sub>0</sub> ) (%)	LOSS(TH) (%)
3072000	2.245	0.5344E-01	0.3367E-01
12288000	4.688	0.2414E-01	0.1274E-01
44192000	7.524	0.14502E-01	0.5002E-02
196804000	11.646	0.11491E-01	0.1950E-02
784432000	20.134	0.7451E-02	0.2606E-02

\*Information bit rate =  $\frac{1}{2}$  : modulation bit rate

Losses - Soft Decision (3 bit), R =  $\frac{1}{3}$ , K = 7, Viterbi Decoding @ BER =  $10^{-5}$

Table D-41. Demodulation Performance - Raytheon Inc. QPSK  
TDMA with "Cesium II" Phase Noise (2 Terminals)

Phase Variances vs. Data Rate\*  
at Optimum PLL Bandwidth:

M-ARY PSK      N = 4

PHASE = 1.0E-10

AUXILIARY CARRIER SYSTEM

TIME DUTY FACTOR = .00100000

AMPLITUDE FACTOR = .707107

DATA (MHz, BITS/SEC)	R	PH-VAR(TOT) (DR-RAU*#2)	PH-VAR(TH) (DR-RAU*#2)	PH-VAR(DN) (DR-RAU*#2)
307200.	2.54E	-14.7814	-22.1777	-23.6464
1228800.	4.17E	-23.0122	-26.0606	-25.4844
4915200.	6.58E	-25.5876	-30.0240	-27.5234
19660800.	10.367	-27.2813	-34.0179	-28.2994
78643200.	15.42E	-28.1975	-37.4711	-24.6804
314572000.	157.57E	-28.4820	-34.0353	-30.6045

DEMODULATION LOSS VS. DATA RATE  
AT OPTIMUM PHASE (TH):

SENSITIVITY RATE (PS) = 16.00  
DEMODULATION LOSSES USING GAUSSIAN  
AMPLITY. ARE ACCURATE WHEN  $\leq 1.40000$  DR

AMPLITUDE FACTOR = .707107

DATA (MHz, BITS/SEC)	R	LOSS(TOT)	LOSS(TH)
307200.	2.54E	.1271E+01	.7503E+00
1228800.	4.17E	.6074E+00	.3004E+00
4915200.	6.58E	.3330E+00	.1206E+00
19660800.	10.367	.2284E+00	.6746E-01
78643200.	15.42E	.1514E+00	.1937E-01
314572000.	157.57E	.1414E+00	.4794E-01

\*Information bit rate =  $\frac{1}{2} \times$  modulation bit rate

{Losses - Soft Decision (3 bit), R =  $\frac{1}{2}$ , K = 7, Viterbi Decoding @ BER =  $10^{-5}$ }

Table D-43. Demodulation Performance - Raytheon Inc. BPSK  
TDMA with "Crystal II" Phase Noise (2 Terminals)

Phase Variances vs. Data Rate\*  
at Optimum PLL Bandwidth

$N = 8$ ,  $R = 1$ ,  $M = 2$

$E_b/N_0 = 1.0$  dB

ANALYTICAL APPROX. SYSTEM  
TIME CONSTANT = 0.00150000  
DATA RATE = 2.7107

DATA RATE	BER	PH-VAR (T/T)	PH-VAR (TH)	SH-VAR (PH)
(10 <sup>6</sup> BPS/SEC)	(-2)	(10 <sup>-2</sup> VAR <sup>-0.2</sup> )	(10 <sup>-2</sup> VAR <sup>-0.2</sup> )	(10 <sup>-2</sup> VAR <sup>-0.2</sup> )
3.072000	0.564	-24.3146	-27.4443	-28.7448
1.224000	1.001	-26.1415	-31.2577	-30.6146
4.416000	1.744	-31.3162	-35.7771	-31.7548
1.4448000	2.464	-31.5270	-34.5171	-32.3474
7.8848000	3.242	-32.3449	-42.2033	-32.8561

DEMODULATION LOSS VS. DATA RATE  
AT OPTIMUM PHASE NOISE:

SENSITIVITY DATA (dB) = 17.00  
DEMODULATION LOSSES (dB) = GAUSSIAN  
APPROX. DATA ACCURACY (BER < 0.0001) = 0.0001

DATA RATE = 2.7107

DATA RATE	LOSS	LOSS (T/T)
(10 <sup>6</sup> BPS/SEC)	(-2)	(-2)
3.072000	0.564	1.326E-01
1.224000	1.001	1.732E-02
4.416000	1.744	2.674E-02
1.4448000	2.464	3.112E-02
7.8848000	3.242	2.473E-02

\*Information bit rate =  $\frac{1}{2} \cdot$  modulation bit rate

{Losses - Soft Decision (3 bit),  $R = \frac{1}{2}$ ,  $K = 7$ , Viterbi Decoding @ BER =  $10^{-5}$ }

Table D-45. Demodulation Performance - Raytheon Inc. QPSK  
TDMA with "Crystal II" Phase Noise (2 Terminals)

Phase Variances vs. Data Rate\*  
at Optimum PLL Bandwidth

N=4812 PPSK      N= 4

FRMSD = 1.3 x 10<sup>-5</sup>

AUXILIARY CARRIER SYSTEM  
TDMA DUTY FACTOR = .00100006  
DAMPING FACTOR = .707107

DMR (MOD. BITS/SEC)	RL (dB)	PH-VAR(TOT) (DMR=4812*2)	PH-VAR(TH) (DMR=4812*2)	PH-VAR(HN) (DMR=4812*2)
307200.	.664	-24.4266	-27.4443	-28.4662
1228800.	1.041	-24.2125	-31.8477	-30.6649
4915200.	1.744	-30.3160	-35.7471	-31.7651
19660400.	2.964	-31.6274	-34.5171	-32.3479
78643200.	4.242	-32.3492	-42.3133	-32.4564
314572800.	17.642	-32.0368	-43.7493	-33.3072

DEMODULATOR LOSS VS. DATA RATE  
AT OPTIMUM BANDWIDTH:

SENSITIVITY GAIN (DH) = 10.00  
DEMODULATION LOSSES USING GAUSSIAN  
AMPLIF. ARE ACCURATE WHEN < .40dB OF DH

DAMPING FACTOR = .707107

DMR (MOD. BITS/SEC)	RL (dB)	LOSS(TOT) (DH)	LOSS(TH) (DH)
307200.	.664	.3476E+00	.1444E+00
1228800.	1.041	.1E31E+00	.7914E-01
4915200.	1.744	.1124E+00	.3203E-01
19660400.	2.964	.4364E-01	.1357E-01
78643200.	4.242	.7003E-01	.7145E-02
314572800.	17.642	.6175E-01	.5063E-02

\*Information bit rate =  $\frac{1}{2}$  x modulation bit rate

{Losses - Soft Decision (3 bit), R =  $\frac{1}{2}$ , K = 7, Viterbi Decoding @ BER = 10<sup>-5</sup>}

Table D-46. Demodulation Performance - Raytheon Inc. QPSK TDMA with "Crystal II" Phase Noise (2 Terminals and 1 Equivalent Satellite)

Phase Variances vs. Data Rate\*  
at Optimum PLL Bandwidth:

$\omega_{PLL}$   $\omega_{RF}$   $\omega_{IF}$   $\omega_{BPF}$

$\omega_{PLL}/\omega_{RF} = 1.0$   $\omega_{IF}/\omega_{BPF} = 1.0$

AUXILIARY TRACKING SYSTEM  
TDMA DUTY FACTOR = .5000000  
DAMPING FACTOR = .707107

DATA (MBPS, BITS/SEC)	1	PH-1 AW (TOT) (0.000000000)	PH-1 AW (T+) (0.000000000)	PH-1 AW (S+) (0.000000000)
307200.	.707	-26.6264	-27.1472	-27.4666
1224000.	1.024	-27.1645	-31.0242	-34.3244
4915200.	2.012	-26.6104	-35.1723	-30.2143
19660800.	3.565	-27.1210	-37.7171	-30.7654
78643200.	4.024	-31.7413	-41.0712	-31.8118
314572800.	24.024	-21.3042	-46.4243	-31.6521

DEMODULATION LOSS vs. DATA RATE  
AT OPTIMUM BANDWIDTH:

SENSITIVITY RATE (FR) = 10.00  
DEMODULATION LOSSES (LOSS IN dB) = 0.000000000  
APPROX. BPF ACCURATE WHEN  $\omega_{BPF}/\omega_{RF} = 0.400000$

DAMPING FACTOR = .707107

DATA (MBPS, BITS/SEC)	1	LOSS(T+T)	LOSS(T+)
307200.	.707	.4172E+00	.2237E+00
1224000.	1.024	.2122E+00	.4114E+00
4915200.	2.012	.1424E+00	.2890E+00
19660800.	3.565	.1141E+00	.1832E+00
78643200.	4.024	.1012E+00	.1649E+00
314572800.	24.024	.0640E+00	.0840E+00

\*Information bit rate =  $\frac{1}{2}$  modulation bit rate

{Losses - Soft Decision (3 bit),  $R = \frac{1}{2}$ ,  $K = 7$ , Viterbi Decoding @ BER =  $10^{-5}$ }

## REFERENCES

1. Paul, H. I., "Performance of USC-28 Operating With an AN/ASC-18 Terminal (U)," Secret, CSC Internal Memorandum, 19 July 1974, Task 4188-21201.
2. Wolfson, C. R., and Giordano, C., "Effects of Phase Jitter On The Probability of Bit Error for PSK Communications Employing Forward Acting Error Control in the Phase II DSCS," Computer Sciences Corporation Report, Contract No. DCA-100-73-C-0008, Task Order 0109, Part 1, Report No. 10901-2, February 1973.
3. Barnes, J. A., et al., "Characterization of Frequency Stability," NBS Technical Note 394, October 1970.
4. Shoaf, J. H., et al., "Frequency Stability and Measurement: High Frequency and Microwave Signals," NBS Technical Note 632, January 1973.
5. Viterbi, A. J., "Principles of Coherent Communications," McGraw-Hill, Inc., 1966.
6. Stiffler, J. J., "Theory of Synchronous Communications," Prentice-Hall, Inc., 1971.
7. Wolfson, C. R., "Comparison of Suppressed Carrier Binary and Quaternary PSK Modulation for DSCS," Computer Sciences Corporation Report, Contract No. DCA-100-72-C-0002, Task Order 0015, Part 1a, August 1972.
8. Kullstam, P. A., "The Influence of Phase Noise From Phase Locked Loops on Coherent PSK Signal Demodulation," to be published in 1974.
9. Kullstam, P. A., "An Analysis of Utilization of the Goddard Networks for 1973-1980," Quarterly Progress Report, Section 2, July 1972.
10. Barnard, S., and Child, J. M., Higher Algebra, McMillan and Company, Ltd., 1964.
11. Hartell, D., "Documentation of a Computer Solution to the Performance of M-ARY PSK Signalling in the Presence of Phase Noise and Thermal Noise," CSC Internal Memorandum, Task 4188-10703, August 1973.
12. Larimore, W. E., and Paul, H. I., "Gated Phase Locked Loop in the Presence of Noise," IEEE Conf. on Communications, Philadelphia, Pa., 1972.

13. Sherwin, R. P., "The Relation Between the Phase II MT /HT Earth Terminal Incidental FM Specification and Its Corresponding Phase Noise Density," Communications & Systems, Inc., Contract No. DCA-100-67-C-0023, Task 24-2404, 27 June 1969.
14. Hewlett Packard Data Sheet: Cesium Beam Frequency Standard, Model 5061A, 1 January 1973.
15. Oscilloquartz SA Tentative Data Sheet: B5400 Crystal, May 1973.
16. Levensky, E. E., LTC, Sig C, Executive Officer, "Performance Data for Improved Phase II Frequency Converter Local Oscillators," Headquarters, U.S. Army Satellite Communications Agency, AMCPM-SC-5E, 28 February 1974.
17. Jones, M. E., et al., "Modulation - TDMA, Progress Report on the DSCS Phase II, Stage 2 Engineering Development Model TDMA," Computer Sciences Corporation Report, Contract No. DCA-100-73-C-0008, Task 109, Part 2, 31 March 1973.
18. Paul, H.I., "Appendix to Documentation of Computer Program to Implement Analysis of a Gated PLL in the Presence of Noise," CSC Internal Memorandum, 17 January 1972, Task 4188-1520.
19. Viterbi, A.J., "Convolutional Codes and Their Performance in Communications Systems," Part II, IEEE Transactions on Communications, 19 April 1971.
20. Gradshteyn, I.S. and Ryzhik, I.M., "Table of Integrals, Series and Products," Academic Press, 1965.
21. Rhodes, S.A., Tunstall, B.P., Lebowitz, S.H., "Effect of a Noisy Phase Reference on Coherent PSK Communications with Convolutional Error Correction Encoding and Viterbi Decoding," to be published in NTC, December, 1974, San Diego, California.

